Regression modeling of baseflow and low flow indices using watershed characteristics in eastern Japan

STANLEY NUNGU CHAPASA

Department of Environmental Science and Technology

Graduate School of Science and Technology

Niigata University

A thesis submitted in fulfilment of the requirement for the degree of

DOCTOR OF PHILOSOPHY

2023

Declaration

This thesis is the result of the author's novel study. It has been produced originally by the author. Additionally, it has not been hitherto submitted, in part or fullness, to any other university or institution for any degree, diploma, or other qualifications.

Signed:

Date:

Acknowledgments

I would like to express my sincere gratitude to the Government of Japan, Niigata University, and Mitsubishi Corporation for providing me with the following scholarships: MEXT Honors and Mitsubishi Corporation International Scholarships. These scholarships have enabled me to finish my Ph.D. study successfully.

Special profound thanks should go to my primary supervisor Prof. Dr. Whitaker for the opportunity he gave me to pursue my interest in Watershed Hydrology Lab. I am very thankful for the belief you held in my capabilities over the previous few years. Many thanks should go to you again and co-supervisors, Professors Dr. Hideo Hasegawa and Dr. Makoto Nakata whose suggestions, guidance, constructive criticism, and advice throughout this study were crucial for the success of this work.

I also wish to thank all lecturers, fellow lab members, Daichi, Shakil, and Kaba, and the entire members and staff of the Faculty of Agriculture and the Graduate School of Science and Technology for their moral support and collaboration throughout the study.

Many thanks should go to my wife Joyce and two daughters, Success and Favour. Your patience and encouragement undoubtedly boosted my morale and gave me the much-needed strength to take me through my academic pursuit. It has not been easy to earn a living and stay alone with our children at home. Your cheers and moral support cannot go without being mentioned. I would also like to thank my mother, whose love, care, and desire was to see me educated up to the Ph.D. level.

Last but not least, my appreciation also goes to a labmate, Daichi Miyajima, for his assistance in collecting some data in Japan.

Abstract

Regression modeling of baseflow and low flow indices using watershed characteristics in eastern Japan

Stanley Nungu Chapasa

Baseflow is the portion of streamflow derived from delayed subsurface pathways. The baseflow index (BFI) is a ratio of baseflow to total streamflow, and is an important hydrological variable when linking watershed characteristics to baseflow. In addition, the BFI and runoff trend analysis could be used to assess the impact of climate change and human activity on river systems. The 'smoothed minima' procedure of baseflow separation was applied to streamflow data (29-67 years) from twenty-six gauges of watersheds in eastern Japan. The Mann-Kendall statistical test and Sen's slope estimator were used to identify trends and estimate the rate of change in annual and seasonal runoff and BFI per decade at 0.01 and 0.05 significance levels. According to what I know, this is the first study to investigate long-term trends in runoff and BFI for watersheds in the large-scale region of eastern Japan. Results showed significant trends in annual runoff and BFI, with a concentration of significant seasonal trends occurring in winter, with five gauges showing trends in runoff and nine gauges showing trends in BFI. The results suggest that the response of annual and seasonal runoff and BFI to climate change can already be seen, which implies that policymakers need more information on the impacts of climate change and human activities to manage water resources sustainably.

A convenient technique was suggested for the matching strip method in determining the recession constant of the master recession curve using the ratio of flow over successive days (Q_{n+1}/Q_n). The procedure was applied to 29 basins (6.1–740 km^2) in

eastern Japan to build linear regression models which estimate low flow indices through the recession constant (λ), and either mean annual precipitation or mean annual runoff. Statistically, significant models with an additive format (no log transformation) were built for dependent variables; $Q7_{10}$ (7-day 10-year low flow), and $Q97_{10}$ (10-year low flow exceeded 97% of time) in the case of all basins, and in particular, the case of basins classified into sedimentary or igneous lithology with the adjusted R^2 up to 0.784. In case of all basins lumped together, regression models based on mean annual runoff as the second independent variable performed better than those based on mean annual precipitation, with adjusted R^2 of 0.705 and 0.717 for the $Q7_{10}$ and $Q97_{10}$ models, respectively.

The thesis also developed models with a multiplicative format (log transformation) to estimate annual BFI and $Q7_{10}$ flow index using the mean annual runoff and either mean elevation or maximum elevation. Five out of the six models developed were significant, with adjusted R^2 values up to 0.482 ($Q7_{10}$ model for sedimentary lithology). These significant regression models could be applied to poorly gauged watersheds to manage water resources sustainably in eastern Japan and contribute towards achieving SDG6.

Preface

The results of this thesis were put together into a series of articles to be published in peer reviewed journals are presented in chapters 4 and 5. Each results chapter has its own abstract, introduction, materials and methods, results and discussion and conclusion. Chapter 6 provided introduction, results and discussion of regression analysis of annual BFI and $Q7_{10}$ models. A text-to-text connection between chapters was written to determine context, relationship, commonalities and harmony between the chapters. The published articles contained in each results chapter were as follows:

Chapter 4

Chapasa, S.N. and Whitaker, A.C., 2023. Assessing characteristics and long-term trends in runoff and baseflow index in eastern Japan. Hydrological Research Letters, 17(1), 1-8.

Chapter 5

Whitaker, A.C, Chapasa, S.N., Sagras, C., Theogene, U., Veremu, R. and Sugiyama, H., 2022. Estimation of base flow recession constant and regression of low flow indices in eastern Japan. Hydrological Sciences Journal, 67(2), 191-204.

The author of this thesis is the corresponding author of the published paper in chapter 4 and has produced the work guided by supervisor Assoc. Professor Andrew C. Whitaker. This thesis was supported by data sourced from the Government of Japan through various ministries, department and agencies and other global data source platforms.

Study Contribution

This thesis has contributed to knowledge in many ways. The study contributions are outlined below:

- New investigations regarding the characterization of distribution and variability of the annual and seasonal BFI values have emerged. Histograms and plot box charts were used to show frequency distribution and variability of the BFI values.
- New knowledge has been generated for Japan using the Mann-Kendall test and Sen's slope estimator. The identification of annual and seasonal trends and rate of change per decade in runoff and BFI values was done across a range of catchments in eastern Japan
- A new proposed convenient procedure for the matching strip method to objectively estimate baseflow recession constant has been discovered.
- New knowledge has been generated for Japan by the development of simple multiple regression models, which could be used to estimate annual BFI values and low flow indices in poorly gauged basins in Japan.

Table of Contents

Declaration **2**

Acknowledgments **3**

Abstract **4**

Preface **6**

Study Contribution **7**

List of Abbreviations and Acronyms **16**

Chapter 1 Introduction **19**

1.1 Background *19*

1.2 Study area and source data *20*

1.3 Research aim and objectives *21*

1.4 Thesis structure *22*

Chapter 2 Literature Review **24**

2.1 Introduction *24*

2.2 Baseflow and baseflow index *24*

2.3 Trend analysis *26*

2.4 Low flow index, $Q7_{10}$ *27*

2.5 Baseflow recession constant *28*

2.6 Regression analysis *29*

2.7 Summary *30*

Chapter 3 Methodology **31**

3.1 Introduction *31*

3.2 Study materials *31*

3.2.1 Data 31

3.2.2 Software 32

3.3 Study methods *33*

3.3.1 Baseflow separation and BFI quantification 33

3.3.2 Analysis of significant trends in annual and seasonal runoff and BFI 34

3.3.3 Determining the baseflow recession constant of the master recession curve 34

3.3.4 Regression modeling of BFI and low flow index, $Q7_{10}$ 35

3.4 Summary *37*

Chapter 4 Assessing Characteristics and Long-Term Trends in Runoff and BFI in Eastern Japan **38**

4.1 Introduction *38*
4.2 Paper (HRL) *39*
4.3 Supplementary material *67*
4.4 Summary *76*
Chapter 5 Estimation of Baseflow Recession Constant and Regression of Low Flow Indices in Eastern Japan **78**
5.1 Introduction *78*
5.2 Paper (HSJ) *79*
5.3 Summary *113*
Chapter 6 Results of Regression Modeling of BFI and $Q7_{10}$ analysis in Japan **114**
6.1 Introduction *114*
6.2 Results *121*
6.3 Discussion *129*
6.3.1 Regression models of the BFI_{ann} and the $Q7_{10}$ in all basins lumped together 129
6.3.2 Regression models of the BFI_{ann} and the $Q7_{10}$ in sedimentary lithology 129
6.3.3 Regression models of the BFI_{ann} and the $Q7_{10}$ in igneous lithology 130
6.4 Summary *131*
Chapter 7 Discussion, Recommendations and Conclusion **142**
7.1 Introduction *142*
7.2 Discussion *143*
7.2.1 Restatement of aim and Objectives 143
7.2.2 Achievement of the study objectives 143
7.2.3 Strengths 145
7.2.4 Limitations 146
7.2.5 Study contribution 147
7.2.6 Filling of the study knowledge gaps 147
7.2.7 Impact of the study 149
7.3 Recommendations *149*
7.3.1 Specific recommendations 150
7.4 Conclusion *150*
References **152**
Appendix A Spreadsheet Procedure to Determine the Master Recession Curve (Modified from Veremu, 2009) for Chapter 5 ..... **160**
Appendix B Determination of Annual BFI Values by the BFI Programme **165**
Appendix C Determination of $Q7_{10}$ Flow Index **166**

List of Figures

Figure 1. Flow diagram of thesis structure outlining chapters. 23

Figure 2. Location map showing gauges (MLIT), streams, and the digital elevation model (DEM), which was processed in ArcGIS 10.5. The DEM was sourced freely online from the ALOS World 3D 30-meter (AW3D30) DEM database (Japan Aerospace Exploration Agency, 2021). 43

Figure 3. Relative frequency histograms for the sample of 26 basins showing the distribution of BFI in the case of (a) annual period, (b) spring season (March-May), (c) summer season (June-August), (d) autumn season (September-November), and (e) winter season (December-February).....47

Figure 4. Box charts representing fundamental BFI from summary statistics for (a) annual period (yellow colour), (b) spring season (cyan colour), (c) summer season (green colour), (d) autumn season (red colour), and (e) winter season (grey colour) for 26 gauges (on horizontal axis) with periods of record ranging from 29 to 67 years. 49

Figure 5. Monthly BFI, precipitation, and runoff for six gauges and Automated Meteorological Data Acquisition System (AMeDAS) stations for (a) Kamiiwakibashi (Hirosaki AMeDAS), (b) Nitadori (Ninohe AMe3D), (c) Nakamura (Oisawa AMeDAS), (d) Imodabashi (Koma AMeDAS), (e) Uonogawa-Horinouchi (Koide AMeDAS) and (f) Ochiai (Ohira AMeDAS). Figures. 5a, c, and e show watersheds located in the Japan Sea region, while Figures 5b, d, and e show watersheds located in the Pacific Ocean region. 51

Figure 6. Location map of the 29 study basins in Eastern Japan, showing the major river systems and their catchment boundaries. 87

Figure 7. Examples of average daily runoff over the period of record in two contrasting basin areas. Arasawa is located near the Japan Sea experiencing high precipitation year round with deep snowpack (December to May), while Shimokubo is located near the Pacific coast with dry winters and little snowpack.....88
Figure 8. Examples of master recession curves for; (a) Yagisawa (basin 11), where the slope of common limb, λ, is -0.0407 based on a minimum recession period of 12 days and the extraction of 15 recession limbs, and (b) Higashiyama (basin 18), where the slope of common limb, λ, is -0.0206 based on a minimum recession period of 14 days and the extraction of 19 recession limbs (Table 9). 89
Figure 9. Example of flow duration curve, reading the runoff value at 97 percent on the time axis (Yagisawa basin for water year 1994). 96
Figure 10. Relative frequency histograms showing the distribution of values of the recession constant (λ) in the case of (a) sedimentary basins, (b) igneous basins, and (c) all basins. 98
Figure 11. Relationship between $Q97_{10}$ and $Q7_{10}$ for the 29 study basins. 101
Figure 12. Location map of the study basins used for regression analysis. 115
Figure 13. Correlation heatmap showing the correlation coefficients of variables.....124
Figure 14. Comparison of observed values and values predicted by BFI_{ann} models (a), (c) and (e), and $Q7_{10}$ models (b), (d) and (f). 141

List of Tables

Table 1. Overview of the data sets used in the thesis study. 32
Table 2. Classification and criteria for assessing the performance of the hydrological model (Cameron and Windmeijer, 1997). 36

Table 3. List of gauging stations used in the analysis for periods of record ranging from 29 to 67 years, including mean annual runoff (MAR) and mean annual precipitation (MAP). 44

Table 4. The Sen's slope of annual and seasonal average runoff per decade for individual gauges (refer to Table 3 for the periods of record). 53

Table 5. The Sen's slope of annual and seasonal average BFI per decade for individual gauges (refer to Table 1 for the periods of record). 55

Table 6. Mann-Kendall trend test results for average annual and seasonal runoff for the 26 gauges with periods of records ranging from 29 to 67 years. 75

Table 7. Mann-Kendall trend test results for average annual and seasonal BFI for the 26 gauges with periods of records ranging from 29 to 67 years. 76

Table 8. Characteristics and locations of the study basins. Period of record is 24 years (1993-2017), except for Ishibuchi (1993-2012), Okumiomote (2003-2017), Misogawa (1997-2017), Shiokawa (1999-2017), and Takiya (2001-2018). 91

Table 9. Low flow indices and characteristics of the master recession curves analyzed for the study basins. 92

Table 10. Sensitivity to minimum recession period and the associated number of recession limbs in the determination of the recession constant (λ) using a random sample of eight basins. 93

Table 11. Sensitivity to period of averaging for the ratio of flow (Q_{n+1}/Q_n) in the determination of the recession constant (λ) for the same random sample of eight basins given in Table 10. 97

Table 12. Regression models developed in the case of predicting $Q7_{10}$ from the recession constant and mean annual precipitation. Units: recession constant, λ (d^{-1}), mean annual precipitation, P (m). Equation coefficients rounded to 4 significant figures.....103
Table 13. Regression models developed in the case of predicting $Q97_{10}$ from the recession constant and mean annual precipitation. Units: recession constant, λ (d^{-1}), mean annual precipitation, P (m). Equation coefficients rounded to 4 significant figures.....103
Table 14. Regression models developed in the case of predicting $Q7_{10}$ from the recession constant and mean annual runoff. Units: recession constant, λ (d^{-1}), mean annual runoff, Q (m). Equation coefficients rounded to 4 significant figures. 104
Table 15. Regression models developed in the case of predicting $Q97_{10}$ from the recession constant and mean annual runoff. Units: recession constant, λ (d^{-1}), mean annual runoff, Q (m). Equation coefficients rounded to 4 significant figures. 104
Table 16. Sensitivity of recession constant to estimation with limited data. Random subsets taken from limbs extracted for Kusaki (basin 8, mean annual runoff 1464 mm, standard deviation 303 mm), Yokokawa (basin 25, mean annual runoff 1389 mm, standard deviation 362 mm), and Miwa (basin 26, mean annual runoff 1318 mm, standard deviation 247 mm) using a minimum recession period of 12 days (total period of record (POR) is 24 years). 108
Table 17. Characteristics and location of study basins. The period of record of the streamflow is 26 years (1993-2019). 116
Table 18. Mean annual precipitation (MAP) and locations of AMeDAS stations which are placed at heights ranged between 2 m and 1465 m above sea level (a.s.l.).....119
Table 19. Watershed characteristics and flow indices for multiple regression modeling. 121

Table 20. Values of watershed characteristics used for Spearman's correlation. 122

Table 21. Regression models developed. 125

Table 22. Analysis of variance of annual BFI and $Q7_{10}$ models. 125

Table 23. Coefficients of determination of annual BFI and $Q7_{10}$ models according to dominant lithology.....126

Table 24. Regression coefficients of annual BFI and $Q7_{10}$ models. 127

Table 25. Variance inflation factor (VIF) and Durbin Watson (DW) statistics of models. 128

Table 26. Normality test (Shapiro-wilk) of the models.....128

Table 27. Relative error values for all basins. 134

Table 28. Relative error values for basins classified into sedimentary lithology. 137

Table 29. Relative error values for basins classified into igneous lithology. 139

List of Equations

Equation 1. Baseflow separation equation 33

Equation 2. Baseflow index equation 34

Equation 3. Multiple linear equation 35

Equation 4. Log transformation equation of multiple regression 35

Equation 5. Additive multiple regression equation 35

Equation 6. Relative error equation 36

Equation 7. R-squared equation.....36

Equations 8-14. Mann-Kendall test equations.....71

Equation 15. Mass balance equation 84

Equation 16. The recession constant limb equation 85

Equation 17. Weibull plotting formula.....93

Equation 18. Multiple regression equation.....100

Equation 19. Formula to determine the number of ranked values of Q_{n+1}/Q_n to estimate the recession constant 107

List of Abbreviations and Acronyms

AMeDAS	Automated Meteorological Data Acquisition System
BFI	Baseflow Index
CV	Coefficient of Variation
DEM	Digital Elevation Model
DW	Durban Watson Statistic
FDC	Flow Duration Curve
FFPRI	Forestry and Forest Products Research Institute
GIS	Geographic Information System
GSJ	Geological Survey of Japan
H_0	Null Hypothesis
H_1	Alternative Hypothesis
H_A	Alternative Hypothesis
HOST	Hydrology of Soil Types
HRL	Hydrological Research Letters
HSJ	Hydrological Sciences Journal
HYSEP	Computer Program for Streamflow Hydrograph Separation and Analysis
IPCC	Intergovernmental Panel on Climate Change
JEES	Japan Educational Exchanges and Services
JHYDROL	Journal of Hydrology
JICA	Japan International Cooperation Agency
JMA	Japan Meteorological Agency
Km^2	Kilometers Squared
M	Meters

m.a.s.l.	Meters Above Sea Level
MAP	Mean Annual Precipitation
MAR	Mean Annual Runoff
MERIT	Multi-Error-Removed Improved-Terrain
MEXT	Ministry of Education, Culture, Sports, Science and Technology
MK	Mann-Kendall
MLIT	Ministry of Lands, Infrastructure, Tourism and Transport
MRC	Master Recession Curve
MS	Microsoft
OLS	Ordinary Least Square
Q_0	Initial Discharge
Q7	7-day Average Minimum Flow
$Q7_{10}$	Seven-day 10-year Low Flow
Q95	Flow Exceeded 95% of the Time
Q97	Flow Exceeded 97% of the Time
$Q97_{10}$	10-year Low Flow Exceeded 97 % of the Time
R^2	R-squared
RE	Relative Error
S1	Supplementary Material Number One
SDGs	Sustainable Development Goals
SO	Study Objective
TBC	To Be Confirmed
UKIH	United Kingdom Institute of Hydrology
UN	United Nations

UNESCO	United Nations Educational, Scientific and Cultural Organization
VIF	Variance Inflation Factor
W	Shapiro–Wilk Test Statistic
WIS	Water Information System
WMO	World Meteorological Organization
<	Less than
>	Greater than
%	Percent

Chapter 1 Introduction

1.1 Background

Baseflow is the portion of streamflow resulting from slow-moving subsurface pathways. The baseflow index (BFI) is a proportion of baseflow to total streamflow. The $Q7_{10}$ low flow index is a 10-year low flow of the seven-day average flow for annual minimum flow. The baseflow recession constant is defined as the slope of streamflow decline on the master recession curve (MRC), an envelope to all recession limbs. The baseflow recession constant is commonly expressed as an exponential function. The baseflow, indices of baseflow and low flow, and baseflow recession constants are essential in evaluating low flow hydrology, water supply, water quality, and water resources planning in watersheds (Hall, 1968, Smakhtin, 2001, Tallaksen, 1995).

Trend analysis is the mathematical technique of collecting information and spotting patterns or trends in the data (Meals et al., 2011). Trend analysis can reveal the response of annual and seasonal runoff and BFI to climate change, thereby aiding policymakers in acquiring needful information on the influences of the changing climate and human activities to manage water resources sustainably. A regression model is an equation that expresses the linkage between dependent variables and independent variables (Smakhtin, 2001). Regression analysis provides a convenient approach to estimating baseflow recession constant, BFI, and low flow index in ungauged and poorly gauged watersheds. This study theme aligns with the UN-Water and Sustainable Development Goals (SDGs) and especially targets of the goal 6 (UN-Water, 2015).

1.2 Study area and source data

The thesis covers a study area located in Japan with the geographic coordinates between 35° N, 136° E and 41° N, 142° E. The elevation of the watersheds ranges from -4 m to 3092 m above sea level. Specific details about the study area are found in respective thesis chapters 4, 5 and 6.

Flow regulations or flow diversions upstream of the stream gauge, greatly affect the streamflow measurements in Japan. The stream gauges for watersheds upstream of reservoirs were used for study without flow regulation or diversion structures in the headwaters. Hydrological flow data for dam basins in Japan, are easily obtained online (www.mudam.nilim.go.jp). The data contain daily series of reservoir water levels, the water gauged at the dam, and reservoir inflows which are determined by means of the mathematical expression of mass balance: Inflow = Outflow discharge ± Difference in storage.

Difference in storage is measured from the relationship determined between water level and storage as it is estimated through the surveying. For analysis, the estimated reservoir inflows were used to represent the unregulated natural discharge from a source of the stream. The climate and hydrological regimes are highly variable across Japan, with areas on the Japan Sea side facing substantial snowfall and summer precipitation. In contrast, the Pacific Ocean side has dry winters and a more significant impact from typhoons. The hydrological year runs from the beginning of October to the end of September. The dominant lithology of each watershed was estimated to be either igneous or sedimentary with confirmation on the Seamless Digital Geological Map of Japan (1:200,000) as available on website (https://gbank.gsj.jp/seamless/v2/viewer/?lang=en).

Trend analysis required us to select stream gauges which had the following factors: (1) those limited to upstreams without dams or flow regulations, such as Nakamura and Shirakawa-Hirokawara in Mogami River system and (2) regional scale basins that contain many dams or flow regulations such as Uonogawa-Horinouchi and Shinano-Ojiya gauges in Shinano River system. Twenty-six stream gauges with daily data were obtained from the Ministry of Land, Infrastructure, Transport and Tourism (MLIT) database, available at http://www1.river.go.jp/. The period of record for daily streamflow data averaged 45.8 years (29-67 years). The precipitation data were sourced from Automated Meteorological Data Acquisition System (AMeDAS) stations (https://www.jma.go.jp/jma/indexe.html) near the gauges. The average annual precipitation (1991-2020) for the study region was 1718 mm, ranging between 1034 mm and 3052 mm, with the highest values appearing for basins on the Sea of Japan side. In addition, long-term temperature and snowfall measurements were obtained from Tokamachi Forestry and Forest Products Research Institute (FFPRI).

1.3 Research aim and objectives

The study aimed to build a regression model to estimate BFI, baseflow recession constant, and low flow index using watershed characteristics that would allow the determination and characterization of BFI and low flow indices in ungauged or poorly gauged basins in Japan. The main aim was achieved through the following specific study objectives:

① to characterize the distribution and variability of annual and seasonal BFI

② to identify annual and seasonal trends in runoff and BFI across a range of watersheds in eastern Japan.

③ (a) to explore and evaluate realistic regression model that can be used to appropriately used for estimating $Q7_{10}$ and $Q97_{10}$ by means of the recession constant (λ) of MRC combined with other catchment or climatic characteristics.

(b) to develop regression models that can be used to estimate annual BFI and $Q7_{10}$ based on watershed characteristics such as mean annual runoff (Q) and elevation.

The study has important implications for providing critical new insights into the behavior of BFI in watersheds to support sustainable water resources management in Japan. The study outputs have the potential to form the basis for decision-making in water management under a changing climate.

1.4 Thesis structure

Following this introductory chapter, the thesis contains six chapters, as described below. A flow diagram of the thesis is provided in Figure 1.

- Chapter 2 presents a general overview of the study topic and the context of the overall study. It also identifies knowledge gaps in the literature
- Chapter 3 provides a synopsis of the study methodology, which was designed and adopted to address the study objectives
- Chapter 4 is the 1st of the results chapters and presents assessing characteristics and long-term trends in runoff and BFI in eastern Japan (HRL paper)
- Chapter 5 is the 2nd of the results chapters and shows how to estimate baseflow recession constant using the proposed matching strip method and regression analysis of low flow indices in eastern Japan (HSJ paper)
- Chapter 6 is the 3rd of the results chapters and expands the study basins from 29 to 67 basins. The sixty-seven dam basins show the application of the study

approach provided in Chapter 5 on regional-scale basins that are more widely distributed across eastern Japan (regression analysis results).

- Chapter 7 provides a discussion of the results chapters in the context of the aim of the study. It discusses the study achievements, strengths, and limitations. It also contains recommendations for future work and ends with a short conclusion.

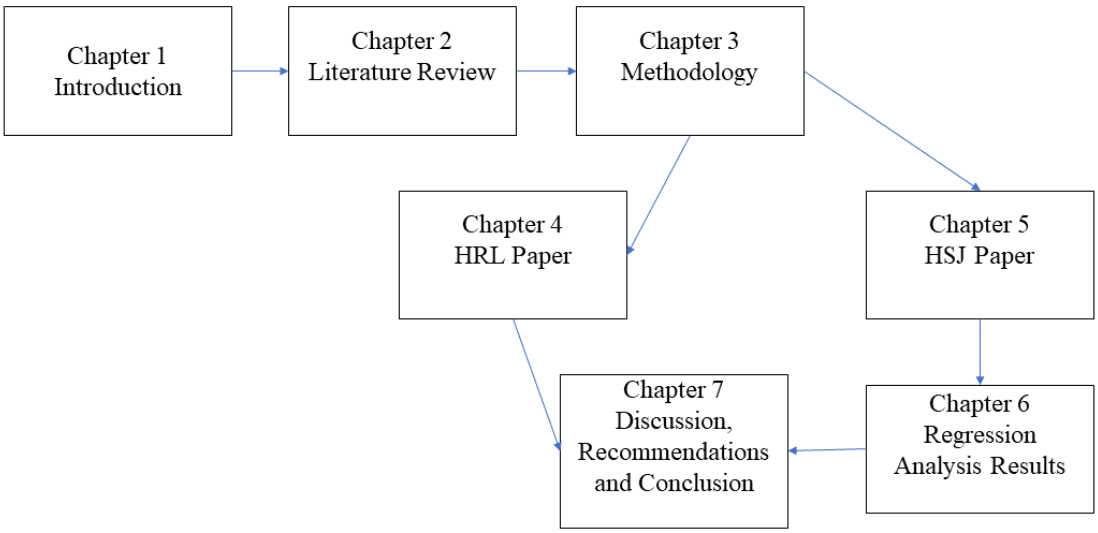

Figure 1.Flow diagram of thesis structure outlining chapters.

Chapter 2 Literature Review

2.1 Introduction

Chapter 1 presented a brief background to the study problem, which this thesis aims to solve together with the study aim and objectives. It also gives an outline of the study area in Japan. The results chapters of this thesis are structured as a sequence of articles for publication in peer-review journals, as mentioned in the thesis preface. A single research article has a detailed literature review within the introduction section per the publication format. This chapter, thus, presents a general synopsis of the study theme and context of the overall study. It also shows the study gaps in the literature for Japan and worldwide.

2.2 Baseflow and baseflow index

Baseflow is a substantial genetic portion of streamflow, originating from groundwater storage or other delayed sources such as shallow subsurface storage, lakes, melting snow, or ice (Smakhtin, 2001). Baseflow results from the partitioning of the whole streamflow hydrograph by many separation techniques of baseflow. We can find assessments of these techniques in many types of research (Aksoy et al., 2008, 2009, Eckhardt, 2005). Most of these methods focus on baseflow separation from a flood hydrograph and are directed to calculating the overland flow portion of a flood (Smakhtin, 2001). There are two main groups of separation methods: (1) those that presume that baseflow reacts to a storm event alongside overland flow and (2) those that account for the delaying effects of bank storage. The quantifiable characteristics of these techniques are, to some extent, subjective, primarily because of the challenges associated with estimating the timing and rate of baseflow rise and identifying the point on a storm hydrograph at which overland flow is presumed to cease. The baseflow proportion sustains the streamflow during the

year's dry season (Smakhtin, 2001). Specialists and experts in the study used numerous other methods to separate the streamflow into its basic components (Brodie et al., 2005).

Other techniques separate baseflow from hydrographs for a long-term period of record, usually using a particular type of digital filter which partitions daily streamflow time series into overland flow and baseflow (Nathan and McMahon, 1990). The physically based algorithm for baseflow separation was digitized and standardized by the United States Geological Survey and then computerized by Sloto et al. (1996). The 'smoothed minima' method (Institute of Hydrology, 1980) and 'recursive digital filter' (Nathan and McMahon, 1990) are the most well-known techniques of baseflow separation. The 'smoothed minima' method was analyzed and reviewed (Piggott et al., 2005) and proved to be as efficient as other methods in baseflow separation. Furthermore, the 'smoothed minima' methods were filtered and reviewed to discover their practical aspects (Aksoy et al., 2009, 2008).

The Baseflow Index (BFI) is a result of dividing the baseflow volume by the total streamflow volume and is unitless. The Baseflow Index (BFI) is essential to low flow research as it indicates the geological impact on low flows (Smakhtin, 2001; Bloomfield et al., 2009a). BFI is, from time to time, also known as the 'reliability index' (Smakhtin, 2001). BFI may be calculated for each annual record or total record period (Gustard et al., 1992). Detailed literature reviewed distinguishing BFI values for numerous streams in other regions (Beck et al., 2013a). According to Price (2011) and Smakhtin (2001), an understanding of BFI and the baseflow regime is essential for the following reasons:

- advancement of watershed management policies (mainly for drought conditions)
- making links between aquatic organisms and their environmental assessment of small to medium water supplies, water quality, and salinity management and

- calculation of water budgets of lakes

The baseflow analysis closely relates to the streamflow recession characteristics analysis (Whitaker et al., 2022). Several written works across the globe have outlined studies on BFI (Singh et al., 2019; Zhang et al., 2019; Bosch et al., 2017; Hagedorn and Meadows, 2021; Arai et al., 2021; Yoshida and Troch, 2016; Beck et al., 2013; Kelly et al., 2019; Bloomfield et al., 2009). Further details on BFI studies can be found in Chapter 4. As far as I am aware, there are no investigations regarding long-term BFI values for watersheds in the large-scale region of eastern Japan.

Knowledge gap 1:

Therefore, there is a need to describe the distribution and variability of annual and seasonal BFI across a range of watersheds in eastern Japan. The results of this study will present critical innovative perceptions into the behavior of BFI in watersheds to support sustainable water resources management in Japan.

2.3 Trend analysis

Trend analysis refers to the method of gaining information and attempting to identify a pattern, or trend, in the data. In other words, trend analysis can be defined as a mathematical technique that uses past results to predict future outcomes. Trend analysis could be used to evaluate uncertain events in the past, even though trend analysis is mainly used to forecast future events. A trend in data is a persistent, long-term rise or fall, while a seasonal variation is a pattern in data that repeats itself at known regular intervals of time. Trends can happen in two ways: a slight change over time that is constantly happening in a direction (monotonic) or an abrupt shift at a specific point in time (step trend) (Meals et al., 2011).

Trend analysis has advantages and disadvantages for evaluating hydrometeorological data, depending on the specific situation. The benefits of simple trend analysis in the data are as follows: it can be done from a single gauging station, does not require a calibration period, applies to large receiving waterbodies that may be subject to many influences, and is helpful for best management plans that develop slowly or situations with long lag times. However, simple trend analysis has the following disadvantages: it usually requires long continuous data records, it is difficult to account for data variability solely related to land management changes, and it provides no insight into the causes of trends (Meals et al., 2011).

The trend analysis can suggest the response of annual and seasonal runoff and BFI to climate change, implying that policymakers need more information on the impacts of climate change and anthropogenic activities to manage water resources sustainably. To the best of my understanding, no study has explored long-term trends in runoff and BFI for watersheds in the large-scale region of eastern Japan.

Knowledge gap 2:

There is a need to identify annual and seasonal trends in runoff and BFI across a range of watersheds in eastern Japan.

2.4 Low flow index, $Q7_{10}$

Sugiyama et al. (2003) introduced the stochastic flow duration curve that was constructed by using the distribution characteristics of a set of probability graphs of streamflow estimated by the Weibull plotting equation at appropriate time intervals from zero to one hundred percent on the time axis. The flow duration curve (FDC) graphically shows the relationship between the exceedance probability of streamflow and its magnitude. It can be applied to assess the flow regimes and has provided helpful details for sustainable

integrated water resources management in the upstreams (Smakhtin, 2001). LeBoutillier and Waylen (1993) stochastically quantified low flow indices. Sadegh et al. (2016) used a mathematical expression of the flow duration curve for planning, designing, and managing water use systems and resources.

Researchers in hydrology have become curious about forecasting baseflow recession rate or recession constant to express estimates of a single low flow index, the $Q7_{10}$ or $Q97_{10}$ flow (Sugiyama, 1996; Tallaksen, 1995; Berhanu et al., 2015; Brandes et al., 2005; Caruso, 2000; Castiglioni et al., 2009; Rifai et al., 2000; Sugiyama et al., 2003).

Knowledge gap 3:

There is a need to build and assess realistic regression models that can appropriately be used to determine low flow indices using the recession constant (λ) and other catchment or climatic characteristics in Japan where there is less related literature.

2.5 Baseflow recession constant

The baseflow recession constant is the slope of streamflow decline on the master recession curve (MRC), commonly expressed as an exponential equation (Vogel and Kroll, 1996). MRC envelopes all recession limbs to indicate the common recession behavior of the catchments (Tallaksen, 1995). The baseflow recession constant is essential for low flow studies, including water supply, water quality, and water resources planning in watersheds (Hall, 1968; Tallaksen, 1995; Smakhtin, 2001). Chapter 5 contains a further literature review, including methods for determining the MRC and models to estimate baseflow recession characteristics (recession constant, base flow index) from several watershed characteristics.

2.6 Regression analysis

The regression model statistically expresses the relationship between dependent and independent variables (Smakhtin, 2001). Simple regression is a regression built by two variables, while multiple regression describes the relationship of more than two variables (Senocak and Tasci, 2022). Regression can be analyzed using statistical software packages such as OriginPro, XLSTAT, and MS Excel.

The regression analyses in various regions have been undertaken using statistical methods to associate BFI with catchment characteristics such as geology, land cover, and precipitation, along with others (Bloomfield et al., 2009a; Senocak and Tasci, 2022; Lyu et al., 2022). Past researchers have considerably conducted regression analyses to assess baseflow at ungauged and poorly basins in many parts of the world (Nathan and McMahon, 1992; Jolánkai and Koncsos, 2018; Ahiablame et al., 2013). Regression models associate BFI with river basin physical features in sites that have not been gauged. Many physical features of river basins are widely reported to affect baseflow and streamflow variations (Smakhtin, 2001; Stuckey, 2006; Price, 2011). Some of these catchment features include topography, relief, climate, precipitation, evapotranspiration, slope, basin drainage area, geologic and hydrogeologic variables, soil infiltration rate, baseflow factor, and land cover. Gustard et al. (1992) performed a regression analysis of low flow using 12 low flow Hydrology of Soil Types (HOST) to accurately predict the Q95 low flow indices at ungauged basins in the UK.

Knowledge gap 4:

There is a need to develop a regression model that can be appropriately used for estimating BFI by means of catchment or climatic characteristics in Japan. This regression model can be applied in ungauged and poorly gauged catchments.

2.7 Summary

This chapter presents a general outline of the study topic and the context of the overall study work. It expresses baseflow and baseflow index, trend analysis, low flow index, and regression analysis using characteristics of watersheds in Japan. It presents the importance of baseflow or BFI to water resources management sustainably. In line with the review, the key gaps in the study are as follows:

- Knowledge gap 1: The study needs to characterize annual and seasonal BFI distribution and variability across a range of watersheds in eastern Japan.
- Knowledge gap 2: There is a need to identify annual and seasonal trends in runoff and BFI across a range of watersheds in eastern Japan.
- Knowledge gap 3: There is a need to discover and assess accurate regression models that can be suitably used for quantifying low flow indices by means of the recession constant (λ) of the master recession curve (determined by using an easy-to-use technique for the matching strip method) collectively together with other basin or climatic characteristics in Japan.
- Knowledge gap 4: There is a need to develop a regression model that can efficiently and effectively quantify BFI using watershed or climatic characteristics in Japan.

The subsequent chapter provides the study method intended to realize the study objectives.

Chapter 3 Methodology

3.1 Introduction

The preceding chapter described quite a few knowledge gaps in the study. As stated in the preface, the thesis results chapters were structured as a collection of articles to be published in scholarly journals. Each article contains its own study materials and method section, as required in the publication. In this chapter, the study method for the thesis is described with the study materials and methods; however, in order to avoid a repeat, reference is made to the specific articles wherever suitable.

3.2 Study materials

3.2.1 Data

The study focused on collecting the existing data, and no field investigations were performed. The current data were collected for Japan on a regional scale, as described in the following sections. It included hydrometeorological data (precipitation, streamflow) and climate data such as long-term temperature. It also included geographical information system (GIS) files (streams, topographical maps, lithological maps, etc.). The data had been collected by ministries, departments, and agencies of the government of Japan (Table 1).

Table 1. Overview of the data sets used in the thesis study.

Characteristic	Source/description	Reference	Resolution
Streamflow	Water information system (WIS) of the Ministry of Land, Infrastructure, Transport and Tourism (MLIT)	http://www1.river.go.jp/	Daily
Mean annual runoff and basin area	Dam database of Japan	http://mudam.nilim.go.jp/	Daily
Digital elevation model (DEM)	Multi-Error-Removed Improved-Terrain DEM (MERIT DEM)	(Yamazaki et al., 2017)	90 m
	ALOS World 3D-30 Meter DEM	(Japan Aerospace Exploration Agency, 2021)	30 m
Long-term temperature and snowfall	Tokomachi Forestry and Forest Products Research Institute (FFPRI)	https://www2.ffpri.go.jp/labs/fwdb/sites/indexE.htm	Daily and seasonal
Mean annual precipitation	The Automated Meteorological Data Acquisition System (AMeDAS) stations run by Japan Meteorological Agency (JMA)	https://www.jma.go.jp/jma/en/Activities/amedas/amedas.html	Yearly
Lithology	Global lithological map (GLiM) v1.0	https://doi.org/10.1594/PANGAEA.788537	0.5°
	Geological Survey of Japan (GSJ)	https://gbank.gsj.jp/	Static

3.2.2 Software

The following software (programmes) were used throughout the thesis:

- BFI Programme for performing baseflow separation (Tallaksen and van Lanen, 2004)
- Microsoft Excel for data analysis, viewing, editing and data creation
- OriginPro for data analysis and graphing
- XLSTAT-Forecast for performing the Mann-Kendall test and Sen's slope estimation (https://www.xlstat.com/en/)
- ArcGIS/ArcMap for viewing, editing and geospatial data analysis

3.3 Study methods

3.3.1 Baseflow separation and BFI quantification

The BFI Programme was used to calculate the BFI (http://europeandroughtcentre.com/). It is an Excel-based tool developed by Martin Morawietz at the Department of Geosciences at the University of Oslo, Norway. It was originally prepared for the textbook; Hydrological Drought-Processes and Estimation Methods for Streamflow and Groundwater (Tallaksen and van Lanen, 2004). The BFI Programme is free to download on the European Drought Centre website http://europeandroughtcentre.com/. The BFI Programme carries out the filtering method called the 'smoothed minima procedure' (Institute of Hydrology, 1980). The 'smoothed minima' technique of baseflow separation (Institute of Hydrology, 1980) was used throughout this study. The technique gives a value that determines the low flow characteristics of a stream (Senocak and Tasci, 2022). The baseflow is separated from the total stream flow by using the daily time series of the streamflow. The streamflow data are partitioned into five groups, and the minimum value for each group is determined. If the minimum value is less than 0.9 for the group before and after the groups in question, this value is taken as the minimum turning point (Piggott et al., 2005). The mathematical expression of this baseflow separation technique is as follows:

$$0.9q_i < \min(q_i - 1, q_i + 1) \quad (1)$$

Where 0.9 is a factor or parameter used to estimate baseflow, q_i is the baseflow at (i) time. When the 'smoothed minima' technique is used in a dry stream, the condition $0.9q_i \leq \min$ ($q_i - 1$, $q_i + 1$) is satisfied. The BFI is estimated using Equation (2) is the base flow equation:

$$\text{BFI} = \frac{\text{Baseflow volume}}{\text{Total flow volume}} \quad (2)$$

3.3.2 Analysis of significant trends in annual and seasonal runoff and BFI

The Mann-Kendall (MK) trend test, a non-parametric test, was used to identify a trend in a series of BFI and runoff, even if there is a seasonal component in the series. The XLSTAT statistical software was used to perform the MK test. The MK test was first revealed by Mann (1945). This MK test was further researched by Kendall (1975) and improved by Hirsch et al. (1982), who allowed it to include a seasonality.

The MK test has the following hypotheses: (1) the null hypothesis (H_0) is that there is no trend in the data, and (2) the alternative hypothesis (H_A) is that there is a negative or positive trend. The MK is based on the calculation of Kendall's tau measure of the correlation between two samples, which is itself built on the ranks with samples. The calculations assume that the observations are autonomous. The XLSTAT was also used to perform Sen's slope (Sen, 1968) BFI and runoff series trends. Chapter 4 contains further details about analyzing of statistically significant trends in annual and seasonal runoff and BFI.

3.3.3 Determining the baseflow recession constant of the master recession curve

The mathematical expression that represents the part of recession limb during a long period without rain or snowmelt can be expressed exponentially by: $Q_t = Q_0 \exp(-\lambda t)$.

where *Qt* is the discharge at time *t*, Q_0 is the initial discharge and λ is the recession constant. The following listed below are the steps to be adhered to when determining the recession constant, you need to:

1. apply certain rules to objectively extract recession limbs from the streamflow record.
2. define a suitable recession limb that will depend to some extent on the study objectives.
3. carry out the smoothing of the streamflow data such as a 3-day moving average as in Vogel and Kroll (1992).
4. choose a method to fit the synthetic master recession curve to the extracted recession limbs.

Chapter 5 contains further information of the analysis of baseflow recession constants.

3.3.4 Regression modeling of BFI and low flow index, $Q7_{10}$

Multiple linear regression was used to develop equations for estimating annual BFI and $Q7_{10}$, which is the drought flow or minimum flow of streamflow which occurs for a consecutive 7-day period one time in 10 years. Multiple linear regression is expressed in the following Equation:

$$Q_b = k_0 X_1^{k_1} X_2^{k_2} X_3^{k_3} \ldots\ldots X_n^{k_n} \quad (3)$$

where, Qb is the predicted $Q7_{10}$ or annual BFI; k_0 is the regression constant; k_1, k_2, k_3, …, k_n are regression coefficients; X_1, X_2, X_3, …, X_n are watershed characteristics and ε is the term for error. The log-transformation of Equation (3) is written as:

$$\log(Q_b) = \log(k_0) + k_1\log(X_1) + k_2\log(X_2) + k_3\log(X_3) + \ldots.+ k_n\log(X_n) + \varepsilon \quad (4)$$

$$Y = b_o + b_1X_1 + b_2X_2 + b_3X_3 + \ldots.+ b_nX_n + \varepsilon_i \quad (5)$$

where, Y is the predicted value (dependent variable), X_i is the independent variable, ε_i is error and b_i are partial regression coefficients.

The models developed were evaluated using Relative Error (RE) and R^2 shown respectively, as indicated by Garg et al. (2003) and Krause et al. (2005):

$$RE = \frac{Q_{b(pred)}(i) - Q_{b(obs)}(i)}{Q_{b(obs)}(i)} \times 100 \quad (6)$$

$$R^2 = 1 - \frac{\sum_{i=1}^{n}\left[Q_{b(obs)}(i) - Q_{b(pred)}(i)\right]^2}{\sum_{i=1}^{n}\left[Q_{b(obs)}(i) - \overline{Q}_{b(obs)}(i)\right]^2} \times 100 \quad (7)$$

Where $Q_{b(obs)}(i)$ is the observed $Q7_{10}$ which was estimated by the best-fit line at the ten per cent probability value on the ordinate of a plot of Q7 against a non-exceedance probability or annual BFI which was quantified from the daily streamflow of entire period of record by the BFI Programme; $Q_{b(pred)}(i)$ is the predicted $Q7_{10}$ or BFI; $\overline{Q}_{(obs)}$ is the mean of $Q_{b(obs)}$, and n is the total number of observations. These statistical model performance indicators are commonly used to assess the performance of hydrologic and water quality models (Garg et al., 2003; Krause et al., 2005). Cameron and Windmeijer (1997) assessed and classified the performance of the hydrological model, as shown in the Table 2.

Table 2. Classification and criteria for assessing the performance of the hydrological model (Cameron and Windmeijer, 1997).

Statistical indicator	Range	Performance
$R^2 = 1 - \frac{\sum_{i=1}^{n}\left[Q_{b(obs)}(i) - Q_{b(pred)}(i)\right]^2}{\sum_{i=1}^{n}\left[Q_{b(obs)}(i) - \overline{Q}_{b(obs)}(i)\right]^2} \times 100$	0.85 to 1.00	Very good
	0.70 to 0.85	Good
	0.60 to 0.70	Satisfactory
	0.40 to 0.60	Acceptable
	R2 < 0.40	Unsatisfactory

The OriginPro and XLSTAT statistical analysis software and MS Excel were used for the analysis. After the independent variables were selected, regression models were built at a significance level (alpha or α) of 5% using the Model-Selection methods, the RSQUARE and Adjusted R^2 Selection (https://support.sas.com). The best models

with the highest R^2 and adjusted R^2 values of combined explanatory variables were selected (Ahiablame et al., 2013). Then, *p*-values of separate explanatory variables were examined for significance.

3.4 Summary

This chapter presented the study approach used in the thesis to achieve the aim of the study. The raw data were collected for the study area, which included streamflow, precipitation, digital elevation model (DEM) and geological maps. Additionally, ArcGIS 10.5 version was used to present the study area and spatially analyze GIS layers. The watershed characteristics gathered and determined for further analysis included the basin drainage area, annual runoff, BFI, low flow indices, annual precipitation, DEM and flow length.

The 'smoothed minima' method was used to separate baseflow from the total streamflow for each basin. The BFI Programme was used to implement baseflow separation and quantify BFI, as shown in Chapter 4. The Mann-Kendall test was used to detect statistically significant trends in annual and seasonal runoff and BFI, as shown in Chapter 4. Estimation of the baseflow recession constant using the matching strip method was demonstrated, and the baseflow recession constant was used as one of the predictors to estimate low flow indices ($Q97_{10}$ and $Q7_{10}$). In addition, as already mentioned, selected watershed characteristics were used as independent variables to build regression models for estimating annual BFI and $Q7_{10}$.

The next chapter assesses characteristics and long-term trends in runoff and BFI in eastern Japan.

Chapter 4 Assessing Characteristics and Long-Term Trends in Runoff and BFI in Eastern Japan

4.1 Introduction

The previous chapter showed the methods to accomplish the aim of the thesis. The methods revealed the baseflow separation and quantification of BFI implemented by the widely used BFI Programme (Tallaksen and van Lanen, 2004). Since the BFI is an essential variable for linking baseflow to watershed characteristics(Smakhtin, 2001; Price, 2011; Bloomfield et al., 2009a, 2011), it was also necessary for methods to include the analysis of statistically significant trends in annual and seasonal runoff and BFI in eastern Japan. Regression analysis which provides an easy alternative technique to estimate baseflow index and low flow indices, was explained.

As described in the methods, the 'smoothed minima' technique of baseflow separation was used throughout this thesis. The Mann-Kendall test (Mann, 1945a; Kendall, 1975) and Sen's slope estimator (Sen, 1968)were used to identify runoff and BFI trends and their rate of change per decade. This chapter provides an assessment of characteristics and long-term trends in runoff and BFI in eastern Japan. This study output was achieved through one study article published in the peer-review journal, Hydrological Research Letter (HRL), as follows:

Chapasa, S.N. and Whitaker, A.C., 2023. Assessing characteristics and long-term trends in runoff and baseflow index in eastern Japan. Hydrological Research Letters, 17(1), 1-8.

To link this article: https://doi.org/10.3178/hrl.17.1

This published article is presented in the following section, and the author's contributions were as follows: Conceptualization, S.N.C. and A.C.W.; Funding acquisition, A.C.W.; Formal analysis, S.N.C.; Methodology, S.N.C.; Resources, A.C.W.; Supervision, A.C.W.; Validation, S.N.C. and A.C.W.; Visualization, S.N.C.; Writing—original draft, S.N.C.; Writing—review & editing, S.N.C., and A.C.W.

4.2 Paper (HRL)

Assessing characteristics and long-term trends in runoff and baseflow index in eastern Japan

Stanley N. Chapasa[1*] and Andrew C. Whitaker[2]

[1]Graduate School of Science and Technology, Niigata University, Japan

[2]Faculty of Agriculture, Niigata University, Japan

*Correspondence to: Stanley Nungu Chapasa, Graduate School of Science and Technology, Niigata University, 8050 Ikarashi 2-no-cho, Nishi-ku, Niigata 950-2181, Japan. E-mail: snunguchapasa@gmail.com

Received: 30 September 2022; Accepted: 29 November 2022; Published: TBC

Abstract

Baseflow is the portion of streamflow derived from delayed subsurface pathways. The baseflow index (BFI) is a ratio of baseflow to total streamflow, and is an important hydrological variable when linking watershed characteristics to baseflow. The 'smoothed minima' procedure of baseflow separation was applied to streamflow data (29-67 years) from twenty-six gauges of watersheds in eastern Japan. The Mann-Kendall statistical test and Sen's slope estimator were used to identify trends and estimate the rate of change in annual and seasonal runoff and BFI per decade at 0.01 and 0.05 significance levels. To the best of our knowledge, this is the first study to investigate long-term trends in runoff and BFI for watersheds in the large-scale region of eastern Japan. Results showed significant trends in annual runoff and BFI, with a concentration of significant seasonal trends occurring in winter with five gauges showing trends in runoff and nine gauges showing trends in BFI. The results suggest that the response of annual and seasonal runoff and BFI to climate change can already be seen, which implies that policymakers need more information on the impacts of climate change and human activities to manage water resources sustainably.

Keywords: runoff; baseflow; climate change; baseflow index; trend analysis; eastern Japan

Introduction

Baseflow is defined as the slowly varying portion of the discharge originating from groundwater storage and other delayed sources such as connected lakes, wetlands, melting snow, temporary storage in the banks of the stream channel, and slow-moving interflow (Tallaksen, 1995; Hall, 1968). Baseflow is commonly expressed as the baseflow index (BFI), defined as the ratio of the long-term baseflow to the total river flow (Tallaksen and van Lanen, 2004). Baseflow varies spatially and temporally and can sustain streamflow during prolonged periods of dry weather (Bosch et al., 2017). Baseflow or BFI is influenced by several factors, including geology, topography, climatic season, and anthropogenic activities (Bloomfield et al., 2011; Carlier et al., 2018; Zhang et al., 2017). BFI is used as a catchment descriptor in low flow studies (Smakhtin, 2001) and as a proxy indicator of groundwater discharge to streams (Price, 2011). Long-term changes in BFI or baseflow can indicate the impacts of climate change and human activities on hydrological processes and streamflow variation (Saedi et al., 2022; Easterling et al., 2000), and understanding these variations in baseflow is crucial for sustainable water resources management (Bosch et al., 2017b). Information and attribution of these changes is fundamental for infrastructure design, water management strategies, and risk mitigation policies (Serinaldi and Kilsby, 2016).

BFI studies have been undertaken by many researchers across the globe, including a global assessment based on over 3000 watersheds (Beck et al., 2013b), national scale assessments in Malawi (Kelly et al., 2020), Great Britain (Bloomfield et al., 2021) and New Zealand (Singh et al., 2019), and regional studies such as in the Loess Plateau, China (Zhang et al., 2019), the Gulf Atlantic Coastal Plain, USA (Bosch et al., 2017b), and the Great Lakes region of Michigan, USA (Hagedorn and Meadows, 2021).

However, few studies have investigated BFI in Japan. Arai et al. (2021) proposed a method of using the BFI to improve the performance of an analytical probabilistic streamflow model in 57 basins throughout Japan, while Yoshida and Troch (2016) found a significant correlation between drainage density and BFI in volcanic catchments in north eastern Japan.

To the best of our knowledge, there have been no investigations regarding long-term trends in runoff and BFI for watersheds in the large-scale region of eastern Japan. Therefore, the objectives of this study are: (1) to characterize the distribution and variability of annual and seasonal BFI, and (2) to identify annual and seasonal trends in runoff and BFI across a range of watersheds in eastern Japan. The findings of this study provide critical new insights into the behavior of BFI in watersheds to support sustainable water resources management in Japan.

Study region and data

The gauging stations are located across the six prefectures of Aomori, Akita, Iwate, Yamagata, Miyagi, and Niigata in eastern Japan (Figure 2). According to Whitaker *et al*. (2022) and Whitaker and Yoshimura (2012), the climate and hydrological regimes vary significantly across this region. Areas on the Japan Sea side (Figure 2) experience some of the heaviest snowfalls in the world (e.g. maximum annual snowfall > 21 m for Tokamachi) as well as heavy summer precipitation, while the Pacific Ocean side (Figure 2) has very dry winters and a more significant influence from typhoons (late summer to autumn). The dominant geology of the study region is determined to be sedimentary with some individual catchments dominated by plutonic rocks or volcanic rocks

(https://gbank.gsj.jp/seamless/v2/viewer/?lang=en). Upstream areas of watersheds in the study region are covered with forests.

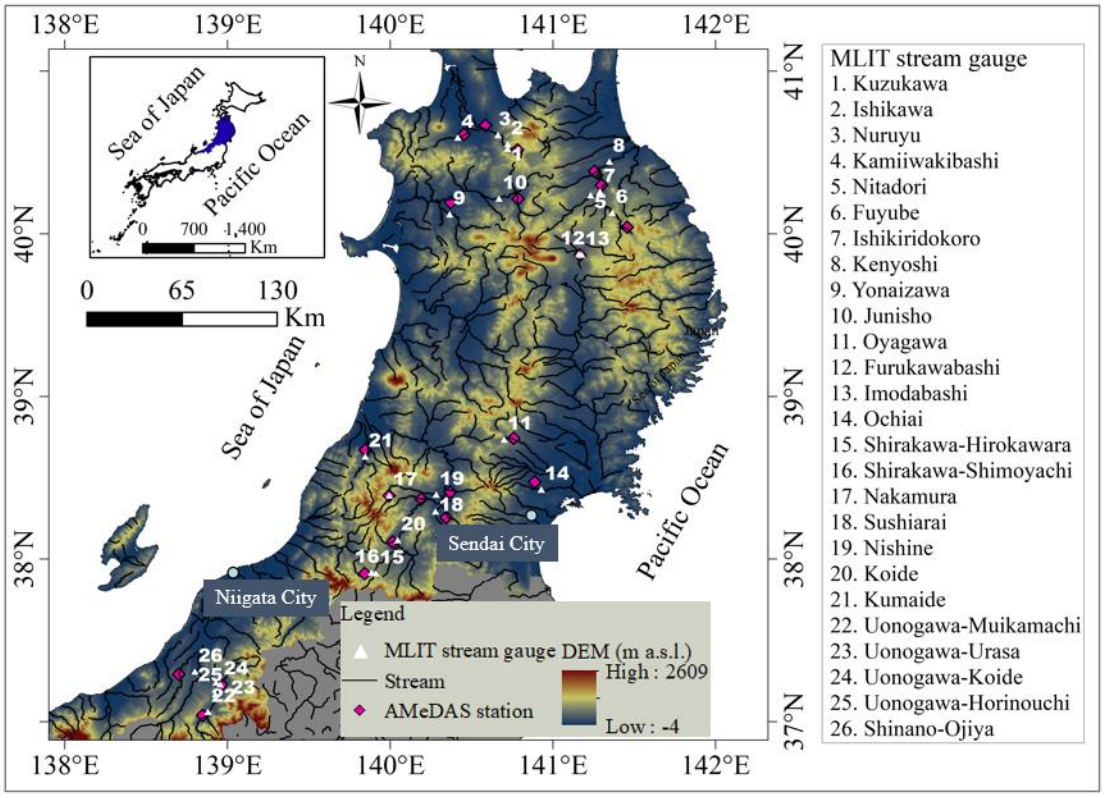

Figure 2. Location map showing gauges (MLIT), streams, and the digital elevation model (DEM), which was processed in ArcGIS 10.5. The DEM was sourced freely online from the ALOS World 3D 30-meter (AW3D30) DEM database (Japan Aerospace Exploration Agency, 2021).

Selected gauges included: (1) those limited to headwaters without dams or flow regulations (e.g. Nakamura and Shirakawa-Hirokawara in Mogami stream system) and (2) regional scale watersheds that include many dams or flow regulations (e.g. Uonogawa-Horinouchi and Shinano-Ojiya gauges in Shinano stream system) (Figure 2; Table 3). Streamflow records in Japan are widely affected by flow regulations or flow diversions upstream of the gauging point, which can significantly impact low flows (Whitaker et al., 2022). Twenty-six gauges with daily streamflow data were selected from

the Ministry of Land, Infrastructure, Transport and Tourism (MLIT) database, available at http://www1.river.go.jp/. The average period of record for daily streamflow data is 45.8 years (29-67 years), and the hydrological characteristics are summarised in Table 3. The precipitation data were taken from Automated Meteorological Data Acquisition System (AMeDAS) stations (https://www.jma.go.jp/jma/indexe.html), which were located close to the gauges. The average annual precipitation (1991-2020) is 1718 mm, ranging between 1034 mm and 3052 mm, with the largest values occurring for watersheds on the Japan Sea side (Figure 2; Table 3). Long-term temperature and snowfall data were obtained from Tokamachi Forestry and Forest Products Research Institute (FFPRI).

Table 3. List of gauging stations used in the analysis for periods of record ranging from 29 to 67 years, including mean annual runoff (MAR) and mean annual precipitation (MAP).

No	Stream system	Gauge name	Gauge id	Watershed area (km^2)	Elevation of gauge (m)	Latitude, Longitude (°)	Missing data (%)	Period of record	MAR (mm)	MAP (mm)
1	Iwaki	Kuzukawa	302071282222040	128*****	351	40.5239, 140.7231	0	1989-2017	2293	1744
2	Iwaki	Ishikawa	302071282201100	284	407	40.5519, 140.5467	0	1969-2017	1680	1744
3	Iwaki	Nuruyu	302071282222030	302	121	40.6075, 140.6636	2	1989-2017	2003	1060
4	Iwaki	Kamiiwakibashi	302071282201070	410	47	40.5919, 140.4167	0	1960-2017	1918	1255
5	Mabechi	Nitadori	302051282201070	402*****	168	40.2375, 141.2333	1	1985-2017	1260	1034
6	Mabechi	Fuyube	302051282201060	424*****	342	40.1303, 141.3653	6.7	1973-2017	731	1038
7	Mabechi	Ishikiridokoro	302051282201050	964	117	40.2594, 141.2906	5.2	1986-2017	1209	1034
8	Mabechi	Kenyoshi	302051282201040	1751	18	40.4444, 141.3481	0	1963-2017	867	1131
9	Yoneshiro	Yonaizawa	302082182211130	683.6	51	40.1208, 140.3664	3.4	1959-2017	2405	1603
10	Yoneshiro	Junisho	302082182211120	1167.4	89	40.2167, 140.6703	3.6	1962-2017	1562	1454
11	Kitakami	Oyagawa	302041282223030	58.24	184	38.7358, 140.7017	2.5	1974-2011	1842	1697
12	Kitakami	Furukawabashi	302041282220150	411*****	206	39.8742, 141.1608	7	1975-2017	1707	1179
13	Kitakami	Imodabashi	302041282220140	618*****	201	39.8722, 141.1781	14.3	1983-2017	641	1179
14	Naruse	Ochiai	302031282207150	197.2	10	38.4281, 140.9294	0	1974-2019	1028	1315
15	Mogami	Shirakawa-Hirokawara	302111282221020	59*****	391	37.9131, 139.9147	4.4	1980-2017	3182	1907
16	Mogami	Shirakawa-Shimoyachi	302041282207210	73.6*****	386	37.9181, 139.8861	1.5	1980-2017	4022	1907
17	Mogami	Nakamura	302111282221050	85.7*****	460	38.3919, 139.9961	2.4	1977-2017	5223	2719
18	Mogami	Sushiarai	302111282214180	422	97	38.2925, 140.2792	0	1960-2017	1172	1088
19	Mogami	Nishine	302111282214160	478	101	38.3969, 140.2836	0	1965-2019	2589	1088
20	Mogami	Koide	302111282214090	1350	195	38.1169, 140.0469	0	1953-2019	1749	1857
21	Akagawa	Kumaide	302121282215020	551.5	69	38.6306, 139.8478	2	1966-2015	3656	2412
22	Shinano	Uonogawa-Muikamachi	304031284403150	355*****	162	37.0617, 138.8814	1.3	1981-2019	3298	2266
23	Shinano	Uonogawa-Urasa	304031284403140	674	144	37.1697, 138.9272	0	1981-2019	3387	2635
24	Shinano	Uonogawa-Koide	304031284403130	879	130	37.2300, 138.9567	0	1981-2019	3293	2635
25	Shinano	Uonogawa-Horinouchi	304031284403110	1408	95	37.2419, 138.9311	0	1960-2019	3560	2635
26	Shinano	Shinano-Ojiya	304031284403070	9719	41	37.3086, 138.8008	0	1961-2020	1637	3052

***** asterisk indicates that no dam is visible. The confirmation of dam visibility is done through the website https://maps.gsi.go.jp/

Methods

Baseflow separation was necessary to analyse the streamflow and determine BFI. Baseflow separation methods include manually performed graphical methods (Lott and Stewart, 2016; Eckhardt, 2008) and computerized automatic filtering methods (Brodie et al., 2007). Various filtering methods are widely available, and implemented by computer programs (Eckhardt, 2005; Sun et al., 2021). Although subjectivity is involved in choosing an appropriate filtering method, the decisions of selecting a filtering method and implementation tool are commonly based on the study objectives (Kelly et al., 2019).

Our needs dictated that the baseflow separation program should be automated, freely available, easy to learn, and capable of selecting seasonal periods from the input data, all of which is possible with the BFI Programme (http://europeandroughtcentre.com/software/software-from-textbook-hydrological-drought-tallaksen-and-van-lanen-2004/). Kelly et al. (2019) suggested that the BFI Programme has advantages compared with other BFI tools in a comparative assessment of several implementation tools. Full details of baseflow separation and implementation can be found in the Text S1.

The Mann-Kendall (MK) test was used to identify statistically significant trends in the annual and seasonal runoff and BFI (Kendall, 1975; Mann, 1945b). The statistical software XLSTAT was used to apply the MK test (https://www.xlstat.com/en/). The test parameters were as follows: 'normal' MK test, 'exact *p*-value' method, 'ignore missing data,' and significance level of 5%. Theil-Sen's slope was used to estimate the slope of the monotonic trends (Sen, 1968). Analyses of Sen's slope were done using XLSTAT

with a 95 % confidence interval parameter setting. All calculations of Sen's slope were done separately for individual stream gauges. Further information can be found in the supplement (Text S1).

Results and discussion

Overall distribution of BFI

Figure 3 shows relative frequency histograms of BFI for all 26 gauges drawn with a class interval of 0.05, considering the annual period and the four seasons, namely spring (March-May), summer (June-August), autumn (September-November), and winter (December-February). For the annual period, two peak frequencies of BFI occurred in the range of 0.55-0.60 and 0.65-0.70, respectively. Minimum and maximum annual BFIs were 0.38 and 0.75, respectively. The average BFI for the annual period was 0.62, and the standard deviation was 0.08. Additionally, the coefficient of variation (CV) for the annual period was 12 % (Figure 3a).

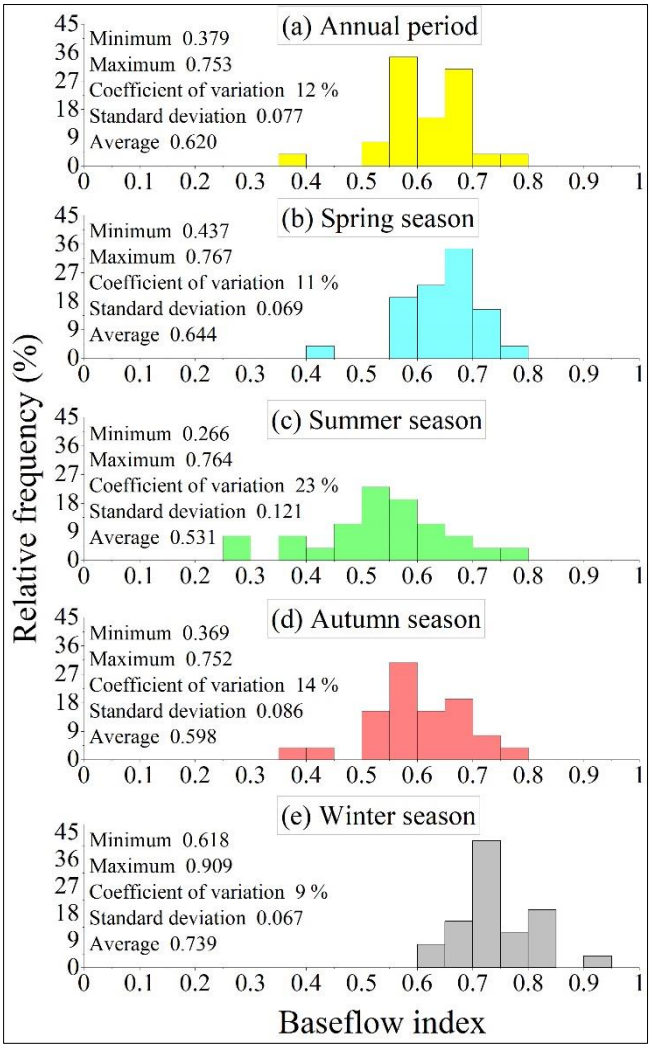

Figure 3. Relative frequency histograms for the sample of 26 basins showing the distribution of BFI in the case of (a) annual period, (b) spring season (March-May), (c) summer season (June-August), (d) autumn season (September-November), and (e) winter season (December-February).

Seasonally, the highest frequency distributions of BFI in Figures 3(b-e) occurred in ranges 0.65-0.70 (spring), 0.50-0.55 (summer), 0.55-0.60 (autumn) and 0.70-0.75 (winter). In winter, about 96 % of all BFIs occurred within the band 0.60-0.85 (Figure 3e). The minimum and maximum BFIs for each of the four seasons were 0.44 and 0.77 (spring), 0.27 and 0.76 (summer), 0.37 and 0.75 (autumn), and 0.62 and 0.91 (winter), respectively. The average BFI for each season was 0.64 (spring), 0.53 (summer), 0.60

(autumn) and 0.74 (winter). In addition, the standard deviations of seasonal BFI ranged between 0.12 (summer) and 0.07 (winter/spring). The CV of seasonal BFI ranged between 9 % for the winter and 23 % for the summer.

While our sample of gauges is relatively small, there is evidence in these histograms that the distribution of BFI changes with the seasons. Both the peak frequencies and the summary statistics reveal considerable variability between seasons. The CV for the annual period (12 %) was much lower than the CV for the summer (23 %). These differences in variability show the changing behavior of BFI with the seasons (Kelly et al., 2019). In the case of variations between annual and seasonal BFI, as seen in these results, it is vital to use the appropriate seasonal BFI, as an incorrect BFI could lead to inaccurate water resources assessments. For example, BFI is a hydrogeological parameter useful in modeling ungauged basins (Wahl and Wahl, 1995), which is believed to represent the effect of geology on basin low flow (Gustard et al., 1992; Bloomfield et al., 2009) (see Text S2).

Annual and seasonal BFI for each basin

The most remarkable result to emerge from the data (Figure 4) is that high BFIs with low variability were associated with the influence of large seasonal snowpacks (regional hydroclimatology). For example, Uonogawa and Shinanogawa basins showed high BFIs in spring due to consistent heavy snowmelt. However, there were also high BFIs for some basins which do not get such heavy snow, such as Yonaizawa in the Yoneshiro stream system (see Text S2).

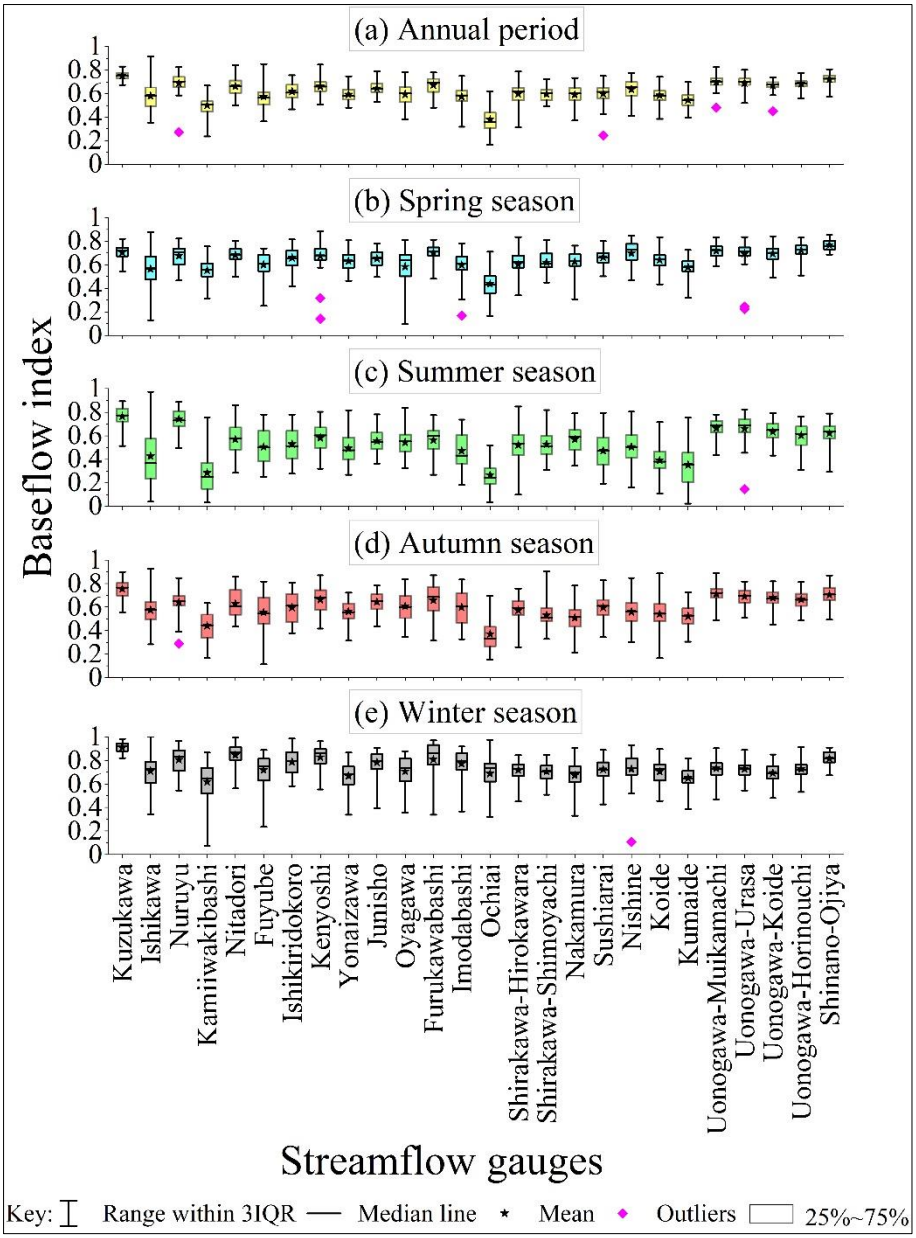

Figure 4. Box charts representing fundamental BFI from summary statistics for (a) annual period (yellow colour), (b) spring season (cyan colour), (c) summer season (green colour), (d) autumn season (red colour), and (e) winter season (grey colour) for 26 gauges (on horizontal axis) with periods of record ranging from 29 to 67 years.

Monthly BFI, runoff, and precipitation

Figure 5 shows the graphs of monthly values of BFI, precipitation, and runoff for six selected gauges, which represent the contrasting hydrometeorological conditions in the

Japan Sea and Pacific regions (see section Study Region and Data). The five gauges of Kamiiwakibashi (Figure 5a), Nitadori (Figure 5b), Nakamura (Figure 5c), Imodabashi (Figure 5d), and Uonogawa-Horinouchi (Figure 5e) show similar seasonal BFI patterns with two BFI peaks that occur in January and May. While for Ochiai (Figure 5f), a BFI peak was observed in January only. It is interesting to note that all six gauges showed low BFI in July. Similar seasonal runoff patterns are shown for Kamiiwakibashi (Figure 5a), Nitadori (Figure 5b), Nakamura (Figure 5c), Imodabashi (Figure 5d), and Uonogawa-Horinouchi (Figure 5e) with high monthly values observed in April. On the other hand, gauge Ochiai (Figure 5f) showed high monthly runoff in September. All gauges observed minimum runoff in February or June (Figure 5). The three gauges of Kamiiwakibashi (Figure 5a), Nakamura (Figure 5c), and Uonogawa-Horinouchi (Figure 5e), which are located in the Japan Sea region, show similar seasonal precipitation patterns with high monthly values occurring in December and July. On the contrary, the other three gauges of Nitadori (Figure 5b), Imodabashi (Figure 5d), and Ochiai (Figure 5f), which are located in the Pacific Ocean region, show different precipitation patterns with high monthly values occurring from July to October.

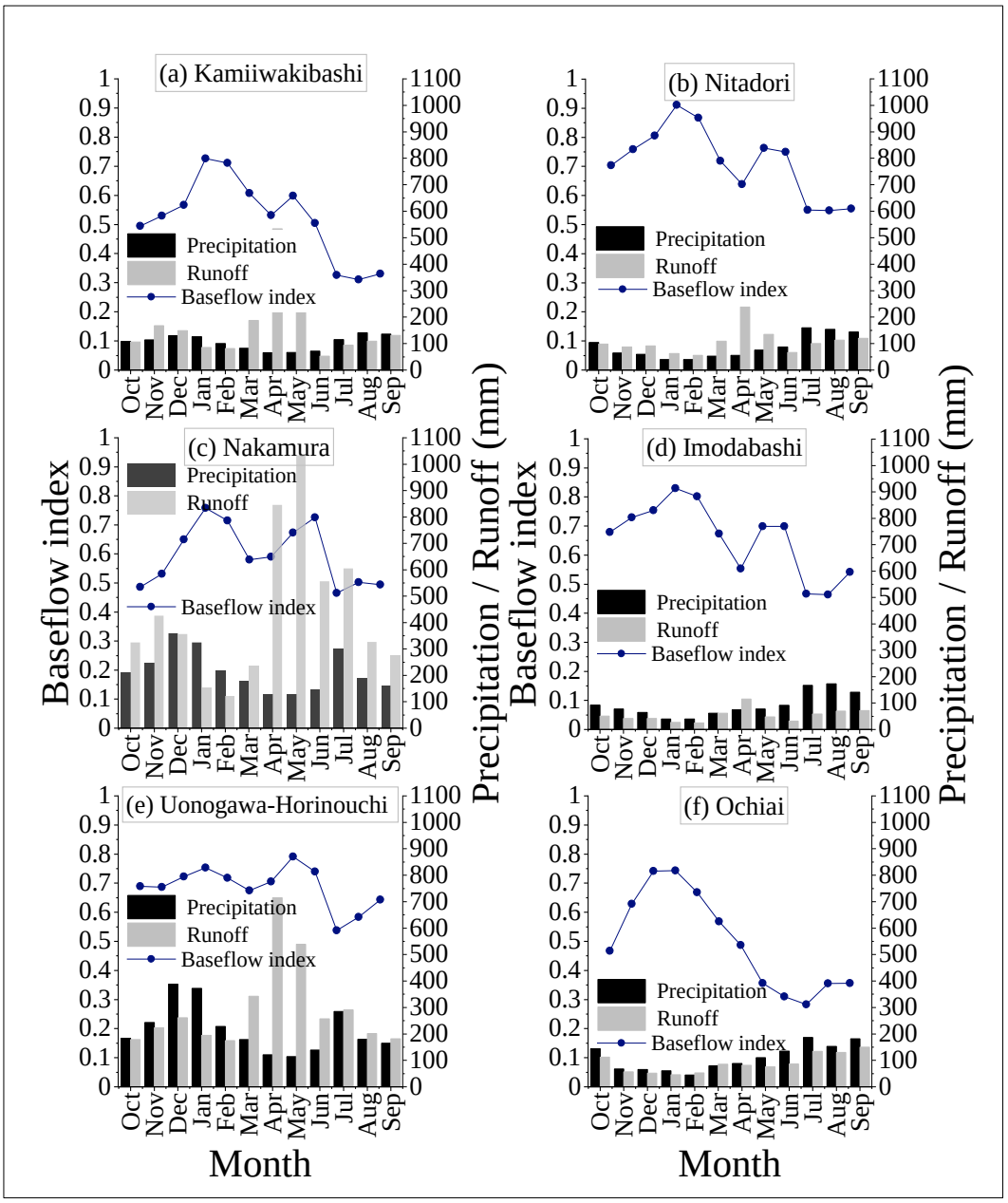

Figure 5. Monthly BFI, precipitation, and runoff for six gauges and Automated Meteorological Data Acquisition System (AMeDAS) stations for (a) Kamiiwakibashi (Hirosaki AMeDAS), (b) Nitadori (Ninohe AMe3D), (c) Nakamura (Oisawa AMeDAS), (d) Imodabashi (Koma AMeDAS), (e) Uonogawa-Horinouchi (Koide AMeDAS) and (f) Ochiai (Ohira AMeDAS). Figures. 5a, c, and e show watersheds located in the Japan Sea region, while Figures 5b, d, and e show watersheds located in the Pacific Ocean region.

The above results reveal seasonal patterns in BFI, and the peak BFI and monthly runoff suggest the influence of snowmelt season on runoff and baseflow (see Text S2).

Trends in annual and seasonal runoff

In order to identify statistically significant trends in both annual and seasonal runoff, we used the Mann-Kendall test and calculated Sen's slope per decade over the full period of record for each individual gauge (Tables 2 and 6). Seasonal trends, or both seasonal and annual trends, were significant in seven (27 %) of the 26 gauging records. For the annual period, the runoff showed a significant increasing trend in three (12 %) of the 26 gauges, while only one gauge showed a decreasing trend, and the rest (84 %) showed no trend. Significant increasing annual trends occurred in two basins in northeastern Tohoku, at Fuyube and Furukawabashi gauges in the Mabechi and Kitakami stream systems (Sen's slope of 60 mm decade^{-1} and 78 mm decade^{-1}, respectively). However, the neighbouring basins of Sushiarai and Nishine in the Mogami stream system in southern Tohoku showed contradicting positive and negative annual trends (Sen's slope of 69 mm decade^{-1} and -76 mm decade^{-1}, respectively). Each of these four basins showing significant annual runoff trends are important regional-scale catchments with basin areas exceeding 400 km^2.

Table 4. The Sen's slope of annual and seasonal average runoff per decade for individual gauges (refer to Table 3 for the periods of record).

No	Stream system	Gauge name	Mean runoff (mm yr^{-1})	Annual period	Spring season	Summer season	Autumn season	Winter season
				Sen's Slope (mm $decade^{-1}$)	Sen's Slope (mm $decade^{-1}$)	Sen's Slope (mm $decade^{-1}$)	Sen's Slope (mm $decade^{-1}$)	Sen's Slope (mm $decade^{-1}$)
1	Iwaki	Kuzukawa	2293	18.03	28.28	11.02	-23.06	-7.62
2	Iwaki	Ishikawa	1680	-59.11	32.03	-28.93	-27.25	-14.15
3	Iwaki	Nuruyu	2003	-46.00	-38.95	28.88	-10.84	-15.30
4	Iwaki	Kamiiwakibashi	1918	89.6	-15.30	-12.20	**29.49***	2.18
5	Mabechi	Nitadori	1260	25.87	34.73	6.44	4.94	-13.16
6	Mabechi	Fuyube	731	**59.63***	**24.01***	5.91	10.03	7.88
7	Mabechi	Ishikiridokoro	1209	4797	18.92	-15.30	29.41	22.21
8	Mabechi	Kenyoshi	867	23.74	1.26	5.82	12.51	2.55
9	Yoneshiro	Yonaizawa	2405	37.09	24.66	-9.69	9.42	-3.31
10	Yoneshiro	Junisho	1562	21.24	-3.25	1.66	9.81	2.06
11	Kitakami	Oyagawa	1842	-137.95	-30.67	-38.71	-16.35	-9.82
12	Kitakami	Furukawabashi	1707	**77.76****	**31.20****	25.44	13.75	**11.01***
13	Kitakami	Imodabashi	641	23.09	0.13	0.00	11.30	5.07
14	Naruse	Ochiai	1028	16.89	-2.81	-13.04	19.16	**10.92***
15	Mogami	Shirakawa-Hirokawara	3182	209.82	82.54	48.56	39.47	30.92
16	Mogami	Shirakawa-Shimoyachi	4022	-53.42	-15.13	25.34	-7.01	-4.21
17	Mogami	Nakamura	5223	-161.59	-83.95	-47.32	-45.45	-11.11
18	Mogami	Sushiarai	1172	**68.72****	**16.40***	**23.36****	**20.44****	**10.10***
19	Mogami	Nishine	2589	**-76.40***	**-53.02***	-07.51	-19.87	**15.57***
20	Mogami	Koide	1749	23.95	7.05	3.33	10.55	6.85
21	Akagawa	Kumaide	3656	-88.26	-30.56	-10.12	-24.49	-1.87
22	Shinano	Uonogawa-Muikamachi	3298	65.64	-30.94	4.62	16.10	2.33
23	Shinano	Uonogawa-Urasa	3387	-8.71	6.89	-29.04	-6.36	7.86
24	Shinano	Uonogawa-Koide	3293	79.54	30.61	6.52	7.75	24.70
25	Shinano	Uonogawa-Horinouchi	3560	-21.06	-33.41	-20.55	-0.03	**19.46****
26	Shinano	Shinano-Ojiya	1637	61.50	48.60	-10.53	23.99	14.57

***** indicates *p*-value <0.05, ****** indicates *p*-value <0.01 and significant Sen's slopes are highlighted in black bold

When we look at the seasonal runoff trends, we can see that, in all three basins where significant increasing annual trends were identified, there were also significant increasing trends in the spring season runoff (Sen's slope ranging from 16 mm $decade^{-1}$ for Sushiarai to 31 mm $decade^{-1}$ for Furukawabashi). On the other hand, the decreasing annual trend at Nishine was associated with a significant decreasing trend in spring runoff (Sen's slope -53 mm $decade^{-1}$), indicating the importance of spring runoff in contributing to annual runoff trends. Summer and autumn seasons exhibited the least number of significant trends (one basin and two basins, respectively). The greatest number of

significant trends in seasonal runoff were identified in the winter season (five basins or 19 % of the total), and in all cases the trends were positive (Sen's slope ranging from 10 mm decade^{-1} for Sushiarai to 19 mm decade^{-1} for Uonogawa-Horinouchi). In addition, winter temperatures with period of record 1918-2021 for Tokamachi in Shinano stream system showed a significant increasing trend (Sen's slope of 0.121 °C decade^{-1}). The basin of Sushiarai was notable in that significant trends in runoff (positive) were identified in the annual period, and in each of the four seasons.

With the progression of climate change and warming temperatures during the period of record analysed in this research (IPCC, 2021), we might expect to see certain patterns in the seasonal runoff trends due to changes in snowmelt (e.g. Yamanaka et al., 2012) and/or changes in precipitation amount or phase (e.g. Wakiyama and Yamanaka, 2014). Snowpack has been in decline across Japan in recent decades (e.g. Hara et al., 2008), and there is evidence that winter season precipitation phase is shifting to a decrease in the snow fraction with warming temperatures (Whitaker and Yoshimura, 2012). Text S2 contains further discussion.

Trends in annual and seasonal BFI

Table 5 and supplement Table 7 show the results of the Mann-Kendall test and Sen's slope for the annual and seasonal BFI. Annually, BFI showed significant increasing trends for three gauges (11.5 %), while twenty gauges (77 %) showed no significant trend, and three gauges (11.5 %) showed a significant decreasing trend. Significant positive Sen's slope occurred in a range between 0.023 decade^{-1} for Ochiai and 0.034 decade^{-1} for Ishikiridokoro, while significant negative Sen's slope occurred in a range between -0.052 decade^{-1} for Ishikawa and -0.007 decade^{-1} for Shinano-Ojiya.

Table 5. The Sen's slope of annual and seasonal average BFI per decade for individual gauges (refer to Table 1 for the periods of record).

No	Stream system	Gauge name	Annual period	Spring season	Summer season	Autumn season	Winter season
			Sen's slope decade^{-1}	Sen's slope decade^{-1}	Sen's slope decade^{-1}	Sen's slope decade^{-1}	Sen's slope decade^{-1}
1	Iwaki	Kuzukawa	-0.015	0.000	**-0.045***	-0.013	-0.014
2	Iwaki	Ishikawa	**-0.052****	**-0.049****	**-0.057***	**-0.057****	-0.008
3	Iwaki	Nuruyu	0.019	0.035	-0.008	0.031	-0.042
4	Iwaki	Kamiiwakibashi	0.003	-0.011	0.022	0.010	**0.033****
5	Mabechi	Nitadori	-0.031	-0.004	-0.036	**-0.042***	**-0.044****
6	Mabechi	Fuyube	-0.003	0.004	0.005	-0.013	-0.023
7	Mabechi	Ishikiridokoro	**0.034***	0.014	0.051	0.036	-0.022
8	Mabechi	Kenyoshi	-0.003	0.006	-0.005	-0.011	0.002
9	Yoneshiro	Yonaizawa	-0.006	0.006	-0.016	**-0.021****	-0.009
10	Yoneshiro	Junisho	0.006	0.011	0.010	-0.003	0.006
11	Kitakami	Oyagawa	0.000	-0.006	0.022	-0.029	-0.026
12	Kitakami	Furukawabashi	**-0.013***	-0.004	-0.023	**-0.032***	**-0.030****
13	Kitakami	Imodabashi	0.011	-0.011	0.008	0.020	0.014
14	Naruse	Ochiai	**0.023***	0.032	**0.033****	-0.016	0.008
15	Mogami	Shirakawa-Hirokawara	-0.009	-0.012	-0.011	-0.012	-0.019
16	Mogami	Shirakawa-Shimoyachi	-0.013	-0.012	-0.010	-0.005	0.013
17	Mogami	Nakamura	-0.012	-0.015	-0.011	-0.009	-0.009
18	Mogami	Sushiarai	0.009	**0.010***	**0.041****	-0.008	0.002
19	Mogami	Nishine	**0.021****	**0.029****	0.009	**0.026***	**0.018***
20	Mogami	Koide	0.001	0.003	**0.019***	-0.004	-0.001
21	Akagawa	Kumaide	-0.008	**-0.016***	-0.015	0.004	0.005
22	Shinano	Uonogawa-Muikamachi	-0.004	0.006	0.010	-0.010	**-0.041****
23	Shinano	Uonogawa-Urasa	0.009	**0.026****	-0.005	-0.003	**-0.032****
24	Shinano	Uonogawa-Koide	0.004	**0.025****	-0.004	-0.001	**-0.046****
25	Shinano	Uonogawa-Horinouchi	-0.003	0.002	0.002	-0.003	**-0.024****
26	Shinano	Shinano-Ojiya	**-0.007***	-0.005	0.011	**-0.020***	**-0.016****

***** indicates *p*-value < 0.05, ****** indicates *p*-value < 0.01 and significant Sen's slopes are highlighted in black bold

Considering seasonal BFI, the winter season showed the highest occurrence of significant trends with nine gauges (35 %), compared to six gauges (23 %) for both spring and autumn, and five gauges (19 %) for the summer season (Tables 5 and 7). It is notable that the majority of the significant trends for the winter season BFI are negative trends (*p*-value <0.01 in all cases), including all five gauges in the Shinano stream system (Sen's slope ranging from -0.016 decade^{-1} to -0.046 decade^{-1}), and one gauge in each of the Mabechi and Kitakami stream systems. The majority of the significant trends for the autumn season BFI are also negative, including gauges from the Iwaki, Mabechi,

Yoneshiro, Kitakami, and Shinano stream systems. In contrast, for the spring and summer seasons, the majority of significant trends for seasonal BFI are positive, with several examples in the Mogami and Shinano stream systems.

Aside from flow regulation due to dams and irrigation diversions, there are various possible explanations for the detection of either positive or negative trends in the annual and seasonal BFI. The detection of positive trends could be associated with increases in groundwater levels due to increased infiltration and groundwater recharge in the watersheds (Smakhtin, 2001; Price, 2011), despite the fact that Japan is experiencing decreasing trends for snowpack (Whitaker et al., 2008; Iwata et al., 2010). Positive trends in BFI could be caused by a decrease in rainfall intensity, which reduces overland flow to streams (Meriano et al., 2011; Penna et al., 2015), but this seems unlikely here as increasing trends in rainfall intensity have been reported for Japan (Yamada et al., 2020; Fujibe et al., 2005). The recovery of forest cover is more likely to have played a role in these positive BFI trends, because it is associated with high infiltration and recharge of basin subsurface storage (Troendle and King, 1985; Lins and Slack, 2005).

The detection of negative trends in annual and seasonal BFI could be associated with more surface runoff occurring from intense rainfall events, and/or shifts in the precipitation phase from snow to rain due to the impact of climate change (Hagedorn and Meadows, 2021). The significant negative trends in winter BFI for the Shinano stream system may be attributed to increases in air temperature, which reduces snow storage and snow water equivalent due to snow fraction sensitivity during the winter (Nedelcev and Jenicek, 2021). Importantly, these negative trends in winter BFI occur in combination with evidence of positive trends in winter runoff (Table 4), and positive trends in winter

temperature (e.g. Tokamachi showed significant trends (p-value <0.01) in temperature) which lends support to our hypothesis of decreasing snow fraction.

Meanwhile, the absence of significant trends in either annual or seasonal BFI is evident for nine gauges (35 % of total), indicating that runoff processes in these watersheds have remained stable with minimal impacts from human activities (Hagedorn and Meadows, 2021). In particular, there are three basins in the Mogami stream system (Shirakawa-Hirokawara, Shirakawa-Shimoyachi, and Nakamura) where no significant trends in BFI are evident. All three of these basins are located in snowy high-mountain headwater regions that are protected as part of the Bandai-Asahi National Park (see Text S2).

Conclusions

In this paper, we have presented BFI summary statistics and trends for runoff and BFI at the annual and seasonal time-scales, using the Mann-Kendall test and Sen's slope per decade over the full period of record for each of twenty-six stream gauges in eastern Japan. We showed that seasonal trends, or both seasonal and annual trends, were significant in seven gauges for runoff and seventeen gauges for BFI. Significant winter trends outnumbered other significant seasonal trends (spring, summer, and autumn trends) with five gauges showing trends in runoff and nine gauges showing trends in BFI. In addition, we found that BFI followed a non-normal distribution, which changed with the seasons. High BFIs with low variability were associated with winter and spring seasons, and regional hydroclimatic characteristics such as snowmelt. Our findings suggest that the influence of climate change on annual and seasonal runoff and BFI can already be seen, especially in watersheds with large snowpack such as the Shinano River

system. This implies that policymakers need more information on the impacts of climate change and human activities on hydrological processes to manage water resources sustainably. Future work should investigate how annual and seasonal BFI may respond to continuing changes in climate.

Acknowledgments

This study was supported by Niigata University and Mitsubishi Corporation through the Mitsubishi Corporation International Scholarship (JEES Sponsor-Crowned Scholarship). We thank Mr. Daichi Miyajima and the staff at the Faculty of Agriculture, Niigata University, for their cooperation.

Supplements

Text S1. Methods supplement

Text S2. Discussion supplement

Figure 4. Box charts representing fundamental BFI from summary statistics for (a) annual period (yellow colour), (b) spring season (cyan colour), (c) summer season (green colour), (d) autumn season (red colour), and (e) winter season (grey colour) for 26 gauges (on horizontal axis) with periods of record ranging from 29 to 67 years

Table 6. Mann-Kendall trend test results for average annual and seasonal runoff for the 26 gauges with periods of record ranging from 29 to 67 years

Table 7. Mann-Kendall trend test results for average annual and seasonal BFI for the 26 gauges with periods of record ranging from 29 to 67 years

References

Ahiablame, L., Chaubey, I., Engel, B., Cherkauer, K., and Merwade, V.: Estimation of annual baseflow at ungauged sites in Indiana USA, J Hydrol (Amst), 476, 13–27, https://doi.org/10.1016/j.jhydrol.2012.10.002, 2013.

Aksoy, H., Unal, N. E., and Pektas, A. O.: Smoothed minima baseflow separation tool for perennial and intermittent streams, Hydrol Process, 22, 4467–4476, https://doi.org/10.1002/hyp.7077, 2008.

Aksoy, H., Kurt, I., and Eris, E.: Filtered smoothed minima baseflow separation method, J Hydrol (Amst), 372, 94–101, https://doi.org/10.1016/j.jhydrol.2009.03.037, 2009.

Arai, R., Toyoda, Y., and Kazama, S.: Runoff recession features in an analytical probabilistic streamflow model, J Hydrol (Amst), 597, https://doi.org/10.1016/J.JHYDROL.2020.125745, 2021.

Beck, H. E., van Dijk, A. I. J. M., Miralles, D. G., de Jeu, R. A. M., Bruijnzeel, L. A., McVicar, T. R., and Schellekens, J.: Global patterns in base flow index and recession based on streamflow observations from 3394 catchments, Water Resour Res, 49, 7843–7863, https://doi.org/10.1002/2013WR013918, 2013a.

Beck, H. E., van Dijk, A. I. J. M., Miralles, D. G., de Jeu, R. A. M., Bruijnzeel, L. A., McVicar, T. R., and Schellekens, J.: Global patterns in base flow index and recession based on streamflow observations from 3394 catchments, Water Resour Res, 49, 7843–7863, https://doi.org/10.1002/2013WR013918, 2013b.

Berhanu, B., Seleshi, Y., Demisse, S. S., and Melesse, A. M.: Flow regime classification and hydrological characterization: A case study of Ethiopian rivers, Water (Switzerland), 7, 3149–3165, https://doi.org/10.3390/w7063149, 2015.

Bloomfield, J., Gong, M., Marchant, B., Coxon, G., and Addor, N.: How is Baseflow Index (BFI) impacted by water resource management practices?, Hydrology and Earth System Sciences Discussions, 1–34, https://doi.org/10.5194/hess-2021-259, 2021.

Bloomfield, J. P., Allen, D. J., and Griffiths, K. J.: Examining geological controls on baseflow index (BFI) using regression analysis: An illustration from the Thames Basin, UK, J Hydrol (Amst), 373, 164–176, https://doi.org/10.1016/j.jhydrol.2009.04.025, 2009a.

Bloomfield, J. P., Allen, D. J., and Griffiths, K. J.: Examining geological controls on baseflow index (BFI) using regression analysis: An illustration from the Thames Basin, UK, J Hydrol (Amst), 373, 164–176, https://doi.org/10.1016/j.jhydrol.2009.04.025, 2009b.

Bloomfield, J. P., Bricker, S. H., and Newell, A. J.: Some relationships between lithology, basin form and hydrology: a case study from the Thames basin, UK, Hydrol Process, 25, 2518–2530, https://doi.org/10.1002/hyp.8024, 2011.

Bosch, D. D., Arnold, J. G., Allen, P. G., Lim, K. J., and Park, Y. S.: Temporal variations in baseflow for the Little River experimental watershed in South Georgia, USA, J Hydrol Reg Stud, 10, 110–121, https://doi.org/10.1016/j.ejrh.2017.02.002, 2017a.

Bosch, D. D., Arnold, J. G., Allen, P. G., Lim, K. J., and Park, Y. S.: Temporal variations in baseflow for the Little River experimental watershed in South Georgia, USA, J Hydrol Reg Stud, 10, 110–121, https://doi.org/10.1016/j.ejrh.2017.02.002, 2017b.

Brandes, D., Hoffmann, J. G., and Mangarillo, J. T.: Base flow recession rates, low flows, and hydrologic features of small watersheds in Pennsylvania, USA, J Am Water Resour Assoc, 41, 1177–1186, https://doi.org/10.1111/j.1752-1688.2005.tb03792.x, 2005.

Brodie, R., Sundaram, B., and Hostetler, S.: Tools for assessing groundwater-surface water interactions: a case study in the Lower Richmond catchment, NSW, Canberra, 2005.

Brodie, R., Sundaram, B., Tottenham, R., Hostetler, S., and Ransley, T.: An overview of tools for assessing groundwater-surface water connectivity, Canberra, 133: 1-133 pp., 2007.

Cameron, A. C. and Windmeijer, F. A. G.: An R-squared measure of goodness of fit for some common nonlinear regression models, J Econom, 77, 329–342, https://doi.org/10.1016/s0304-4076(96)01818-0, 1997.

Carlier, C., Wirth, S. B., Cochand, F., Hunkeler, D., and Brunner, P.: Geology controls streamflow dynamics, J Hydrol (Amst), 566, 756–769, https://doi.org/10.1016/J.JHYDROL.2018.08.069, 2018.

Caruso, B. S.: Evaluation of low-flow frequency analysis methods, Journal of Hydrology (NZ), 19–47 pp., 2000.

Castiglioni, S., Castellarin, A., and Montanari, A.: Prediction of low-flow indices in ungauged basins through physiographical space-based interpolation, J Hydrol (Amst), 378, 272–280, https://doi.org/10.1016/j.jhydrol.2009.09.032, 2009.

Chiew, F. H. S. and McMahon, T. A.: Detection of trend or change in annual flow of Australian rivers, International Journal of Climatology, 13, 643–653, https://doi.org/10.1002/JOC.3370130605, 1993.

Douglas, E. M., Vogel, R. M., and Kroll, C. N.: Trends in floods and low flows in the United States: Impact of spatial correlation, J Hydrol (Amst), 240, 90–105, https://doi.org/10.1016/S0022-1694(00)00336-X, 2000.

Easterling, D. R., Karl, T. R., Gallo, K. P., Robinson, D. A., Trenberth, K. E., and Dai, A.: Observed climate variability and change of relevance to the biosphere Is the hydrologic cycle changing? Is the weather and climate becoming more extreme or variable?, JOURNAL OF GEOPHYSICAL RESEARCH, 101–121 pp., https://doi.org/10.1029/2000JD900166, 2000.

Eckhardt, K.: How to construct recursive digital filters for baseflow separation, Hydrol Process, 19, 507–515, https://doi.org/10.1002/HYP.5675, 2005.

Eckhardt, K.: A comparison of baseflow indices, which were calculated with seven different baseflow separation methods, J Hydrol (Amst), 352, 168–173, https://doi.org/10.1016/j.jhydrol.2008.01.005, 2008.

Fujibe, F., Yamazaki, N., Katsuyama, M., and Kobayashi, K.: The Increasing Trend of Intense precipitation in Japan Based on Four-hourly Data for a Hundred Years, SOLA, 1, 041–044, https://doi.org/10.2151/sola.2005-012, 2005.

Garg, V., Chaubey, I., and Haggard, B. E.: Impact of Calibration Watershed on Runoff Model Accuracy, Transactions of the American Society of Agricultural Engineers, 46, 1347–1353, https://doi.org/10.13031/2013.15445, 2003.

Gustard, A., Bullock, A., and Dixon, J. M.: Low flow estimation in the United Kingdom, Report No. 108, Crowmarsh Gifford, Wallingford, Oxfordshire, OXIO 8BB, United Kingdom, 1992.

Hagedorn, B. and Meadows, C.: Trend analyses of baseflow and BFI for undisturbed watersheds in Michigan-constraints from multi-objective optimization, Water (Switzerland), 13, https://doi.org/10.3390/w13040564, 2021.

Hall, F. R.: Base-Flow Recessions—A Review, Water Resour Res, 4, 973–983, https://doi.org/10.1029/WR004I005P00973, 1968.

Hara, M., Yoshikane, T., Kawase, H., and Kimura, F.: Estimation of the Impact of Global Warming on Snow Depth in Japan by the Pseudo-Global-Warming Method, Hydrological Research Letters, 2, 61–64, https://doi.org/10.3178/hrl.2.61, 2008.

Helsel, D. R., Hirsch, R. M., Ryberg, K. R., Archfield, S. A., and Gilroy, E. J.: Statistical Methods in Water Resources Techniques and Methods 4 – A3, USGS Techniques and Methods, Reston, VA, 458 pp., https://doi.org/10.3133/tm4a3, 2020.

Hirsch, R. M. and Slack, J. R.: A Nonparametric Trend Test for Seasonal Data With Serial Dependence, Water Resour Res, 20, 727–732, 1984.

Hirsch, R. M., Slack, J. R., and Smith, R. A.: Techniques of Trend Analysis for Monthly Water Quality Data, Water Resour Res, 18, 107–121, 1982.

Hodgkins, G. A. and Dudley, R. W.: Historical summer base flow and stormflow trends for New England rivers, Water Resour. Res, 47, 7528, https://doi.org/10.1029/2010WR009109, 2011.

Institute of Hydrology: Low Flows Studies Report No 3, Wallingford, UK, 1980.

IPCC: Summary for Policymakers. In: Climate Change 2021: The Physical Science Basis. Contribution of Working Group I to the Sixth Assessment Report of the Intergovernmental Panel on Climate Change, edited by: Masson-Delmotte, V., P. Zhai, A. Pirani, S. L. Connors, C. Péan, S. Berger, N. Caud, Y. Chen, L. Goldfarb, M. I. Gomis,

M. Huang, K. Leitzell, E. Lonnoy, J.B.R. Matthews, T. K. Maycock, T. Waterfield, O. Yelekçi, R. Y. and B. Z., Cambridge University Press. In Press, 3949P pp., 2021.

Iwata, Y., Hirota, T., Hayashi, M., Suzuki, S., and Hasegawa, S.: Effects of frozen soil and snow cover on cold-season soil water dynamics in Tokachi, Japan, Hydrol Process, 24, 1755–1765, https://doi.org/10.1002/hyp.7621, 2010.

Jacques, J. M. S. and Sauchyn, D. J.: Increasing winter baseflow and mean annual streamflow from possible permafrost thawing in the Northwest Territories, Canada, Geophys Res Lett, 36, https://doi.org/10.1029/2008GL035822, 2009.

Japan Aerospace Exploration Agency: ALOS World 3D - 30 meter DEM. V3.2, Jan 2021. Distributed by OpenTopography, https://doi.org/10.5069/G94M92HB, 2021.

Jolánkai, Z. and Koncsos, L.: Base flow index estimation on gauged and ungauged catchments in Hungary using digital filter, multiple linear regression and artificial neural networks, Periodica Polytechnica Civil Engineering, 62, https://doi.org/10.3311/PPci.10518, 2018.

Kelly, L., Kalin, R. M., Bertram, D., Kanjaye, M., Nkhata, M., and Sibande, H.: Quantification of temporal variations in base flow index using sporadic river data: Application to the Bua catchment, Malawi, Water (Switzerland), 11, 901, https://doi.org/10.3390/w11050901, 2019.

Kelly, L., Bertram, D., Kalin, R., Ngongondo, C., and Sibande, H.: A National Scale Assessment of Temporal Variations in Groundwater Discharge to Rivers: Malawi, American Journal of Water Science and Engineering, 6, 39–49, https://doi.org/10.11648/j.ajwse.20200601.15, 2020.

Kendall, M. G.: Rank Correlation Methods, 4th ed., Griffin, London, UK, 1975.

Krause, P., Boyle, D. P., and Bäse, F.: Comparison of different efficiency criteria for hydrological model assessment, Advances in Geosciences, 5, 89–97, https://doi.org/10.5194/adgeo-5-89-2005, 2005.

LeBoutillier, D. W. and Waylen, P. R.: A stochastic model of flow duration curves, Water Resour Res, 29, 3535–3541, https://doi.org/10.1029/93WR01409, 1993.

Lei, Y., Jiang, X., Geng, W., Zhang, J., Zhao, H., and Ren, L.: The variation characteristics and influencing factors of base flow of the hexi inland rivers, Atmosphere (Basel), 12, 356, https://doi.org/10.3390/atmos12030356, 2021.

Lins, H. F. and Slack, J. R.: Seasonal and Regional Characteristics of U.S. Streamflow Trends in the United States from 1940 to 1999, Phys Geogr, 26, 489–501, https://doi.org/10.2747/0272-3646.26.6.489, 2005.

Lott, D. A. and Stewart, M. T.: Base flow separation: A comparison of analytical and mass balance methods, J Hydrol (Amst), 535, 525–533, https://doi.org/10.1016/J.JHYDROL.2016.01.063, 2016.

Lyu, S., Zhai, Y., Zhang, Y., Cheng, L., Kumar Paul, P., Song, J., Wang, Y., Huang, M., Fang, H., and Zhang, J.: Baseflow signature behaviour of mountainous catchments around the North China Plain, J Hydrol (Amst), 606, https://doi.org/10.1016/j.jhydrol.2022.127450, 2022.

Mann, H. B.: Nonparametric Tests Against Trend, Econometrica, 13, 245, https://doi.org/10.2307/1907187, 1945a.

Mann, H. B.: Nonparametric Tests Against Trend, Econometrica, 13, 245, https://doi.org/10.2307/1907187, 1945b.

Meals, D. W., Spooner, J., Dressing, S. A., and Harcum, J. B.: Statistical analysis for monotonic trends, nonpoint source monitoring: Tech Notes, U.S. Environmental Protection Agency, 2011.

Meriano, M., Howard, K. W. F., and Eyles, N.: The role of midsummer urban aquifer recharge in stormflow generation using isotopic and chemical hydrograph separation techniques, J Hydrol (Amst), 396, 82–93, https://doi.org/10.1016/j.jhydrol.2010.10.041, 2011.

Mori, N., Takemi, T., Tachikawa, Y., Tatano, H., Shimura, T., Tanaka, T., Fujimi, T., Osakada, Y., Webb, A., and Nakakita, E.: Recent nationwide climate change impact assessments of natural hazards in Japan and East Asia, Weather Clim Extrem, 32, 100309, https://doi.org/10.1016/j.wace.2021.100309, 2021.

Nathan, R. J. and McMahon, T. A.: Evaluation of automated techniques for base flow and recession analyses, Water Resour Res, 26, 1465–1473, https://doi.org/10.1029/WR026I007P01465, 1990.

Nathan, R. J. and McMahon, T. A.: Estimating low flow characteristics in ungauged catchments, Water Resources Management, 6, 85–100, https://doi.org/10.1007/BF00872205, 1992.

Nedelcev, O. and Jenicek, M.: Trends in seasonal snowpack and their relation to climate variables in mountain catchments in Czechia, Hydrological Sciences Journal, 66, 2340–2356, https://doi.org/10.1080/02626667.2021.1990298, 2021.

Oki, D. S.: Trends in streamflow characteristics at long-term gaging stations, Hawaii, U.S. Geological Survey Scientific Investigations Report 2004-5080, 120 pp., 2004.

Penna, D., van Meerveld, H. J., Oliviero, O., Zuecco, G., Assendelft, R. S., Dalla Fontana, G., and Borga, M.: Seasonal changes in runoff generation in a small forested mountain catchment, Hydrol Process, 29, 2027–2042, https://doi.org/10.1002/HYP.10347, 2015.

Piggott, A. R., Moin, S., and Southam, C.: A revised approach to the UKIH method for the calculation of baseflow/Une approche amélioréede la méthode de l'UKIH pour le calcul de l'écoulement de base, Hydrological Sciences Journal, 50, 5, 2005.

Price, K.: Effects of watershed topography, soils, land use, and climate, on baseflow hydrology in humid regions: A review, Prog Phys Geogr, 35, 465–492, https://doi.org/10.1177/0309133311402714, 2011.

Rifai, H. S., Brock, S. M., Ensor, K., and Bedient, P. B.: Determination of Low-Flow Characteristics for Texas Streams, Journal of Water Resources Planning and Management , 126, 2000.

Rougé, C., Ge, Y., and Cai, X.: Detecting gradual and abrupt changes in hydrological records, Adv Water Resour, 53, 33–44, https://doi.org/10.1016/j.advwatres.2012.09.008, 2013.

Sadegh, M., Vrugt, J. A., Gupta, H. v., and Xu, C.: The soil water characteristic as new class of closed-form parametric expressions for the flow duration curve, J Hydrol (Amst), 535, 438–456, https://doi.org/10.1016/j.jhydrol.2016.01.027, 2016.

Saedi, J., Sharifi, M. R., Saremi, A., and Babazadeh, H.: Assessing the impact of climate change and human activity on streamflow in a semiarid basin using precipitation and baseflow analysis, Sci Rep, 12, 9228, https://doi.org/10.1038/s41598-022-13143-y, 2022.

Senocak, S. and Tasci, S.: Shaping a baseflow model through multiple regression analysis: The Çoruh watershed example, Water Supply, 22, 2117–2132, https://doi.org/10.2166/WS.2021.362, 2022.

Sen, P. K.: Estimates of the Regression Coefficient Based on Kendall's Tau, J Am Stat Assoc, 63, 1379–1389, https://doi.org/10.1080/01621459.1968.10480934, 1968.

Serinaldi, F. and Kilsby, C. G.: The importance of prewhitening in change point analysis under persistence, Stochastic Environmental Research and Risk Assessment, 30, 763–777, https://doi.org/10.1007/s00477-015-1041-5, 2016.

Singh, S. K., Pahlow, M., Booker, D. J., Shankar, U., and Chamorro, A.: Towards baseflow index characterisation at national scale in New Zealand, J Hydrol (Amst), 568, 646–657, https://doi.org/10.1016/j.jhydrol.2018.11.025, 2019.

Sloto, R. A., Crouse, M. Y., and Eaton, G. P.: HYSEP: A COMPUTER PROGRAM FOR STREAMFLOW HYDROGRAPH SEPARATION AND ANALYSIS. Water-Resources Investigation Report 96-4040, Lemoyne, Pennsylvania, 1996.

Smakhtin, V. U.: Low flow hydrology: A review, J Hydrol (Amst), 240, 147–186, https://doi.org/10.1016/S0022-1694(00)00340-1, 2001.

Stoelzle, M., Schuetz, T., Weiler, M., Stahl, K., and Tallaksen, L. M.: Beyond binary baseflow separation: a delayed-flow index for multiple streamflow contributions, Hydrol Earth Syst Sci, 24, 849–867, https://doi.org/10.5194/hess-24-849-2020, 2020.

Stuckey, M. H.: Low-flow, base-flow, and mean-flow regression equations for Pennsylvania streams, 84 pp., 2006.

Sugiyama, H.: Analysis and extraction of low flow recession characteristics, Water Resources Bulletin, 32, 491–497, https://doi.org/10.1111/j.1752-1688.1996.tb04047.x, 1996.

Sugiyama, H., Vudhivanich, V., Whitaker, A. C., and Lorsirirat, K.: Stochastic flow duration curves for evaluation of flow regimes in rivers, J Am Water Resour Assoc, 39, 47–58, https://doi.org/10.1111/j.1752-1688.2003.tb01560.x, 2003.

Sun, J., Wang, X., Shahid, S., and Li, H.: An optimized baseflow separation method for assessment of seasonal and spatial variability of baseflow and the driving factors, Journal of Geographical Sciences, 31, 1873–1894, https://doi.org/10.1007/S11442-021-1927-8, 2021.

Tallaksen, L. and van Lanen, H. A.: Hydrological drought. Processes and estimation methods for streamflow and groundwater, edited by: Tallaksen, L. and van Lanen, H. A. J., Elsevier B.V., Amsterdam, 579 pp., 2004.

Tallaksen, L. M.: A review of baseflow recession analysis, J Hydrol (Amst), 165, 349–370, https://doi.org/10.1016/0022-1694(95)92779-d, 1995.

Troendle, C. A. and King, R. M.: The Effect of Timber Harvest on the Fool Creek Watershed, 30 Years Later, Water Resour Res, 21, 1915–1922, https://doi.org/10.1029/WR021I012P01915, 1985.

Vogel, R. M. and Kroll, C. N.: Estimation of baseflow recession constants, Water Resources Management, 10, 303–320, https://doi.org/10.1007/BF00508898, 1996.

Wahl, K. L. and Wahl, T. L.: Determining the Flow of Comal Springs at New Braunfels, Texas, Unknown, 95, 16–17, 1995.

Wakiyama, Y. and Yamanaka, T.: Year-to-year variation in snowmelt runoff from a small forested watershed in the mountainous region of central Japan, Hydrological Research Letters, 8, 90–95, https://doi.org/10.3178/hrl.8.90, 2014.

Whitaker, A. C. and Yoshimura, A.: Climate Change Impacts on the Seasonal Distribution of Runoff in a Snowy Headwater Basin, Niigata, Hydrological Research Letters, 6, 7–12, https://doi.org/10.3178/hrl.6.7, 2012.

Whitaker, A. C., Sugiyama H., and Hayakawa K.: Effect of snow cover conditions on the hydrologic regime: case study in a pluvial-nival watershed, Japan, Journal of American Water Resources Association, 44, 814–828, https://doi.org/10.1111/j.1752-1688.2008.00206.x, 2008.

Whitaker, A. C., Chapasa, S. N., Sagras, C., Theogene, U., Veremu, R., and Sugiyama, H.: Estimation of baseflow recession constant and regression of low flow indices in eastern Japan, Hydrological Sciences Journal, 67, 191–204, https://doi.org/10.1080/02626667.2021.2003368, 2022.

WMO: Manual on Low-flow Estimation and Prediction – Operational Manual Hydrology Report No. 50, edited by: Gustard, A. and Demuth, S., World Meteorological

Organization, German National Committee for the International Programme (IHP) of UNESCO and the Hydrology and Water Resources Programme (HWRP) of WMO, Koblenz, 1–138 pp., 2009.

Yamada, T. J., Seang, C. N., and Hoshino, T.: Influence of the long-term temperature trend on the number of new records for annual maximum daily precipitation in Japan, Atmosphere (Basel), 11, https://doi.org/10.3390/ATMOS11040371, 2020.

Yamanaka, T., Wakiyama, Y., and Suzuki, K.: Is snowmelt runoff timing in the Japanese Alps region shifting toward earlier in the year?, Hydrological Research Letters, 6, 87–91, https://doi.org/10.3178/hrl.6.87, 2012.

Yamazaki, D., Ikeshima, D., Tawatari, R., Yamaguchi, T., O'Loughlin, F., Neal, J. C., Sampson, C. C., Kanae, S., and Bates, P. D.: A high-accuracy map of global terrain elevations, Geophys Res Lett, 44, 5844–5853, https://doi.org/10.1002/2017GL072874, 2017.

Yang, Y., Chen, R., Liu, G., Liu, Z., and Wang, X.: Trends and variability in snowmelt in China under climate change, Hydrol Earth Syst Sci, 26, 305–329, https://doi.org/10.5194/hess-26-305-2022, 2022.

Yoshida, T. and Troch, P. A.: Coevolution of volcanic catchments in Japan, Hydrol Earth Syst Sci, 20, 1133–1150, https://doi.org/10.5194/hess-20-1133-2016, 2016.

Yue, S., Pilon, P., and Cavadias, G.: Power of the Mann–Kendall and Spearman's rho tests for detecting monotonic trends in hydrological series, J Hydrol (Amst), 259, 254–271, https://doi.org/10.1016/S0022-1694(01)00594-7, 2002.

Zhang, J., Zhang, Y., Song, J., and Cheng, L.: Evaluating relative merits of four baseflow separation methods in Eastern Australia, J Hydrol (Amst), 549, 252–263, https://doi.org/10.1016/j.jhydrol.2017.04.004, 2017.

Zhang, J., Song, J., Cheng, L., Zheng, H., Wang, Y., Huai, B., Sun, W., Qi, S., Zhao, P., Wang, Y., and Li, Q.: Baseflow estimation for catchments in the Loess Plateau, China, J Environ Manage, 233, 264–270, https://doi.org/10.1016/j.jenvman.2018.12.040, 2019.

Zhang, X., Vincent, L. A., Hogg, W. D., and Niitsoo, A.: Temperature and precipitation trends in Canada during the 20th century, Atmosphere-Ocean, 38, 395–429, https://doi.org/10.1080/07055900.2000.9649654, 2000.

4.3 Supplementary material

Supplementary material for

Assessing characteristics and long-term trends in runoff and baseflow index in eastern Japan

Stanley N. Chapasa[1] and Andrew C. Whitaker[2]

[1]Graduate School of Science and Technology, Niigata University, Japan

[2]Faculty of Agriculture, Niigata University, Japan

Correspondence to: Stanley Nungu Chapasa, Graduate School of Science and Technology, Niigata University, 8050 Ikarashi 2-no-cho, Nishi-ku, Niigata 950-2181, Japan. E-mail: snunguchapasa@gmail.com

Received: 30 September 2022; Accepted: 29 November 2022; Published: TBC

Contents:

Text S1. Methods supplement

Text S2. Discussion supplement

Figure 4. Box charts representing fundamental BFI from summary statistics for (a) annual period (yellow colour), (b) spring season (cyan colour), (c) summer season (green colour), (d) autumn season (red colour), and (e) winter season (grey colour) for 26 gauges (on horizontal axis) with periods of record ranging from 29 to 67 years

Table 6. Mann-Kendall trend test results for average annual and seasonal runoff for the 26 gauges with periods of record ranging from 29 to 67 years

Table 7. Mann-Kendall trend test results for average annual and seasonal BFI for the 26 gauges with periods of record ranging from 29 to 67 years

Text S1. Supplement methods

Baseflow separation method and implementation

The BFI Programme implements the widely used filtering method called the 'smoothed minima procedure', which uses smoothing and separation techniques to process a stream hydrograph (Gustard et al., 1992). The BFI Programme is an Excel-based tool developed by Martin Morawietz at the Department of Geosciences at the University of Oslo, Norway. The BFI Programme was initially prepared for the textbook (Tallaksen and van Lanen, 2004) "Hydrological Drought-Processes and Estimation Methods for Streamflow and Groundwater", which demonstrates a working example of how to use the tool. The BFI Programme is open and accessible freely to the public on the European Drought Centre website http://europeandroughtcentre.com/. Daily streamflow data is partitioned into 5-day increments (also known as non-overlapping consecutive blocks of 5 days) (WMO, 2009), and the minimum flow in each period (or block of 5 days) is identified. The minimum flow value of each block is compared to the minimum of the two adjacent blocks with a turning point parameter (also known as a multiplying factor f). A turning point is identified if the minimum value multiplied by 0.9 (a multiplying factor f) is less than or equal to the two adjacent minima (Aksoy et al., 2009; Tallaksen and van Lanen, 2004). Turning points are placed in the series of minimum flows and connected by straight

lines to draw the baseflow hydrograph. The BFI is calculated by dividing the baseflow volume (the baseflow hydrograph) by the total flow volume (the stream hydrograph) for each period. The precise details of the procedure are also provided in the Low Flow Studies Report No 3 by the (Institute of Hydrology, 1980) and in many studies (Tallaksen, 1995; Aksoy et al., 2008; Stoelzle et al., 2020; Wahl and Wahl, 1995).

The streamflow data were screened before baseflow separation to identify any periods of missing data. Before proceeding with the analysis, two options were available to deal with the missing data: (1) infill the missing data or (2) not infill the missing data, disregarding the data gaps, and analysed only the primary data (raw data). Although there were merits to infilling data (Jacques and Sauchyn, 2009), we did not infill data; we instead only analysed the primary streamflow data to determine BFI, as agreed by most studies (Hodgkins and Dudley, 2011; Oki, 2004; Zhang et al., 2019). So, in this study, the streamflow data were prepared by disregarding periods of missing values and grouping them into periods of non-missing values (Kelly et al., 2020). The periods of missing data were counted and converted to a percentage based on the total number of years of record as defined by several months (Table 3). For example, stream gauge Fuyube had missing data for 3 full annual periods (1979-1980 and 1984), which equates to approximately 6.7 % of 45 years of record, while Ishikiridokoro had missing data for 1 full annual period and 8 months, which equates to approximately 5.2 % of the period of record (1986 to 2017). For this study, the missing data ranges between 1 % and 14.3 % of the data records, as shown in Table 3. Although there is no specific rule, Helsel et al. (2020) advise using monotonic trend analysis rather than step trend if the missing data is less than one-third of the total record.

The assessment periods selected were annual and seasonal periods defined by months. The annual period was taken as the water year used in Japan by the Government of Japan's MLIT and ran from October 1 to September 30. The seasonal periods selected were the spring season defined as March-May, the summer season defined as June-August, the autumn season defined as September-November, and the winter season defined as December-February. The baseflow separation was implemented by using the BFI Programme in the following steps:

1. For each year of streamflow data, the baseflow separation was performed, producing a separate annual BFI value where there was enough data. The average annual BFI was therefore determined based on individual years,
2. The baseflow separation was performed for each monthly and seasonal period in the same manner as the annual period described above,
3. The total flow, baseflow, and surface runoff flow from each baseflow separation were summed for each period and
4. Descriptive statistics for BFI values (average, maximum, minimum, etc.) were determined for the annual, seasonal, and monthly periods.

Statistically significant trend analysis

The MK is recommended by the World Meteorological Organization (WMO, 2009) and is used globally in many studies (Hirsch and Slack, 1984; Chiew and McMahon, 1993; Lei et al., 2021; Douglas et al., 2000; Zhang et al., 2000; Rougé et al., 2013; Kelly et al., 2019; Nedelcev and Jenicek, 2021; Yue et al., 2002). The advantage of the MK test over the parametric test is that the MK test is insensitive to the missing data, which is commonly encountered in hydrological time series (Hirsch et al., 1982; Hirsch and Slack, 1984). The MK test provides higher statistical power in the case of non-normality of data,

and it is robust against outliers and large data gaps (Helsel et al., 2020; Meals et al., 2011). The null hypothesis H0 is that a sample of data {Xi, I = 1, 2…n} is independent and identically distributed. The alternative hypothesis H1 is that a monotonic trend exists in X. The equations for calculating the MK test are expressed below. The statistic *S* (MK 'S') test is calculated as follows:

$$S=\sum_{i=1}^{n-1}\sum_{j=i+1}^{n} sgn(X_j-X_i) \tag{8}$$

where n is the data length, X_i and X_j (the sequential data values) indicate data values at the i and j times, respectively.

$$sgn(x_j+x_i) = \begin{cases} 1; & X_j>X_i \\ 0; & X_j=X_i \\ -1; & X_j<X_i \end{cases} \tag{9}$$

Kendall (1975) and Mann (1945) suggested that the statistic S is approximately normally distributed with the mean and variance when $n \geq 10$ as follows:

$$E(S)=0\ , \tag{10}$$

$$Var(S)=\left[n(n-1)(2n+5)-\sum_{i=1}^{p} t_i(t_i-1)(2t_i+5)\right]/18\ , \tag{11}$$

where p denotes the number of tied groups, there is equal data in the time series. t_i indicates how many times a datum repeats. Finally, the standardized test statistic Z (Z value) is calculated by:

$$Z = \begin{cases} \frac{S-1}{\sqrt{Var(S)}}, & S>0 \\ 0, & S=0 \\ \frac{S+1}{\sqrt{Var(S)}}, & S<0 \end{cases} \tag{12}$$

The standardized MK statistic *Z* follows the standard normal distribution with mean = 0 and variance = 1. The probability value *p* of the MK statistic *S* of sample data can be estimated using the normal cumulative distribution function as follows:

$$P = \frac{1}{\sqrt{2\pi}} \int_{-\infty}^{Z} e^{-r^2/2}\, dt \qquad (13)$$

For independent sample data without a trend, the *p*-value should be equal to 0.5. For the data with a largely positive trend in data values, the *p*-value should be closer to 1.0, whereas a large negative trend should yield a *p*-value closer to 0.0. Similarly, the existence of the trend in data values is investigated with the null hypothesis. Suppose the absolute value of the calculated *Z* value is greater than the standardized *Z* value corresponding to the chosen significance level (0.01 or 0.05). In that case, the null hypothesis is rejected, in which case there is a trend.

The sign of the MK '*S'* value determines the direction of the trend (positive means an increasing trend, negative means a decreasing trend). Otherwise, there is no trend in the data value, and the null hypothesis is accepted. Using the seasonal Kendall test, MK test statistics for each season are calculated, and these are added to for seasonal test statistics (Hirsch et al., 1982; Hirsch and Slack, 1984):

$$S_k = \sum_{i=1}^{m} S_i \qquad (14)$$

For this test, the season can be monthly or quarterly or follow any other definition. In this study, monthly values were selected as the season. The significance of the trend was investigated as in the classical MK test.

Text S2. Supplement discussion

Overall distribution of BFI

We can see that the distribution of BFI is not normally distributed, which supports our decision to use a nonparametric test of trend analysis as recommended by many researchers (Hirsch and Slack, 1984).

Annual and seasonal BFI for each basin

Annual and seasonal BFIs show temporal and spatial variability in the study region, and they are influenced by the regional climate in eastern Japan. Variability in the data may be due to many factors, including changes in hydrology and weather, natural changes, human activities and management, among others (Meals et al., 2011; Helsel et al., 2020).

Monthly BFI, runoff, and precipitation

Regularly repeated single peak (n-shaped) or double peak (m-shaped) patterns of monthly BFI, runoff, and precipitation in basins, highlight distinct hydrological regimes (Figure 5). Basins in the Japan Sea region, such as Kamiiwakibashi, Nakamura, and Uonogawa-Horinouchi (Figures 2 and 5), experience heavy snowfall and heavy summer precipitation (Whitaker et al., 2022; Mori et al., 2021), while basins in the Pacific Ocean region, such as Nitadori, Imodabashi, and Ochiai, have very dry winters and a more significant influence from typhoons in late summer to autumn.

Trends in annual and seasonal runoff

Our results show that about 20 % of the basins have significantly increasing winter runoff, which suggests that we are seeing the influence of climate change through increased winter rainfall and/or rain fraction. In the case of reductions in snowpack, we might

expect to see decreasing trends in spring runoff in those basins where winter runoff is increasing. However, increasing trends in spring runoff could be caused by snowmelt shifting from early summer to April and May, or changes in spring season precipitation.

Trends in annual and seasonal BFI

Our findings appear to be well supported by trends and spatial variability in snowmelt, as suggested by Yang et al. (2022), which could influence large-scale water resources assessments. Additionally, increased air temperatures reduce baseflow and BFI due to increased evapotranspiration in the summer season (Mori et al., 2021). Similarly, Easterling et al. (2000) suggested that anthropogenic decreases in watershed infiltration capacity could exacerbate climate change effects on baseflow and BFI. Thus, with reduced recharge, the baseflow becomes a smaller fraction of total annual and seasonal streamflow as suggested by Price (2011) and Smakhtin (2001).

Table 6. Mann-Kendall trend test results for average annual and seasonal runoff for the 26 gauges with periods of records ranging from 29 to 67 years.

No	Gauge name	Period of record	Annual		Spring		Summer		Autumn		Winter	
			MK 'S'	Trend	MK 'S'	Trend	MK 'S'	Trend	MK 'S'	Trend	MK 'S'	Trend
1	Kuzukawa	1989-2017	26	↔	50	↔	28	↔	-60	↔	-48	↔
2	Ishikawa	1969-2017	-114	↔	182	↔	-162	↔	-120	↔	-98	↔
3	Nuruyu	1989-2017	-26	↔	-38	↔	62	↔	-20	↔	-62	↔
4	Kamiiwakibashi	1960-2017	53	↔	-135	↔	-125	↔	**306***	↑	45	↔
5	Nitadori	1985-2017	20	↔	86	↔	16	↔	10	↔	-56	↔
6	Fuyube	1973-2017	**195***	↑	**209***	↑	51	↔	114	↔	181	↔
7	Ishikiridokoro	1986-2017	39	↔	47	↔	-29	↔	51	↔	103	↔
8	Kenyoshi	1963-2017	221	↔	13	↔	161	↔	253	↔	147	↔
9	Yonaizawa	1959-2017	136	↔	252	↔	-76	↔	94	↔	-74	↔
10	Junisho	1962-2017	149	↔	-41	↔	23	↔	159	↔	69	↔
11	Oyagawa	1974-2011	-98	↔	-44	↔	-76	↔	-62	↔	-34	↔
12	Furukawabashi	1975-2017	**220****	↑	**242****	↑	156	↔	98	↔	**214***	↑
13	Imodabashi	1983-2017	44	↔	0	↔	0	↔	52	↔	68	↔
14	Ochiai	1974-2019	59	↔	-33	↔	-60	↔	86	↔	**235***	↑
15	Shirakawa-Hirokawara	1980-2017	148	↔	144	↔	132	↔	104	↔	122	↔
16	Shirakawa-Shimoyachi	1980-2017	-47	↔	-13	↔	49	↔	-23	↔	-8	↔
17	Nakamura	1977-2017	-138	↔	-158	↔	-76	↔	-130	↔	-41	↔
18	Sushiarai	1960-2017	**716****	↑	**324***	↑	**428****	↑	**574****	↑	**358***	↑
19	Nishine	1965-2019	**-303***	↓	**-351***	↓	-41	↔	-249	↔	**301***	↑
20	Koide	1953-2019	254	↔	70	↔	72	↔	276	↔	226	↔
21	Kumaide	1966-2015	-108	↔	-96	↔	-46	↔	-114	↔	-8	↔
22	Uonogawa-Muikamachi	1981-2019	71	↔	-29	↔	11	↔	53	↔	9	↔
23	Uonogawa-Urasa	1981-2019	-9	↔	21	↔	-81	↔	-31	↔	51	↔
24	Uonogawa-Koide	1981-2019	115	↔	79	↔	21	↔	39	↔	141	↔
25	Uonogawa-Horinouchi	1960-2019	-122	↔	-246	↔	-186	↔	0	↔	**424****	↑
26	Shinano-Ojiya	1961-2020	210	↔	300	↔	-62	↔	132	↔	228	↔

***** indicates *p*-value <0.05, ****** indicates *p*-value <0.01, ↓ indicates a decreasing trend, ↑ indicates an increasing trend, ↔ indicates no trend, and MK 'S' means Mann-Kendall's statistic and significant values are highlighted in black bold

Table 7. Mann-Kendall trend test results for average annual and seasonal BFI for the 26 gauges with periods of records ranging from 29 to 67 years.

No	Gauge name	Period of record	Annual		Spring		Summer		Autumn		Winter	
			MK 'S'	Trend	MK 'S'	Trend	MK 'S'	Trend	MK 'S'	Trend	MK 'S'	Trend
1	Kuzukawa	1989-2017	-103	↔	0	↔	**-122***	↓	-18	↔	-79	↔
2	Ishikawa	1969-2017	**-511****	↓	**-332****	↓	**-246***	↓	**-386****	↓	-87	↔
3	Nuruyu	1989-2017	49	↔	82	↔	-22	↔	72	↔	-70	↔
4	Kamiiwakibashi	1960-2017	107	↔	-233	↔	252	↔	162	↔	**461****	↑
5	Nitadori	1985-2017	-122	↔	-8	↔	-60	↔	**-134***	↓	**-185****	↓
6	Fuyube	1973-2017	-42	↔	39	↔	41	↔	-74	↔	-166	↔
7	Ishikiridokoro	1986-2017	**166***	↑	43	↔	107	↔	69	↔	-68	↔
8	Kenyoshi	1963-2017	-62	↔	149	↔	-65	↔	-131	↔	58	↔
9	Yonaizawa	1959-2017	-166	↔	112	↔	-226	↔	**-414****	↓	-162	↔
10	Junisho	1962-2017	160	↔	207	↔	125	↔	-49	↔	166	↔
11	Oyagawa	1974-2011	1	↔	-14	↔	68	↔	-73	↔	-79	↔
12	Furukawabashi	1975-2017	**-329***	↓	-105	↔	-259	↔	**-337***	↓	**-439****	↓
13	Imodabashi	1983-2017	49	↔	-33	↔	19	↔	35	↔	53	↔
14	Ochiai	1974-2019	**225***	↑	203	↔	**298****	↑	-122	↔	-439	↔
15	Shirakawa-Hirokawara	1980-2017	-103	↔	-56	↔	-40	↔	-58	↔	-102	↔
16	Shirakawa-Shimoyachi	1980-2017	-121	↔	-71	↔	-43	↔	-27	↔	66	↔
17	Nakamura	1977-2017	-101	↔	-116	↔	-50	↔	-38	↔	-66	↔
18	Sushiarai	1960-2017	268	↔	**321***	↑	**584****	↑	-150	↔	48	↔
19	Nishine	1965-2019	**420****	↑	**483****	↑	97	↔	**349***	↑	**280***	↑
20	Koide	1953-2019	48	↔	86	↔	**380***	↑	-110	↔	-32	↔
21	Kumaide	1966-2015	-185	↔	**-242***	↓	-84	↔	56	↔	65	↔
22	Uonogawa-Muikamachi	1981-2019	-50	↔	47	↔	59	↔	-73	↔	**-332****	↓
23	Uonogawa-Urasa	1981-2019	151	↔	**227****	↑	-39	↔	-27	↔	**-310****	↓
24	Uonogawa-Koide	1981-2019	75	↔	**223****	↑	-19	↔	-5	↔	**-336****	↓
25	Uonogawa-Horinouchi	1960-2019	-190	↔	86	↔	36	↔	-78	↔	**-838****	↓
26	Shinano-Ojiya	1961-2020	**-316***	↓	-194	↔	272	↔	**-492***	↓	**-657****	↓

***** indicates *p*-value < 0.05, ****** indicates *p*-value < 0.01, ↓ indicates a decreasing trend, ↑ indicates an increasing trend, ↔ indicates no trend, and MK 'S' means Mann-Kendall's statistic and significant values are highlighted in black bold

4.4 Summary

In this chapter, the study used long-term data (29 to 67 years) collected from 26 MLIT stream gauges in eastern Japan. The most remarkable study outcome was that statistically significant trends in annual runoff and BFI with more trends occurring in winter season. The study showed that BFI values were not distributed evenly and changed with seasons.

The study output has important impacts on sustainable water resource management in Japan. The study findings could be used to monitor the impacts of climate change on water resources in eastern Japan.

The next chapter provides the study of estimation of baseflow recession constant and regression of low flow indices in eastern Japan.

Chapter 5 Estimation of Baseflow Recession Constant and Regression of Low Flow Indices in Eastern Japan

5.1 Introduction

The previous chapater demonstrated, using the Mann-Kendall test and Sen's slope estimator, how to identify trends and the rate of change per decade per in annual and seasonl runoff and BFI values at 1 % and 5 % significance levels. Annual and seasonal frequency analyses of distribution of BFI values using histograms and box plots were performed for each of 26 basins over full period of record (29-67 years). The study results suggested that climate change has influence on the runoff and BFI trends and the regional hydroclimatic condition could influence the variability of BFI and runoff values in eastern Japan.

This chapter introduces a peer reviewed published article that demonstrates how to estimate the baseflow recession constant and development of regression models that can be used to estimate low flow indeces in eastern Japan. The paper was published in the Hydrological Sciences Journal (HSJ) as follows:

Whitaker, A.C, Chapasa, S.N., Sagras, C., Theogene, U., Veremu, R. and Sugiyama, H., 2022. Estimation of base flow recession constant and regression of low flow indices in eastern Japan. Hydrological Sciences Journal, 67(2), 191-204.

To link this article: https://doi.org/10.1080/02626667.2021.2003368

This published article is presented in the following section, and the author's contributions were as follows: Conceptualization, A.C.W., S.N.C., H.S. and R.V..; Funding acquisition, A.C.W and H.S.; Formal analysis, A.C.W, S.N.C., C.S., H.S; Methodology, A.C.W, H.S, S.N.C.; Resources, A.C.W.; Supervision, A.C.W and H.S.; Validation, A.C.W, S.N.C., C.S., U.T., R.V. and H.S.; Visualization, A.C.W, S.N.C.,

C.S., U.T., R.V. and H.S..; Writing—original draft, A.C.W and H.S.; Writing—review & editing, A.C.W, S.N.C., C.S., U.T., R.V. and H.S.

5.2 Paper (HSJ)

Estimation of base flow recession constant and regression of low flow indices in eastern Japan

Andrew C. Whitaker[1], Stanley N. Chapasa[2], Cristencio Sagras[2], Uwitonze Theogene[3], Ronald Veremu[4], Hironobu Sugiyama[5]

Corresponding author: Andrew C. Whitaker

Niigata University, Ikarashi 2-nocho 8050, Nishi-ku, Niigata City 950-2181, Japan

Tel/Fax: +81-25-262-6656

Email: whitaker@agr.niigata-u.ac.jp

1 Associate Professor, Faculty of Agriculture, Niigata University, Japan

2 Graduate School of Science and Technology, Niigata University, Japan

3 Senior Rural Engineer, Rwanda Agriculture and Animal Resources Development Board, Rwanda

4 Ministry of Lands, Agriculture & Rural Resettlement, Zimbabwe

5 Former Professor, University of Tsukuba & Niigata University, Japan

Received: 4 November 2020; Accepted: 15 October 2021; Published: 14 January 2022

Abstract

We propose a convenient procedure for the matching strip method in determining the recession constant of the master recession curve using the ratio of flow over successive days (Q_{n+1}/Q_n). The method is applied to 29 basins (6.1–740 km^2) in Eastern Japan to develop linear regression models which estimate low flow indices through the recession constant (λ), and either mean annual precipitation or mean annual runoff. Significant models were developed for $Q7_{10}$ (7-day 10-year low flow), and $Q97_{10}$ (10-year low flow exceeded 97% of time) in the case of all basins, and in particular the case of basins classified into sedimentary or igneous geology (adjusted R^2 up to 0.784). When basins were not classified by geology, models based on mean annual runoff as the second independent variable performed better than those based on mean annual precipitation, with adjusted R^2 of 0.705 and 0.717 for the $Q7_{10}$ and $Q97_{10}$ models, respectively.

Keywords: low flow indices; flow duration curve; base flow; recession constant; master recession curve; regression analysis, eastern Japan

1 Introduction

In the evaluation of low flow hydrology, the determination of base flow recession characteristics or low flow indices is important when considering water supply, water quality, and water resources planning in river basins (Hall 1968, Tallaksen 1995, Smakhtin 2001). The synthetic master recession curve (MRC), generally expressed as an exponential function, has been widely applied to evaluate the low flow characteristics in a basin (e.g. Singh and Stall 1971, Beran and Gustard 1977, Eng and Milly 2007, Croker *et al.* 2003, Thomas *et al*. 2015). It has been suggested that the MRC, as an envelope to all recession limbs, shows the general recession behavior of the basin (Tallaksen 1995), and the slope of streamflow decline on the MRC is commonly referred to as the base flow recession constant (Vogel and Kroll 1996). However, questions remain regarding how the MRC can be determined objectively and easily from individual recession limbs in the streamflow record. Hydrologists have proposed various methods for determining the MRC, including manual graphical methods such as the correlation method and the matching strip method (e.g. Snyder 1939, Nathan and McMahon 1990), and automated mathematical techniques that rely on base flow separation through application of a digital filter (e.g. Arnold et al. 1995, Arnold and Allen 1999, Beck *et al*. 2013). Manual graphical methods allow visual control over the inclusion of the most representative recessions, although they are time-consuming. Automated methods appear to be the most objective, although they are not without their difficulties in the application of base flow separation techniques which require the selection of filter parameter values and decisions on the number of filter passes.

Numerous regional studies have developed models to estimate base flow recession characteristics (recession constant, base flow index) from various catchment

characteristics (geology, soils, topography, basin area, climate, land cover) for application to ungauged basins (e.g. Zecharias and Brutsaert 1988, Brandes et al. 2005, Van Dijk 2010, Pena-Arancibia et al. 2010, Krakauer and Temimi 2011). In addition, other models have been developed to estimate low flow indices as a function of basin characteristics, in some cases including the recession constant (or recession index) which acts as a surrogate for both basin hydraulic conductivity and drainable soil porosity (e.g. Bingham 1986, Curran 1990, Vogel and Kroll 1992, Reilly and Kroll 2003, Stuckey 2006, Castiglioni et al. 2009). The inclusion of the recession constant or other hydrogeological explanatory variables has produced more efficient models (e.g. Vogel and Kroll 1996, Kroll et al. 2004). Although gauging data is needed for an estimate of the recession constant from hydrograph analysis, a relatively short period of record may be sufficient to allow the application of regression models predicting, for example, the 7-day 10-year probability flow index.

The flow duration curve (*FDC*), graphically depicting the relationship between the exceedance probability of streamflow and its magnitude, has been applied in order to evaluate the severity of high, ordinary, and low flow regimes, and has provided useful information for sustainable planning and/or management of water resources in the upper reaches of streams. A stochastic estimation of low flow (e.g. LeBoutillier and Waylen 1993) and mathematical expressions describing the flow duration curve (e.g. Sadegh *et al.* 2016) have been developed for the planning, development, and management of water resources and/or water use systems. Sugiyama *et al*. (2003) defined the stochastic flow duration curve as one which is drawn by using the distribution characteristics of a set of probability plots of streamflow calculated by the Weibull plotting formula at suitable time intervals from 0 to 100 percent on the time axis.

In order to provide estimates of a single low flow index, hydrologists have taken interest in predicting the base flow recession rate or recession constant (e.g. Tallaksen 1995, Sugiyama 1996), the $Q7_{10}$ flow (the 7-day, 10-year low flow, e.g. Caruso 2000, Rifai *et al*. 2000, Brandes *et al*. 2005, Castiglioni *et al*. 2009, Berhanu *et al*. 2015) and the $Q97_{10}$ flow (the 10-year low flow equaled or exceeded 97 percent of time on the annual flow duration curve, e.g. Sugiyama *et al*. 2003). However, further work is needed to develop methods that are not dependent on base flow separation techniques and which are simple and easy to apply. In addition there is also benefit in exploring alternative forms of regression models used to estimate low flow indices in regions such as Japan, where fewer studies have been published compared to other regions.

The overall objective of this paper is to explore and evaluate realistic regression models that can be appropriately used for estimating low flow indices by means of the recession constant (λ) of the master recession curve combined with other catchment or climatic characteristics. The location of eastern Japan was chosen because this region is climatologically and geologically diverse, and many of the streams are influenced by snow accumulation and snowmelt processes in addition to seasonal rains. Firstly, a convenient procedure for the matching strip method is proposed to objectively determine the recession constant (λ) of the master recession curve, based on the ratio of streamflow values on successive days during flow recession limbs (see Appendix). Secondly, the $Q7_{10}$ and $Q97_{10}$ flows, representing low flow indices, are predicted by means of multiple linear regression analysis. Thirdly, we explore the potential of using information on the dominant geology of the basins to improve the predictive performance of such regression models.

2 Location and data

Stream flow records in Japan are widely influenced by flow regulations or flow diversions upstream of the gauging point, which can have a major impact on measured low flows. We opted to use hydrological records for headwater catchments upstream of reservoirs, with the restriction that there are no regulation or diversion structures in the upstream reaches. Hydrological records for reservoir catchments in Japan, arranged in a dataset for about the recent twenty five years, are easily obtained on-line (www.mudam.nilim.go.jp). These records contain daily data on reservoir water levels, water discharged at the dam, and reservoir inflows which are estimated based on the mass balance:

$$\text{Inflow} = \text{Release discharge} \pm \text{Change in storage} \quad (15)$$

Change in storage is estimated from the relationship between water level and storage as determined through surveying. In our analysis we use the estimated reservoir inflows to represent the natural unregulated discharge from the headwater catchments. Twenty nine catchments located in eastern Japan are selected here with basin areas ranging from 6.1 to 740 km^2 and mean annual runoff ranging from 695 to 4690 mm (Figure 6, Table 8). All basins are located in headwater forested mountain areas, with elevations at the gauging point ranging from 32 to 1123 m above sea level, and maximum elevations ranging up to about 3000 m. The climate and hydrological regimes are extremely variable across this region, with areas on the Japan Sea side experiencing heavy snowfall and heavy summer precipitation, while the Pacific Ocean side has very dry winters and a greater influence from typhoons (late summer to autumn). The water year runs from the beginning of October to the end of September. The dominant geology of each basin was determined to be either igneous or sedimentary by referring to the

Seamless Digital Geological Map of Japan (1:200,000) as published on-line (https://gbank.gsj.jp/seamless/v2/viewer/?lang=en).

The fluctuation of average daily runoff during the period of record (24 years) at two contrasting study basins (wettest and driest) is shown in Figure 7. Peak snowmelt runoff in the heavy snow regions of the Japan Sea coast, such as Arasawa basin, typically occur during April or May. Even at low elevations in Arasawa basin, average precipitation during snowfall season (November to March) exceeds 1500 mm, with average annual snowfall >13 m and average peak snow depth >2.5 m. On the other hand, basins located on the Pacific Ocean side, such as Shimokubo basin, do not have significant snowpack and so peak runoff occurs from August to September during the typhoon season. In Shimokubo basin, average precipitation during the cold season (November to March) is only about 200 mm, compared to >400 mm over just two months in late summer (August to September). Both the cold season precipitation and the mean annual runoff for Arasawa basin are about seven times greater than that of Shimokubo basin, indicating the importance of cold season precipitation and snowmelt as a water resource, and the extreme variability in climate and hydrological regime within the study area.

3 Methods

3.1 How to determine the recession constant of the master recession curve

The exponential equation below has been quoted by many hydrologists as the expressional equation that represents the recession limb during a long period without rain or snowmelt (Barnes 1939). According to this equation, base flow recedes exponentially with time. Therefore, at least part of the recession limb can be expressed by:

$$Q_t = Q_0 \exp(-\lambda t) \quad (16)$$

where Q_t is the discharge at time t, Q_0 is the initial discharge and λ is the recession constant.

As a first step, certain criteria or rules must be applied to objectively extract recession limbs from the streamflow record. The definition of a suitable recession limb will depend to some extent on the research objectives. Smoothing of the streamflow data may also be applied as part of the criteria (e.g. 3-day moving average as in Vogel and Kroll, 1992). In the second step, a method must be chosen to fit the synthetic master recession curve to the extracted recession limbs. We chose the matching strip method (Snyder, 1939), which was adapted to spreadsheet use by Veremu (2009) and further developed here.

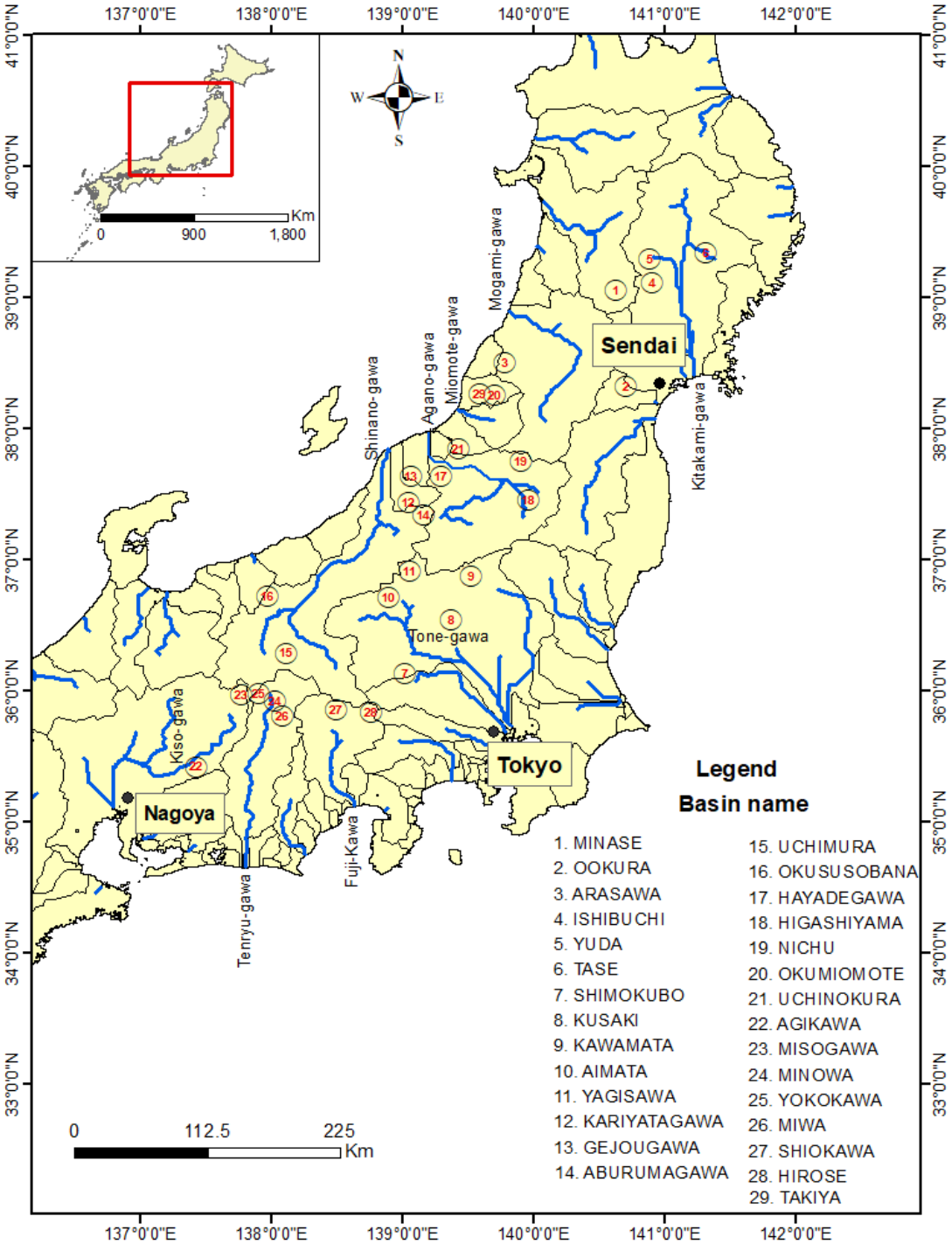

Figure 6. Location map of the 29 study basins in eastern Japan, showing the major river systems and their catchment boundaries.

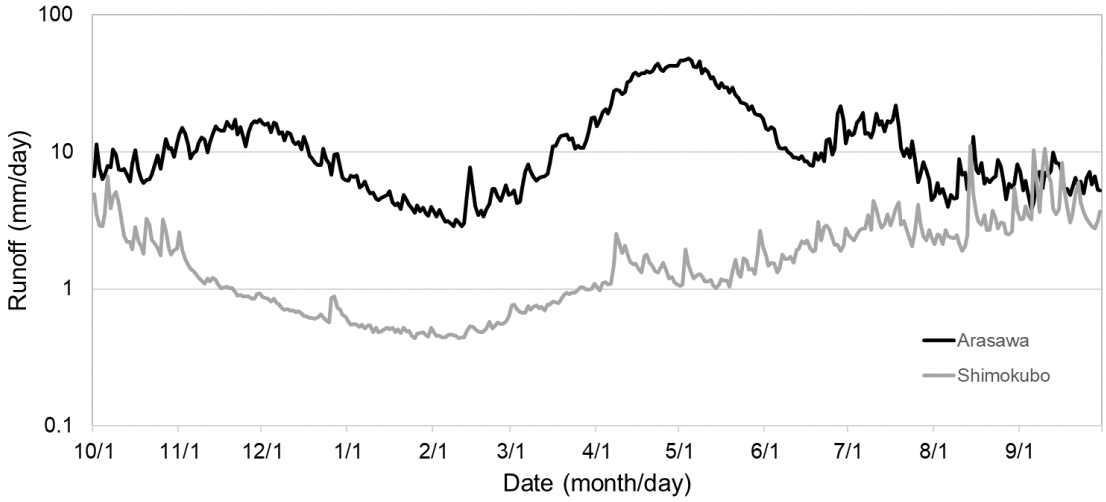

Figure 7. Examples of average daily runoff over the period of record in two contrasting basin areas. Arasawa is located near the Japan Sea experiencing high precipitation year round with deep snowpack (December to May), while Shimokubo is located near the Pacific coast with dry winters and little snowpack.

Due to the presence of seasonal snowpack in most of the study basins, we only considered the period July to November for extracting recession limbs, when the influence of snowmelt on runoff could be considered negligible or absent. We then used a spreadsheet to automatically extract recession limbs based on the following criteria. A 3-day moving average was applied to the original data, and recession limbs extracted based on a minimum recession period, without reference to precipitation data. For each basin, the minimum recession period was set within the range of 12-18 days in order to obtain the longest 15-20 recession limbs (Table 9). We assume that the longer recession limbs are more likely to give information on the true master recession curve, as they are less influenced by surface runoff.

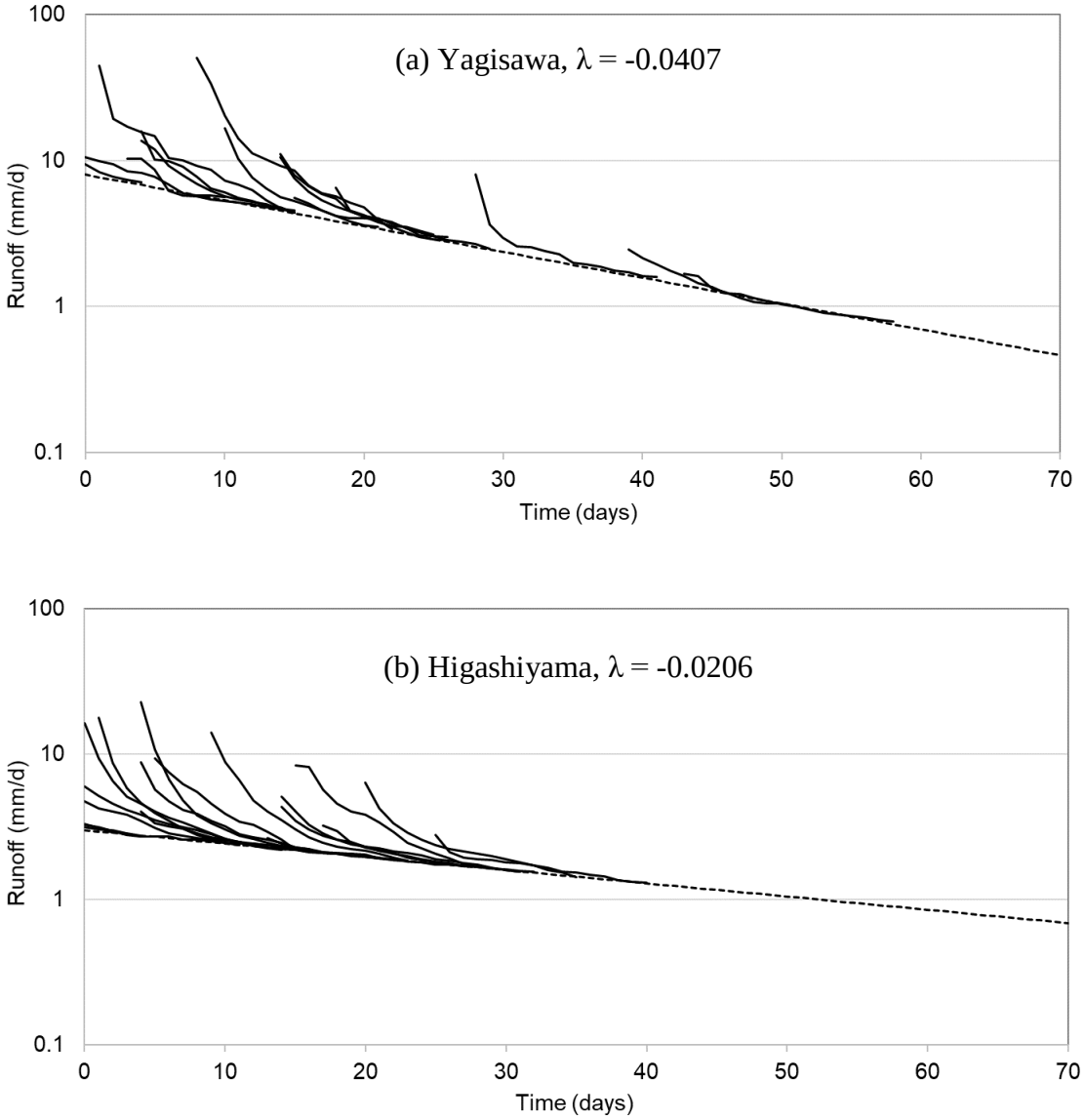

Figure 8. Examples of master recession curves for; (a) Yagisawa (basin 11), where the slope of common limb, λ, is -0.0407 based on a minimum recession period of 12 days and the extraction of 15 recession limbs, and (b) Higashiyama (basin 18), where the slope of common limb, λ, is -0.0206 based on a minimum recession period of 14 days and the extraction of 19 recession limbs (Table 9).

Recessions did not include any increase in the 3-day moving average of daily runoff. Finally, using the moving average values, we calculated the average value for the ratio Q_{n+1}/Q_n over the last 7 days of each recession limb (less likely to be influenced by surface runoff than the early part of the recession), ranked the values, and took the mean of the largest 5 values as an estimate of the slope ($\lambda = 1 - Q_{n+1}/Q_n$) for the master

recession curve. In this way, we numerically determined the recession constant for the master recession curve using the minimum tendency of the slopes of all extracted recession limbs. Full details of the methods used to construct the master recession curves are detailed in the Appendix, including use of a spreadsheet to develop the procedure and confirmation of the result with the matching strip method. A sensitivity analysis of our procedure in estimating the recession constant is presented in the results.

By obtaining a numerical estimate of the slope for the master recession curve, as detailed above, we avoided much of the inherent subjectivity in the matching strip method which generally relies on purely visual judgment in fitting the common limb to the extracted recessions (Nathan and McMahon 1990). Here we use the matching strip plotting method only to visually confirm the slope for the master recession curve which has been already determined objectively by using the ratio Q_{n+1}/Q_n. In the traditional matching strip method, we found that a wide range of slopes for the common limb could be seen to fit the extracted recession limbs, and the problem remained of how to determine the slope in a more objective manner. Figure 8 shows two examples of master recession curves obtained through our method, and the recession constants obtained for each study basin are shown in Table 9.

Table 8. Characteristics and locations of the study basins. Period of record is 24 years (1993-2017), except for Ishibuchi (1993-2012), Okumiomote (2003-2017), Misogawa (1997-2017), Shiokawa (1999-2017), and Takiya (2001-2018).

No.	River system	Basin name	Area (km^2)	P[a] (mm/year)	Q[b] (mm/year)	Geology	Location (latitude,longitude)
1	Omono	Minase	172	1928	2340	Ig	39.056, 140.630
2	Natori	Ookura	89	1569	1808	Ig	38.322, 140.706
3	Aka	Arasawa	162	3158	4690	Ig	38.507, 139.783
4	Kitakami	Ishibuchi	154	2165	2813	Sed	39.116, 140.903
5	Kitakami	Yuda	583	2109	2348	Ig	39.302, 140.885
6	Kitakami	Tase	740	1137	913	Ig	39.343, 141.319
7	Tone	Shimokubo	323	1245	695	Sed	36.133, 139.022
8	Tone	Kusaki	254	1461	1464	Ig	36.542, 139.373
9	Tone	Kawamata	179	1627	1419	Ig	36.878, 139.520
10	Tone	Aimata	111	1755	1687	Ig	36.713, 138.893
11	Tone	Yagisawa	167	2302	3128	Sed	36.912, 139.056
12	Shinano	Kariyatagawa	24	2801	3513	Sed	37.437, 139.052
13	Shinano	Gejougawa	6	2056	1943	Ig	37.639, 139.064
14	Shinano	Aburumagawa	59	3105	4652	Sed	37.343, 139.164
15	Shinano	Uchimura	13	1251	916	Ig	36.292, 138.111
16	Shinano	Okususobana	65	1624	2123	Ig	36.725, 137.967
17	Agano	Hayadegawa	83	3212	4209	Ig	37.642, 139.293
18	Agano	Higashiyama	41	1253	1313	Ig	37.461, 139.966
19	Agano	Nichu	41	1562	2254	Ig	37.753, 139.908
20	Miomote	Okumiomote	175	3215	4116	Ig	38.263, 139.704
21	Kaji	Uchinokura	48	3252	4327	Sed	37.850, 139.424
22	Kiso	Agikawa	82	1785	1350	Sed	35.425, 137.432
23	Kiso	Misogawa	55	1927	1670	Sed	35.977, 137.770
24	Tenryu	Minowa	38	1436	757	Sed	35.928, 138.031
25	Tenryu	Yokokawa	39	1436	1389	Sed	35.978, 137.907
26	Tenryu	Miwa	311	1552	1318	Ig	35.813, 138.082
27	Fuji	Shiokawa	85	1147	866	Ig	35.859, 138.498
28	Fuji	Hirose	77	1636	1451	Ig	35.839,138.764
29	Miomote	Takiya	19	2719	2842	Sed	38.265, 139.592

a: Mean annual precipitation (P) taken from the Japanese Meteorological Agency gauge located closest to the basin mouth (1991-2020). These values will often be significantly lower than actual basin scale precipitation due to under-catch of snowfall precipitation and orographic enhancement of precipitation at higher elevations. Therefore, the situation where Q>P occurs in many basins.

b: Mean annual runoff (Q) given for the period of record for each basin.

Table 9. Low flow indices and characteristics of the master recession curves analyzed for the study basins.

No.	River system	Basin name	$Q97_{10}$ (mmd^{-1})	$Q7_{10}$ (mmd^{-1})	Recession constant, λ (d^{-1})	Minimum recession period (d)	No. of recession limbs
1	Omono	Minase	1.08	0.82	0.0418	13	18
2	Natori	Ookura	1.08	0.89	0.0313	15	15
3	Aka	Arasawa	1.67	1.48	0.0441	12	14
4	Kitakami	Ishibuchi	0.80	0.81	0.0622	13	18
5	Kitakami	Yuda	0.96	0.86	0.0526	13	17
6	Kitakami	Tase	0.84	0.81	0.0205	12	19
7	Tone	Shimokubo	0.23	0.14	0.0346	16	19
8	Tone	Kusaki	0.64	0.50	0.0305	17	19
9	Tone	Kawamata	0.86	0.87	0.0305	17	19
10	Tone	Aimata	0.78	0.74	0.0364	15	20
11	Tone	Yagisawa	1.52	1.42	0.0407	12	15
12	Shinano	Kariyatagawa	1.62	1.48	0.0266	14	18
13	Shinano	Gejougawa	0.34	0.29	0.0651	12	17
14	Shinano	Aburumagawa	1.62	1.53	0.0360	12	21
15	Shinano	Uchimura	0.20	0.18	0.0299	15	19
16	Shinano	Okususobana	0.82	0.73	0.0385	15	18
17	Agano	Hayadegawa	0.55	0.32	0.0787	12	16
18	Agano	Higashiyama	1.00	0.96	0.0206	14	19
19	Agano	Nichu	0.81	0.58	0.0399	14	19
20	Miomote	Okumiomote	1.80	1.72	0.0412	12	14
21	Kaji	Uchinokura	2.32	1.95	0.0335	12	20
22	Kiso	Agikawa	0.82	0.65	0.0420	14	16
23	Kiso	Misogawa	1.07	1.08	0.0299	15	20
24	Tenryu	Minowa	0.66	0.64	0.0159	16	19
25	Tenryu	Yokokawa	0.26	0.50	0.0199	18	21
26	Tenryu	Miwa	0.85	0.81	0.0227	17	22
27	Fuji	Shiokawa	0.83	0.81	0.0227	16	20
28	Fuji	Hirose	1.23	1.20	0.0136	17	20
29	Miomote	Takiya	0.86	0.65	0.0319	12	24

3.2 How to read the daily flow at 97 percent on the time axis

The flow duration curve of daily flows for a water year is drawn by plotting and arranging the daily discharge values in descending order. Figure 9 illustrates how to read the value of daily discharge from the flow duration curve at 97 percent on the time axis. This procedure is continued for each of the given water years.

3.3 How to estimate the $Q97_{10}$ flow

Step 1. Read the *Q*97 of daily flow equaled or exceeded for 97 percent of time (Figure 9). Carry out this step for each of the given water years (obtaining annual *Q*97 values).

Step 2. Rank in ascending order the annual *Q*97 flows.

Step 3. Calculate the plotting position with the following Weibull plotting formula, and plot against non-exceedance probability using a probability scale.

$$P = m / (n+1) \times 100\% \quad (17)$$

where, *P* is the probability of the annual *Q*97 flow being less than or equal to a given value, *m* is the rank, and *n* is the number of years on record.

Step 4. Fit a straight line (best fit by eye or by regression), and read the $Q97_{10}$ flow from the best fit line at the 10 percent probability value on the ordinate.

The procedure above is carried out for each catchment area (see also Sugiyama et al. (2003) for further details).

Table 10. Sensitivity to minimum recession period and the associated number of recession limbs in the determination of the recession constant (λ) using a random sample of eight basins.

No.	Basin name	Minimum recession period (d)	No. of recession limbs	Recession constant, λ (d^{-1})	Percent change in λ (%)[a]
1	Minase	13	18	0.0418	
		12	24	0.0385	-8
3	Arasawa	12	14	0.0441	
		11	24	0.0370	-16
8	Kusaki	17	19	0.0305	
		16	25	0.0285	-7
		12	63	0.0238	-16
14	Aburumagawa	14	14	0.0393	
		12	21	0.0360	-8
20	Okumiomote	12	14	0.0412	
		11	18	0.0412	0
25	Yokokawa	18	21	0.0199	
		15	38	0.0199	0
		12	60	0.0196	-2
26	Miwa	18	17	0.0227	
		17	22	0.0227	0
		12	52	0.0215	-5
29	Takiya	14	16	0.0330	
		12	24	0.0319	-3

3.4 How to estimate the $Q7_{10}$ flow (see the above-mentioned procedure (step 1 to step 4))

Firstly, the annual minimum flow averaged over a consecutive period of seven days ($Q7$) is estimated using daily flow data for each water year during the period of record. Next the discharge estimated is ranked in ascending order, and the plotting position is calculated through equation (3). The $Q7$ flow against non-exceedance probability are plotted using a probability scale, and a best-fit straight line is fitted. Finally, the $Q7_{10}$ flow for the 10-year probability is read from the best-fit line at the 10 percent probability value on the ordinate.

4 Results

4.1 Distribution of the recession constant (λ)

Results for the determination of the recession constant (λ) are shown in Table 9, with values ranging from 0.0136 d^{-1} to 0.0787 d^{-1} and a mean value of 0.0356 d^{-1}. A relative frequency histogram of λ is drawn with a class interval of 0.005 d^{-1} considering geological characteristics in Figure 10. In the case of all basins lumped and the sedimentary basins, the highest frequency occurs in the range 0.030-0.035 d^{-1}, while for igneous basins the peak occurs in the range 0.020-0.025 d^{-1}. For all basins, 76% of values occur within the range 0.020-0.045 d^{-1}. While our sample of basins is relatively small, there is evidence in these histograms that the distribution of λvalues is dependent on the dominant geology.

4.2 Sensitivity analysis in the determination of recession constant (λ)

We would like to stress that our approach is fundamentally based on the matching strip method (Snyder, 1939), which is well established in the literature, commonly used in

practice, and has been extensively compared with other methods (e.g. Nathan and McMahon, 1990). However, as with any method, certain choices made in the approach can influence on the results obtained. Here we examine the sensitivity of our results to choices made in the development of the method, including the criteria used to extract recession limbs, and the use of averaging for the ratio of flow over successive days (Q_{n+1}/Q_n).

4.2.1 *Minimum recession period and number of recession limbs*

Our objective was to extract the longest recession limbs, as the first part of a recession will be influenced by surface runoff and/or stormflow, and therefore cannot be used in the analysis of base flow recession. Due to the high variability in climatic conditions throughout the study region, we had to vary the minimum recession period required for the extraction of recession limbs in order to obtain a similar size sample of limbs. In basins where recession limbs tended to be longer, we increased the minimum recession period up to 17 or 18 days, while in basins where recession limbs tended to be short, we reduced the minimum recession period to 12 days (Table 7). This produced a relatively consistent number of extracted limbs of about 15-20 per basin, or approximately 0.6-1.0 limbs per year of record (mean value of 0.82). Firstly, by considering a random sample of eight basins, we look at the sensitivity of the estimated recession constant to the minimum recession period and the number of limbs extracted (Table 10). For the first four basins given in Table 10, there tended to be a higher sensitivity to minimum recession period with changes of -7 to -16 percent in the estimated recession constant. In all cases, a reduction in the minimum recession period led to a reduction in the value for the estimated recession constant. However, for the last four basins

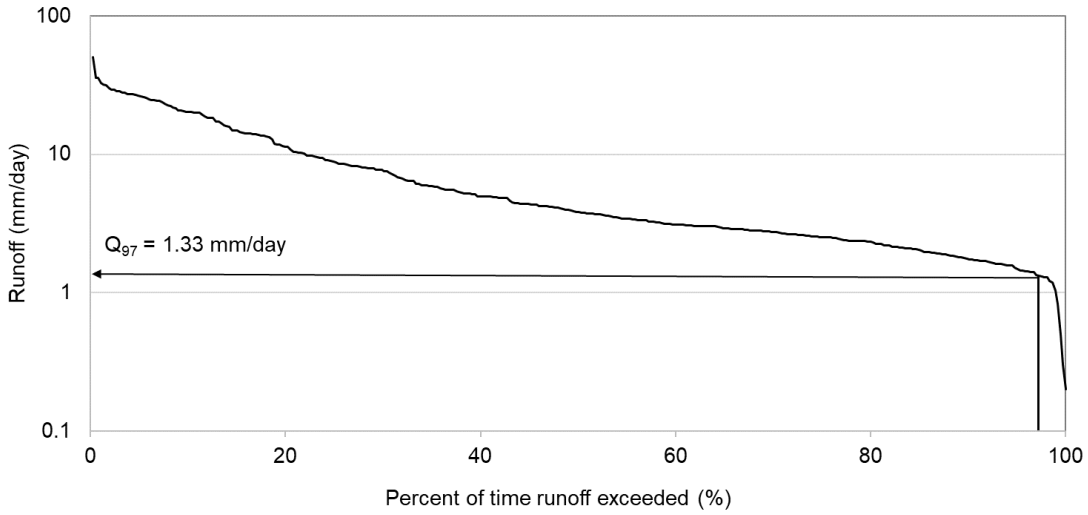

Figure 9. Example of flow duration curve, reading the runoff value at 97 percent on the time axis (Yagisawa basin for water year 1994).

given in Table 10 we found relative insensitivity to minimum recession period, with a maximum change of -5 percent. For basin 25 (Yokokawa), we varied the minimum recession period between 12, 15, and 18 days, giving 60, 38, and 21 extracted recession limbs, respectively. However, the estimated recession constant was the same value when using either 38 limbs or 21 limbs (15 or 18 days minimum recession), and only differed by -2 percent when using 60 limbs. Similarly, for basin 26 (Miwa), there is little or no sensitivity in the estimated recession constant when the minimum recession period is varied between 12 and 18 days. This shows that in these examples, the limbs which have a bearing on the minimum tendency of the slopes of all extracted recession limbs have already been extracted with a minimum recession period of 18 days. Therefore, the resulting estimate of the recession constant is relatively insensitive to the minimum recession period.

In summary, we found little or no sensitivity to minimum recession period and number of limbs extracted when at least 15-20 limbs were extracted from a period of record of 24 years. Where sensitivity occurred, increasing the number of limbs extracted produced a smaller value for the recession constant.

4.2.2 *Period over which ratio of flow (Q_{n+1}/Q_n) was averaged*

In our approach we applied averaging to the ratio of flow over successive days (Q_{n+1}/Q_n) during the last 7 days of each extracted recession limb.

Table 11. Sensitivity to period of averaging for the ratio of flow (Q_{n+1}/Q_n) in the determination of the recession constant (λ) for the same random sample of eight basins given in Table 10.

No.	Basin name	Minimum recession period (d)	Period of averaging for Q_{n+1}/Q_n (d)	Recession constant, λ (d^{-1})	Percent change in λ (%)[a]
1	Minase	13	7	0.0418	
			6	0.0381	-9
			5	0.0337	-12
3	Arasawa	12	7	0.0441	
			6	0.0436	-1
			5	0.0406	-7
8	Kusaki	17	7	0.0305	
			6	0.0305	0
			5	0.0288	-6
14	Aburumagawa	12	7	0.0360	
			6	0.0361	0
			5	0.0349	-3
20	Okumiomote	12	7	0.0412	
			6	0.0389	-6
			5	0.0373	-4
25	Yokokawa	18	7	0.0199	
			6	0.0200	1
			5	0.0199	-1
26	Miwa	17	7	0.0227	
			6	0.0230	1
			5	0.0219	-5
29	Takiya	12	7	0.0319	
			6	0.0272	-15
			5	0.0272	0

a: relative to the case of longer averaging period for Q_{n+1}/Q_n in row above

Here we examine sensitivity of the results to this averaging period. First, we should note that the shortest recession limbs extracted were 12 days in length for basins with few longer recessions.

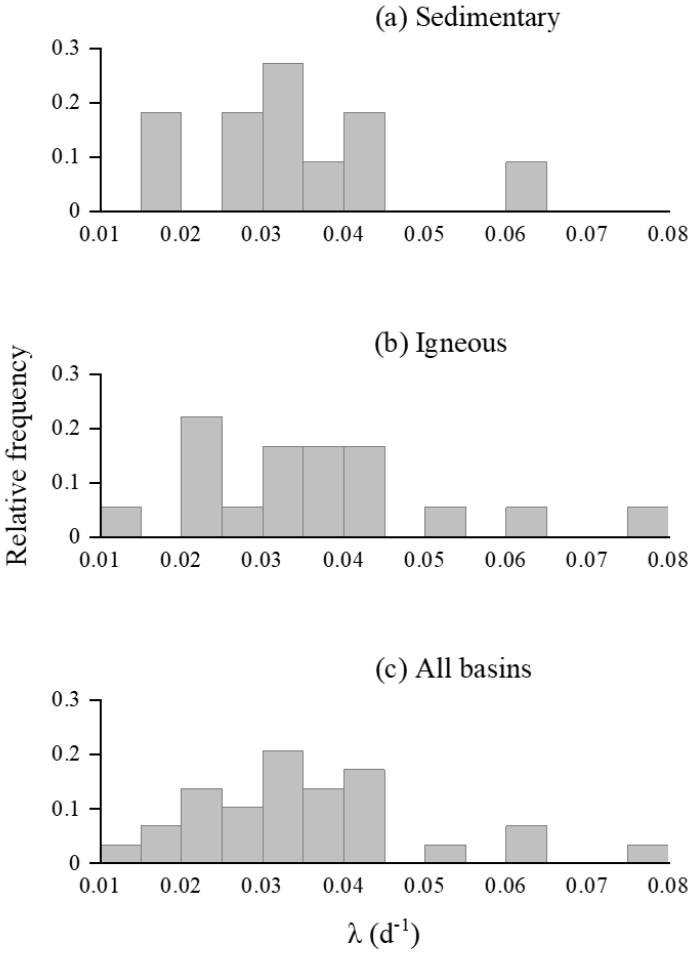

Figure 10. Relative frequency histograms showing the distribution of values of the recession constant (λ) in the case of (a) sedimentary basins, (b) igneous basins, and (c) all basins.

Knowing that the first part of the recession is usually influenced by surface runoff and/or stormflow, we can only consider applying the averaging of (Q_{n+1}/Q_n) over the last 7 days or less of each limb. Therefore, we explore sensitivity of the results to varying the

averaging period over the last 5-7 days for the same random sample of eight basins discussed in the previous section (Table 11).

In five out of the eight basins, reducing the period of averaging for the flow ratio from seven to six days resulted in little or no change in estimated recession constant (-1 to +1 %). When further reducing the period of averaging to five days, the resulting change in estimated recession constant only exceeded 5 percent in three of the eight basins. Overall, the average sensitivity of the recession constant is <5 percent.

On balance, we feel that the 7-day averaging period for Q_{n+1}/Q_n is suitable and reasonable in that it can be applied to basins where the minimum recession period varies between 12 and 18 days, as is the case for our study region where the climate and precipitation regime is highly variable.

4.2.3 *Averaging the highest ranked values of Q_{n+1}/Q_n*

In our approach we ranked the 7-day average values for Q_{n+1}/Q_n and took the mean of the largest 5 values as our estimate of the recession constant ($\lambda = 1 - Q_{n+1}/Q_n$). Here we examine the sensitivity of results to variability in the number of values used in the calculation of the mean (top-3, top-5, and top-7 values). Using the top-5 ranked values, the average estimate across all basins for the recession constant was 0.0356 d^{-1}, compared to 0.0324 d^{-1} and 0.0384 d^{-1} using top-3 and top-7 values, respectively. When we plotted the master recession curves with the matching strip method, we found that the estimates of the recession constant based on the top-3 or top-5 values were in good agreement. However, when using only the top-3 values, the influence of potential outlier values from suspect recession limbs could greatly affect the results. Suspect recession limbs could potentially be included in cases where minor rainfall occurred in some part of the basin

leading to a slowed rate of recession. Using the top-7 values further reduces the influence of potential outliers, but the resulting estimate of the recession constant is less aligned with the minimum tendency of the slopes of all extracted limbs. Furthermore, in the section below on regression modeling, we found that the most significant models were obtained using estimates of recession constant based on the top-3 and top-5 values. In that section, we present models based on the top-5 values because these estimates are; (1) in good agreement with the matching strip method, and (2) less likely to be affected by outlier values.

4.3 Relationship between $Q97_{10}$ and $Q7_{10}$

The $Q7_{10}$ and $Q97_{10}$ flows are summarized in Table 9 and plotted against each other in Figure 11. From Figure 11 we can see that the relationship between $Q7_{10}$ and $Q97_{10}$ is strong and strictly linear (correlation coefficient = 0.975). This result suggests that the $Q7_{10}$ flow is approximately equivalent to the $Q97_{10}$ flow.

4.4 Multiple regression analysis

Regression analysis was used to establish a linear relationship between independent variables and dependent variables. The predicted value (Y) of the dependent variable is generally described as:

$$Y = b_0 + b_1X_1 + b_2X_2 + \text{-------} + b_kX_k + \varepsilon_i \quad (18)$$

where Y is the predicted value (dependent variable), X_i is the independent variable, ε_i is error, and b_i are the partial regression coefficients.

Before attempting multiple regression analysis, we examined the correlation matrix including all dependent ($Q7_{10}$ and $Q97_{10}$) and independent (recession constant,

basin area, minimum elevation, mean annual precipitation and mean annual runoff) variables. From these independent variables, the correlation coefficients were notably high for both annual precipitation (0.612, 0.673) and annual runoff (0.647, 0.708) for $Q7_{10}$ and $Q97_{10}$ dependent variables, respectively. We expected overlap in the predictive information contained in the variables of precipitation and runoff (multicollinearity), and this was confirmed by a correlation value of 0.959.

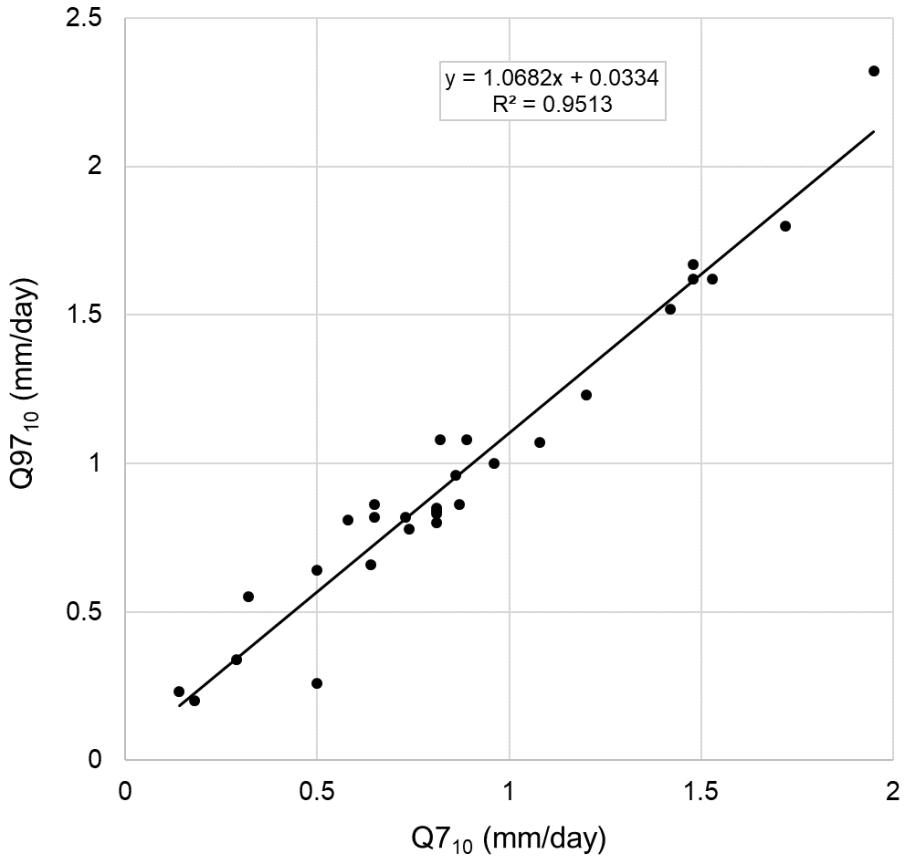

Figure 11. Relationship between $Q97_{10}$ and $Q7_{10}$ for the 29 study basins.

The higher correlation coefficients for annual runoff indicate higher potential for regression modeling, although in data-poor locations it may be easier to estimate mean annual precipitation than mean annual runoff.

Basically we applied the step-wise method of analysis which resulted in regression equations for $Q97_{10}$ and $Q7_{10}$ by means of recession constant (λ) and either mean annual precipitation (P) or mean annual runoff (Q). The value of the partial regression coefficients is found using ordinary least squares. In addition, we explored the possibility of developing regression models based on a classification of the dominant geology of the basins as either sedimentary (n = 11) or igneous (n = 18).

4.4.1 *Regression models based on recession constant (λ) and mean annual precipitation (P)*

Tables 12 and 13 show the regression models for the $Q7_{10}$ and $Q97_{10}$ dependent variables, respectively. For the regression models (3) and (6) representing all basins lumped together, the significance F values are <0.001 and the adjusted R^2 values are 0.636 and 0.645, respectively. The significance of each independent variable is indicated by the p values, with both mean annual precipitation and the recession constant having a high level of significance (p = <0.001 in both models). These results show that the all basin lumped models are viable for the study region, with standard errors of 0.273 and 0.295 for the $Q7_{10}$ and $Q97_{10}$ dependent variables, respectively.

When developing regression models based on dominant geology, we found that significantly higher values for the adjusted R^2 could be achieved (up to 0.77), although standard errors were only reduced for the igneous classification (models 2 and 5) with 0.185 and 0.202, respectively. In the igneous classification models, the significance F and the p values were each <0.001, while for the sedimentary classification models the level of significance was lower. This may be related to the smaller sample size for the sedimentary classification (n = 11) compared to the igneous classification (n = 18).

Table 12. Regression models developed in the case of predicting $Q7_{10}$ from the recession constant and mean annual precipitation. Units: recession constant, λ (d^{-1}), mean annual precipitation, P (m). Equation coefficients rounded to 4 significant figures.

Dominant geology	Equation	Adj. R^2	Signif. F	p value		t value		t. error	eqn. no.
				λ	P	λ	P		
Sedimentary (n = 11)	$Q7_{10}$ = - 0.3536 - 4.334λ +0.6767P	0.655	0.006	0.622	0.002	-0.51	4.56	0.322	(1)
Igneous (n = 18)	$Q7_{10}$ = 0.5477 - 26.51λ + 0.6683P	0.770	<0.001	<0.001	<0.001	-6.90	7.23	0.185	(2)
All basins (n = 29)	$Q7_{10}$ = 0.3691 - 18.92λ + 0.5969P	0.636	<0.001	<0.001	<0.001	-4.70	6.99	0.273	(3)

Table 13. Regression models developed in the case of predicting $Q97_{10}$ from the recession constant and mean annual precipitation. Units: recession constant, λ (d^{-1}), mean annual precipitation, P (m). Equation coefficients rounded to 4 significant figures.

Dominant geology	Equation	Adj. R^2	Signif. F	p value		t value		t. error	eqn. no.
				λ	P	λ	P		
Sedimentary (n = 11)	$Q97_{10}$ = - 0.5976 - 3.636λ + 0.8154P	0.722	0.002	0.692	<0.001	-0.41	5.25	0.337	(4)
Igneous (n = 18)	$Q97_{10}$ = 0.5297 - 24.57λ + 0.6928P	0.736	<0.001	<0.001	<0.001	-5.86	6.86	0.202	(5)
All basins (n = 29)	$Q97_{10}$ = 0.2875 - 18.02λ + 0.6690P	0.645	<0.001	<0.001	<0.001	-4.14	7.25	0.295	(6)

Table 14. Regression models developed in the case of predicting $Q7_{10}$ from the recession constant and mean annual runoff. Units: recession constant, λ (d^{-1}), mean annual runoff, Q (m). Equation coefficients rounded to 4 significant figures.

Dominant geology	Equation	Adj. R^2	Signif. F	p value		t value		St. error	Eqn. no.
				λ	Q	λ	Q		
Sedimentary (n = 11)	$Q7_{10} = 0.3735 - 8.199\lambda + 0.3612Q$	0.714	<0.003	0.327	<0.001	-1.04	5.18	0.292	(7)
Igneous (n = 18)	$Q7_{10} = 0.9398 - 24.17 + 0.3663Q$	0.730	<0.001	<0.001	<0.001	-6.09	6.50	0.201	(8)
All basins (n = 29)	$Q7_{10} = 0.7922 - 19.57 + 0.3527Q$	0.705	<0.001	<0.001	<0.001	-5.41	8.16	0.246	(9)

Table 15. Regression models developed in the case of predicting $Q97_{10}$ from the recession constant and mean annual runoff. Units: recession constant, λ (d^{-1}), mean annual runoff, Q (m). Equation coefficients rounded to 4 significant figures.

Dominant geology	Equation	Adj. R^2	Signif. F	p value		t value		St. error	Eqn. no.
				λ	Q	λ	Q		
Sedimentary (n = 11)	$Q97_{10} = 0.3065 - 7.642\lambda + 0.4150Q$	0.692	<0.004	0.445	<0.002	-0.80	4.91	0.354	(10)
Igneous (n = 18)	$Q97_{10} = 0.9285 - 23.12\lambda + 0.4008Q$	0.784	<0.001	<0.001	<0.001	-6.40	7.81	0.183	(11)
All basins (n = 29)	$Q97_{10} = 0.7619 - 18.74\lambda + 0.3949Q$	0.717	<0.001	<0.001	<0.001	-4.82	8.50	0.264	(12)

4.4.2 *Regression models based on recession constant (λ) and mean annual runoff (Q)*

In the regression analysis here, we substitute the independent variable mean annual precipitation (P) for mean annual runoff (Q). Tables 14 and 15 show the regression models for the $Q7_{10}$ and $Q97_{10}$ dependent variables, respectively. For the regression models (9) and (12) representing all basins lumped together, the significance F values are <0.001 and the adjusted R^2 values are 0.705 and 0.717, respectively. The significance of each independent variable is indicated by the p values, with both mean annual runoff and recession constant showing high significance in each model (p = <0.001). These results show that the all basin lumped models are viable for the study region, with standard errors of 0.246 and 0.264 for the $Q7_{10}$ and $Q97_{10}$ dependent variables, respectively.

When developing regression models based on dominant geology, again we found that higher values for the adjusted R^2 could be achieved (up to 0.784), although as in the previous section, standard errors were only reduced for the igneous classification (models 8 and 11) with 0.201 and 0.183, respectively. In the igneous classification models, the significance F and the p values were each <0.001, while for the sedimentary classification models the level of significance was lower, especially for the p value of the recession constant independent variable. Again, this may be related to the smaller sample size for the sedimentary classification (n = 11) compared to the igneous classification (n = 18), or there could be some other explanation related to differences in process due to geology.

4.4.3 *Overview of regression models predicting $Q7_{10}$ and $Q97_{10}$ dependent variables*

If we look at the functional forms of the regression models in Tables 12 to 15, we can see that the signs for the independent variables of mean annual precipitation and mean annual runoff are always positive. This is as we expect, with higher annual precipitation and higher annual runoff associated with higher low flow indices. When we look at the sign

for the independent variable of recession constant, in all cases we have a negative sign such that the steeper the recession constant, the lower the tendency for low flow indices.

We have presented regression models based on two independent variables; the recession constant in combination with either mean annual precipitation or mean annual runoff. When comparing models based on mean annual precipitation (Tables 5 and 6) with those based on mean annual runoff (Tables 7 and 8), we can see that in the case of all basins lumped, a higher model performance is obtained when using mean annual runoff. However, in the case of models based on dominant geology, the higher performance can go either way between runoff or precipitation as the second independent variable. Overall we obtained a slightly higher model performance when using mean annual runoff as the second independent variable, with an average adjusted R^2 value of 0.724 compared to 0.694 when using mean annual precipitation.

4.5 Gauging data requirements for application of the models

The application of the regression models presented here requires at least limited stream gauging data to estimate the recession constant. Additionally, the best performing model may also require an estimate of mean annual runoff. We evaluated the sensitivity of the recession constant and mean annual runoff to estimation with limited data for three randomly selected basins, where a relatively high number of recession limbs could be extracted (Table 16). A total of 52 to 63 recession limbs were extracted for the Kusaki, Yokokawa and Miwa basins using a minimum recession period of 12 days, and this was divided into 3, 4, and 5 subsets. In the development of the regression models, we ranked the 7-day average values for Q_{n+1}/Q_n and took the mean of the largest 5 values as our estimate of the recession constant ($\lambda = 1 - Q_{n+1}/Q_n$). When working with subsets we

adopted the following formula to determine the number of ranked values of Q_{n+1}/Q_n used to estimate the recession constant:

No. of ranked values of Q_{n+1}/Q_n used $\approx$ POR / 5 (19)

where POR is the period of record for each subset, and the result is rounded to the nearest integer. In developing the regression models, the majority of basins had a POR of 24 years, such that equation (5) gives a value of 5 when rounded to the nearest integer. In this way we can compare between different numbers of subsets in Table 16. We can see that the range and standard deviation of the estimates is broadly similar across the subsets, although the influence of outlier flow ratio values is greater for subset POR of 4.8 and 6 years because only one flow ratio value is used in the estimate of the recession constant. These results seem to indicate that even for basins with high variability in runoff, it is possible to obtain a reasonable estimate of the recession constant with as little as 5-8 years of data.

Furthermore, a moving average was used to evaluate the sensitivity of mean annual runoff to estimation with limited data. For the Yokokawa basin, 6-year moving average values were within 20% of the mean based on the full period of record, while for the Kusaki and Miwa basins, 6-year moving average values were within 10% of the mean based on the full period of record. Although the minimum period of record required to apply the regression models will depend on the runoff characteristics of each basin, the examples given in this section show that it is feasible to apply them after obtaining limited gauging data of approximately 5 to 8 years.

Table 16. Sensitivity of recession constant to estimation with limited data. Random subsets taken from limbs extracted for Kusaki (basin 8, mean annual runoff 1464 mm, standard deviation 303 mm), Yokokawa (basin 25, mean annual runoff 1389 mm, standard deviation 362 mm), and Miwa (basin 26, mean annual runoff 1318 mm, standard deviation 247 mm) using a minimum recession period of 12 days (total period of record (POR) is 24 years).

Basin and No. Subsets	Limbs / subset	Subset POR (years)	Q_{n+1}/Q_n values used in the estimate (≈ subset POR/5)	Mean (range) of estimated recession constant, λ (d^{-1})	Standard deviation of estimates (d^{-1})
Kusaki	63	24	5	0.0238	-
3	21	8	2	0.0265 (0.022-0.0315)	0.0048
4	16	6	1	0.0251 (0.0176-0.0360)	0.0081
5	13	4.8	1	0.0243 (0.0176-0.0287)	0.0049
Yokokawa	60	24	5	0.0196	-
3	20	8	2	0.0203 (0.0182-0.0219)	0.0019
4	15	6	1	0.0209 (0.0152-0.0257)	0.0043
5	12	4.8	1	0.0210 (0.0152-0.0257)	0.0046
Miwa	52	24	5	0.0215	-
3	17	8	2	0.0225 (0.0209-0.0237)	0.0014
4	13	6	1	0.0232 (0.0190-0.0270)	0.0033
5	10	4.8	1	0.0239 (0.0190-0.0297)	0.0045

5 Conclusions

This paper introduces a simple method to develop regression models that are practical for estimating low flow indices through the recession constant of the master recession curve in combination with information on dominant geology and either mean annual precipitation or mean annual runoff. We used average daily flow data in 29 catchments (6.1–740 km^2) located in the mountainous region of eastern Japan which is highly variable in terms of geology and climate, and often influenced by snow accumulation and melt. Firstly, objective criteria were used to automatically extract recession limbs from the streamflow record. By calculating the average value for the ratio Q_{n+1}/Q_n over the last 7 days of each recession limb, we numerically determined the recession constant for the master recession curve, and visually confirmed the result using the matching strip plotting method. Additionally, we evaluated the sensitivity of our results to choices made in the development of the procedure, including the criteria used to extract recession limbs, and the use of averaging for the ratio of flow over successive days (Q_{n+1}/Q_n). We conclude that the procedure is robust, and is a suitable extension of the matching strip method. Secondly, the regression models for the $Q7_{10}$ and $Q97_{10}$ dependent variables were developed by means of multiple linear regression analysis. When developing models based on mean annual runoff, we found that significantly higher values for the adjusted R^2 could be achieved (0.705 and 0.717 for equations (9) and (12)), compared to models based on mean annual precipitation (0.636 and 0.645 for equations (3) and (6)). As expected, higher annual runoff (or annual precipitation) is associated with higher low flow indices. Thirdly, we explored the possibility of developing regression models based on a classification of the dominant geology for each basin as either sedimentary (n=11) or igneous (n=18). Classifying basins by dominant geology leads to an increase in model

performance as indicated by the adjusted R^2 values (up to 0.784), although standard errors were only reduced for the igneous classification. The explanatory variables of recession constant and mean annual precipitation or runoff were significant at the level <0.001 for the igneous classification, while lower significance was achieved in the case of sedimentary geology, especially for the recession constant. For mixed geology models or igneous geology models, the significance F of the models was in each case at the level <0.001. A greater sample size of sedimentary basins would be required to develop more efficient models in this type of dominant geology, perhaps by further sub-dividing sedimentary basins into two or more classifications. Finally, we demonstrated the practical application of the regression models based on limited gauging data. Although the period of record required to sufficiently estimate the recession constant depends on the runoff characteristics of a given basin, we suggest it is feasible with a period of approximately 5 to 8 years of data.

Acknowledgements

This study was carried out by the support of JICA (Japan International Cooperation Agency) at JICA Tsukuba International Center in Japan. We would like to thank the JICA officers of Tsukuba International Center and all of the course participants involved.

References

Arnold, J.G., Allen, P.M., Muttiah, R. and Bernhardt, G., 1995. Automated base flow separation and recession analysis techniques. *Ground Water*, 33 (6), 1010-1018.

Arnold, J.G. and Allen, P.M., 1999. Automated methods for estimating baseflow and ground water recharge from streamflow records. *Journal of the American Water Resources Association*, 35 (2), 411-424.

Barnes, B.S., 1939. The structure of discharge recession curves. *Trans. Am. Geophys. Union*, 20 (4), 721-725.

Beck, H.E., van Dijk, A.I.J.M., Miralles, D.G., de Jeu, R.A.M., Bruijnzeel, L.A., McVicar, T.R. and Schellekens, J., 2013. Global patterns in base flow index and recession

based on streamflow observations from 3394 catchments. *Water Resources Research*, 49, 7843–7863, doi:10.1002/2013WR013918.

Beran, M.A. and Gustard, A., 1977. A study into the low-flow characteristics of British rivers. *Journal of Hydrology*, 35, 147-157. doi:10.1016/0022-1694(77)90083-X

Berhanu, B., Seleshi, Y., Demisse, S. and Melesse, A., 2015. Flow regime classification and hydrological characterization: a case study of Ethiopian rivers. *Water*, 7 (12), 3149-3165. doi:10.3390/w7063149

Bingham, R.H., 1986. Regionalization of low-flow characteristics of Tennessee streams. U. S. Geological Survey Water-Resources Investigations Report 85-4191, 63 p.

Brandes, D., Hoffmann, J.G., and Mangarillo, J.T., 2005. Base flow recession rates, low flows, and hydrologic features of small watersheds in Pennsylvania, USA. *Journal of the American Water Resources Association*, 41 (5), 1177-1186. doi:10.1111/j.1752-1688.2005.tb03792.x

Caruso, B.S., 2000. Evaluation of low-flow frequency analysis methods. *Journal of Hydrology (NZ)*, 39 (1), 19-47.

Castiglioni, S., Castellarin, A., and Montanari, A., 2009. Prediction of low-flow indices in ungauged basins through physiographical space-based interpolation. *Journal of Hydrology*, 378, 272-280. doi:10.1016/j.jhydrol.2009.09.032

Croker, K.M., Young, A.R., Zaidman, M.D. and Rees, H.G., 2003. Flow duration curve estimation in ephemeral catchments in Portugal. *Hydrological Sciences Journal*, 48 (3), 427-439. doi:10.1623/hysj.48.3.427.45287

Curran, J.C., 1990. Low flow estimation based on river recession rate. *J. IWEM*, 4, 350-355.

Eng, K. and Milly, P.C.D., 2007. Relating low-flow characteristics to the base flow recession time constant at partial record stream gauges. *Water Resources Research*, 43, W01201. doi:10.1029/2006WR005293

Hall, F.R., 1968. Base flow recessions: a review. *Water Resources Research*, 4 (5), 973-983.

Krakauer, N.Y., and Temimi, M., 2011. Stream recession curves and storage variability in small watersheds. *Hydrology and Earth System Sciences*, 15, 2377–2389.

Kroll, C., Luz, J., Allen, B., Vogel, R.M., 2004. Developing a watershed characteristics database to improve low streamflow prediction. *J. Hydrol. Eng*., 9 (2), 116–125.

LeBoutillier, D.W. and Waylen, P.R., 1993. A stochastic model of flow duration curves. *Water Resources Research*, 29 (10), 3535-3541. doi:10.1029/93WR01409

Nathan, R.J. and McMahon, T.A., 1990. Evaluation of automated techniques for base flow and recession analyses. *Water Resources Research*, 26 (7), 1465-1473. doi:10.1029/WR026i007p01465

Pena-Arancibia, J.L., van Dijk, A.I.J.M., Mulligan, M. and Bruijnzeel, L.A., 2010. The role of climatic and terrain attributes in estimating baseflow recession in tropical catchments. *Hydrology and Earth System Sciences*, 14, 2193-2205.

Reilly, C.F., and Kroll, C.N., 2003. Estimation of 7-day, 10-year low-streamflow statistics using baseflow correlation, *Water Resources Research*, 39 (9), 1236. doi:10.1029/2002WR001740

Rifai, H.S., Brock, S.M., Ensor, K.B. and Bedient, P.B., 2000. Determination of low-flow characteristics for Texas streams. *Journal of Water Resources Planning and Management*, 126 (5), 310-319. doi:10.1061/(ASCE)0733-9496(2000)126:5(310)

Sadegh, M., Vrugt, J.A., Gupta, H.V. and Xu, C., 2016. The soil water characteristic as new class of closed-form parametric expressions for the flow duration curve. *Journal of Hydrology*, 535, 438-456. doi:10.1016/j.jhydrol.2016.01.027

Singh, K.P. and Stall, J.B., 1971. Derivation of base flow recession curves and parameters. *Water Resources Research*, 7 (2), 292-303. doi:10.1029/WR007i002p00292

Smakhtin, V.Y., 2001. Low-flow hydrology: a review. *Journal of Hydrology*, 240, 147-186. doi:10.1016/S0022-1694(00)00340-1

Snyder, F.F., 1939. A concept of runoff-phenomena. *Eos Trans. AGU*, 20, 725-738.

Stuckey, M.H., 2006. Low-flow, base-flow, and mean-flow regression equations for Pennsylvania streams. U.S. Geological Survey Scientific Investigations Report 2006-5130, 84 p.

Sugiyama, H., 1996. Analysis and extraction of low flow recession characteristics. *Journal of the American Water Resources Association*, 32 (3), 491-497. doi:10.1111/j.1752-1688.1996.tb04047.x

Sugiyama, H., Vudhivanich, V., Whitaker, A.C. and Lorsirirat, K., 2003. Stochastic flow duration curves for evaluation of flow regimes in rivers. *Journal of the American Water Resources Association*, 39 (1), 47-58. doi:10.1111/j.1752-1688.2003.tb01560.x

Tallaksen, L.M., 1995. A review of baseflow recession analysis. *Journal of Hydrology*, 165, 349-370. doi:10.1016/0022-1694(94)02540-R

Thomas, B.F., Vogel, R.M. and Famiglietti, J.S., 2015. Objective hydrograph baseflow recession analysis. *Journal of Hydrology*, 525, 102-112. doi:10.1016/j.jhydrol.2015.03.028

van Dijk, A.I.J.M., 2010. Climate and terrain factors explaining streamflow response and recession in Australian catchments. *Hydrology and Earth System Sciences*, 14, 159-169. doi:10.5194/hess-14-159-2010

Veremu, R., 2009. Impact of variation in annual runoff on evaluation of low flow in the upper reaches of streams. Unpublished thesis, JICA Tsukuba International Center.

Vogel, R.M. and Kroll, C.N., 1992. Regional geohydrologic-geomorphic relationships for the estimation of low-flow statistics. *Water Resources Research*, 28 (9), 2451-2458.

Vogel, R.M. and Kroll, C.N., 1996. Estimation of baseflow recession constants. *Water Resources Management*, 10, 303-320.

Zecharias, Y.B. and Brutsaert, W., 1988. Recession characteristics of groundwater outflow and base flow from mountainous watersheds. *Water Resources Research*, 24 (10), 1651-1658.

5.3 Summary

In this chapter 29 dam basins in eastern Japan were used as study location. The data used for the study was collected from the dam database of Japan. The convenient procedure procedure for the matching method was explored and used to determin baseflow recession constant. Regression models were developed which could be used to estimate low flow indices. Models developed were viable for the study and can be applied to poory gauged basins in eastern Japan. The study outcome has vital impacts on sustainable management of water resources in eastern Japan.

The next chapter demonstrate the regression analysis of annual BFI and low flow index using watershed charateristics to a larger number of basins than the number used in the study above.

Chapter 6 Results of Regression Modeling of BFI and $Q7_{10}$ Analysis in Japan

6.1 Introduction

The previous chapter demonstrated a proposed easy-to-use technique for the matching strip method in estimating the recession constant of the master recession curve using the ratio of streamflow over successive days (Q_{n+1}/Q_n). The procedure was applied to 29 basins in eastern Japan to build regression models that estimate low flow indices ($Q97_{10}$ and $Q7_{10}$) through recession constant and either mean annual precipitation or mean annual runoff (Whitaker et al., 2022).

This chapter presents the results of regression modeling of BFI and low flow index, $Q7_{10}$ (seven-day ten-year low flow), using watershed characteristics such as land surface elevation from DEM, mean annual runoff, and the mean annual precipitation and among others. The ArcGIS 10.5 version and OriginPro software were used to analyze watershed characteristics included in the study for conducting multiple regression.

The mean annual runoff for the study basins is 2533 mm. The basin area ranged between 6.1 km^2 and 254 km^2 (Table 17). The elevation from DEM of each basin ranges from 35.6 m a.s.l. to 3092 m a.s.l. The study region lithology for basins is mainly dominated by either sedimentary (Sed) or igneous rocks (Ig). The annual precipitation (P) ranges between 781 mm and 4257 mm. The average annual precipitation (P) for the study area is about 2051 mm and the AMeDAS stations are shown in Table 18.

This chapter covers a study area located in Japan with the geographic coordinates between 35° N, 136° E and 41° N, 142° E. The elevation of the catchments ranges from -4 m to 3092 m above sea level (Figure 12).

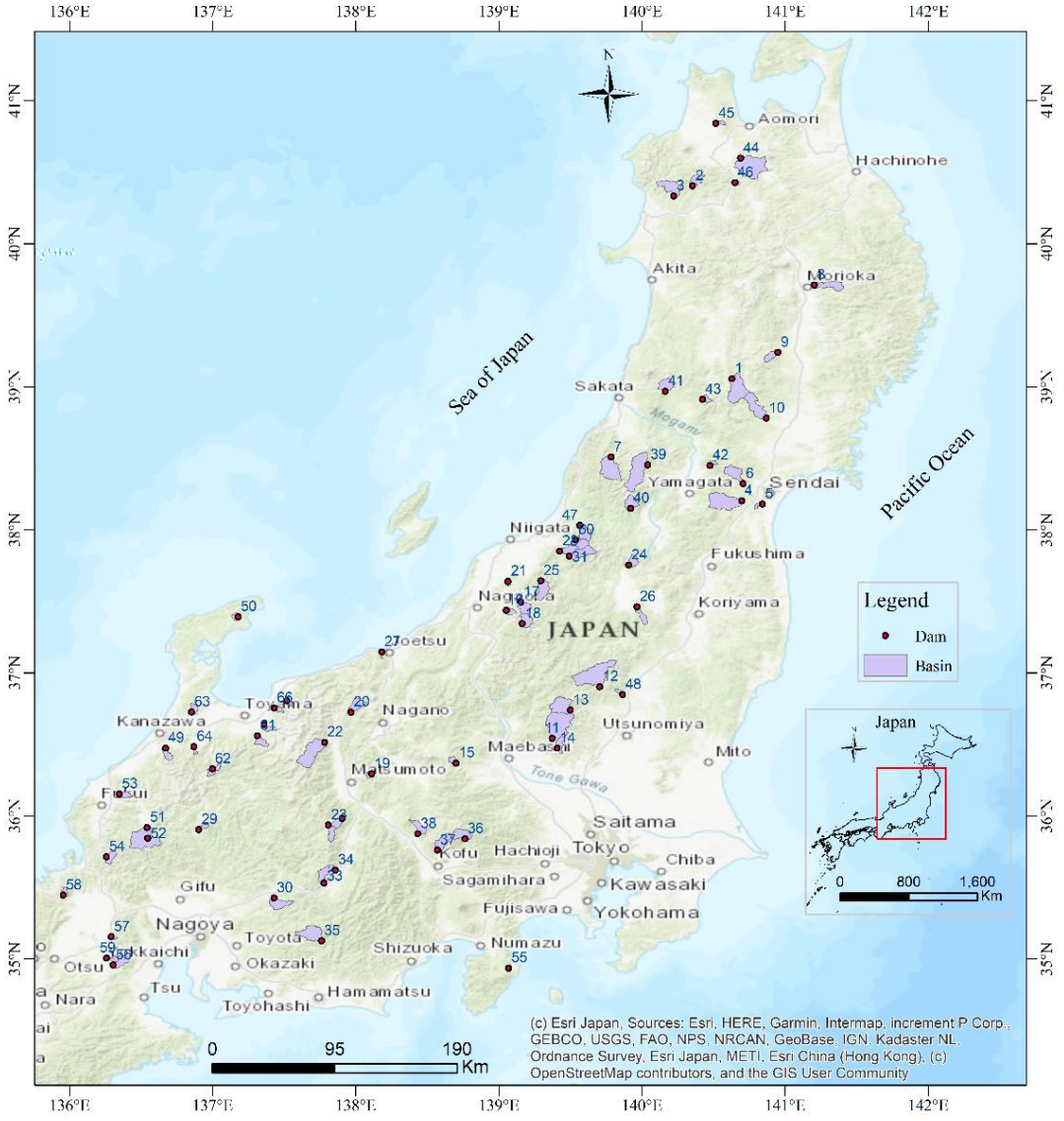

Figure 12. Location map of the study basins used for regression analysis.

Table 17. Characteristics and location of study basins. The period of record of the streamflow is 26 years (1993-2019).

No.	River system	River	Dam	Q (mm/year)	Latitude (°)	Longitude (°)	Area (km^2)	Mean elevation (m a.s.l.)	Lithology
1	Omono	Minase	Minase	2326	140.6291	39.05674	172.0	677	Sed
2	Yoneshiro	Hayaguchi	Hayaguchi	2709	140.3540	40.40531	48.5	699	Sed
3	Yoneshiro	Kasuge	Subari	3188	140.2225	40.33377	100.0	533	Sed
4	Natori	Goishi	Kamafusa	1471	140.6997	38.20028	195.3	491	Sed
5	Natori	Masuda	Tarumizu	813	140.8432	38.17770	9.7	180	Sed
6	Natori	Ookura	Kaihatsu-Okura	1763	140.7060	38.32200	89.0	726	Sed
7	Aka	Arasawa	Arasawa	4722	139.7830	38.50700	162.0	720	Ig
8	Kitakami	Nakatsu	Tsunatori	727	141.2047	39.71119	83.0	621	Ig
9	Kitakami	Geto	Irihata	3173	140.9498	39.24023	38.0	766	Sed
10	Kitakami	Haza	Shoten-Hanayama	1779	140.8683	38.78134	126.9	520	Sed
11	Tone	Watarase	Kusagi	1458	139.3730	36.54222	254.0	1087	Sed
12	Tone	Ojika	Ikari	1980	139.7057	36.90299	169.2	993	Sed
13	Tone	Daiya	Chuzenji	1565	139.4986	36.73833	125.0	1618	Sed
14	Tone	Kiryu	Kiryugawa	1103	139.4078	36.47250	42.0	611	Sed
15	Tone	Kirizumi	Kirizumi	1815	138.7007	36.36863	20.4	1028	Sed
16	Shinano	Kariyatagawa	Kariyata	3492	139.0520	37.43700	24.0	630	Ig
17	Shinano	Ikarashi	Oya	1907	139.4000	37.49500	56.2	563	Ig
18	Shinano	Aburumagawa	Aburumagawa	4653	139.1640	37.34300	59.0	876	Ig
19	Shinano	Uchimura	Uchimura	899	138.1110	36.29200	13.0	1203	Ig
20	Shinano	Susobana	Oku-Susobana	2096	137.9670	36.72500	65.0	1399	Sed
21	Shinano	Shimojo	Gejogawa	1930	139.0644	37.63944	6.1	100	Sed
22	Shinano	Takase	Omachi	2910	137.7822	36.51639	193.0	1913	Ig
23	Shinano	Narai	Narai	1628	137.8106	35.93194	46.0	1605	Ig
24	Agano	Oshikiri	Nitchu	1968	139.9097	37.75389	40.6	956	Ig
25	Agano	Hayade	Hayade	4303	139.2930	37.64200	83.0	640	Sed
26	Agano	Yukawa	Higashiyama	1283	139.9660	37.46100	40.5	735	Sed
27	Sekigawa	Masayoshiji	Shozenji	2771	138.1825	37.14541	6.3	187	Sed
28	Kaji	Uchinokura	Uchinokura	4250	139.4240	37.85000	48.0	695	Sed

29	Kiso	Atagi	Atagi	2286	136.9031	35.90417	16.0	1042	Ig
30	Kiso	Agikawa	Akigawa	1343	137.4320	35.42500	82.0	716	Ig
31	Kaji	Kaji	Kajigawa	3143	139.4923	37.81493	88.0	1018	Ig
32	Tenryu	Yokokawa	Yokokawa	1441	137.9069	35.97806	38.8	1479	Ig
33	Tenryu	Matsukawa	Matsukawa	1353	137.7806	35.52833	60.0	1468	Ig
34	Tenryu	Katagiri-Matsukawa	Katagiri	2702	137.8533	35.61833	15.1	1560	Ig
35	Tenryu	Oiri	Shintoyone	1977	137.7606	35.12593	136.3	820	Ig
36	Fuji	Fuefuki	Hirose	1503	138.7661	35.83500	76.6	1715	Ig
37	Fuji	Arakawa	Arakawa	513	138.5697	35.76028	72.4	1559	Ig
38	Shoro	Daimon	Daimon	522	138.4339	35.87444	51.7	1363	Ig
39	Mogami	Sagae	Sagae	3844	140.0395	38.45450	231.0	864	Ig
40	Mogami	Okitamagawa-Kijiyama	Kijiyama	3526	139.9215	38.14945	63.0	862	Ig
41	Mogami	Sakegawa	Takasaka	3334	140.1635	38.96846	68.2	496	Sed
42	Mogami	Shiramizu	Shiramizugawa	1766	140.4794	38.44583	15.2	695	Sed
43	Mogami	Kanayama	Kamuro	2504	140.4222	38.91280	22.5	729	Sed
44	Iwaki	Asase-Ishikawa	Aseishigawa	1781	140.6964	40.59417	225.5	617	Ig
45	Iwaki	Lizume	Lizume	1071	140.5192	40.84389	11.7	232	Ig
46	Iwaki	Hirakawa	Tobe	3083	140.6542	40.42556	8.3	399	Met
47	Arakawa	Oishi	Oishi	4762	139.5681	38.03056	69.8	681	Ig
48	Naka	Miyagawa	Terayama	1234	139.8692	36.84500	11.5	686	Sed
49	Sai	Uchikawa	Uchikawa	3287	136.6703	36.47361	34.5	594	Met
50	Ukai	Ukai	Oya	1779	137.1778	37.39250	12.8	223	Sed
51	Kuzuryu	Mana	Managawa	1454	136.5409	35.91896	223.7	833	Ig
52	Kuzuryu	Mana-Saso	Sasogawa	2767	136.5475	35.84333	70.7	816	Ig
53	Kuzuryu	Takeda	Ryugahana	3004	136.3492	36.15333	31.1	612	Sed
54	Kuzuryu	Hino	Hirono	2806	136.2047	35.76944	42.3	728	Ig
55	Ito Okawa	Ito-Okawa	Okino	3012	139.0691	34.93739	11.7	321	Sed
56	Yodo	Yasu	Ozuchi	1735	136.3040	34.95597	54.3	607	Ig
57	Yodo	Uso	Usogawa	1342	136.2907	35.15403	7.8	507	Sed
58	Yodo	Ishida	Ishidagawa	3755	135.9555	35.44511	23.4	616	Ig
59	Yodo	Hino	Hinogawa	906	136.2591	35.00517	22.4	455	Sed
60	Tainai	Tainai	Tainai1	2925	139.5367	37.92741	72.2	922	Ig
61	Jinzu	Kumano	Kumanogawa	2970	137.3122	36.55972	39.8	927	Sed

62	shogawa	Toga	Mizunashi	3035	136.9986	36.32778	38.0	1261	Met
63	Oyabe	Konade	Konadegawa	2015	136.8542	36.72499	31.8	224	Sed
64	Oyabe	Yamada	Johana	2622	136.8700	36.48389	10.8	549	Met
65	Shiraiwa	Shiraiwa	Shiroiwakawa	2759	137.3601	36.63935	24.0	509	Sed
66	Kadokawa	Kadokawa	Kadogawa	6750	137.4306	36.75361	16.2	478	Sed
67	Katakai	Fuse	Fusegawa	6406	137.5183	36.80416	13.0	886	Ig

Table 18. Mean annual precipitation (MAP) and locations of AMeDAS stations which are placed at heights ranged between 2 m and 1465 m above sea level (a.s.l.).

Station no.	Station name	P (mm/year)	Period of record	Latitude (°)	Longitude (°)	Gauge height (m a.s.l.)
31296	Goshogawara	1280	1991-2020	40.8083	140.4583	9
31562	Nurukawa	1744	1991-2020	40.5150	140.7833	404
31646	Ikarigaseki	1621	1991-2020	40.4817	140.6200	135
32071	Fujisato	2081	1991-2020	40.3200	140.2933	68
32091	Jinba	2100	1991-2020	40.4033	140.6083	176
32701	Higashinaruse	1928	1991-2020	39.1783	140.6483	191
32771	Yunotai	2104	1991-2020	38.9600	140.5283	335
33371	Yabukawa	1405	1991-2020	39.7833	141.3283	680
33441	Kuzakai	1518	1991-2020	39.6500	141.3533	734
33711	Kanegasaki	1280	1991-2020	39.2250	141.0150	170
34012	Komanoyu	2125	1991-2020	38.9133	140.8283	525
34056	Uguisuzawa	1315	2001-2020	38.8050	140.9483	33
34096	Kawado	1697	1991-2020	38.7433	140.7600	170
34262	Izumigatake	2099	2005-2020	38.4067	140.7217	630
34311	Shinkawa	1569	1991-2020	38.3033	140.6367	265
34392	Sendai	1277	1991-2020	38.2617	140.8967	39
34436	Natori	1124	1991-2020	38.1383	140.9167	2
34462	Zaō	1344	2005-2020	38.1267	140.6800	112
35071	Sasunabe	2811	1991-2020	38.9183	140.2000	88
35116	Kinzan	2078	1991-2020	38.8783	140.3317	170
35256	Arasawa	3158	1991-2020	38.5083	139.7817	272
35334	Higashine	1088	1991-2020	38.4117	140.3700	105
35361	Ōisawa	2719	1991-2020	38.3900	139.9933	440
35456	Nagai	1857	1991-2020	38.1050	140.0150	210
36106	Hibara	1823	1991-2020	37.7217	140.0583	824
36176	Kitakata	1562	1991-2020	37.6583	139.8633	212
36361	Wakamatsu	1253	1991-2020	37.4883	139.9100	212
36426	Tadami	2446	1991-2020	37.3433	139.3133	377
36461	Konan	1342	1991-2020	37.3883	140.0900	536
36562	Yumoto	1635	1991-2020	37.2767	140.0633	646
36726	Tateiwa	1429	1991-2020	37.0917	139.5317	690
41076	Wǔshílǐ	1627	1991-2020	36.9217	139.6950	620
41116	Torobu	1627	1991-2020	36.8917	139.5683	925
41166	Okunikkō	2202	1991-2020	36.7383	139.5000	1292
41181	Shioya	1671	1991-2020	36.7567	139.8833	225
41211	Ashio	1808	1991-2020	36.6467	139.4483	650
42266	Kiryuu	1269	1991-2020	36.4100	139.3250	117
42286	Kamisato	1355	1991-2020	36.3767	138.8950	183
42326	Nishinomaki	1300	1991-2020	36.2450	138.7067	375
48146	Kinasa	1624	1991-2020	36.6883	137.9650	778
48191	Ōmachi	1406	1991-2020	36.5233	137.8317	784
48331	Karuizawa	1246	1991-2020	36.3417	138.5467	999
48371	Shikakyoyu	1251	1991-2020	36.3017	138.1367	721
48536	Kiso Yabuhara	1781	1991-2020	35.9367	137.7867	985
48546	Tatsuno	1436	1991-2020	35.9833	137.9833	732
48571	Nobeyama	1432	1991-2020	35.9483	138.4717	1350
48731	Ījima	2014	1991-2020	35.6533	137.8983	728
48767	Iida	1688	1991-2020	35.5233	137.8217	516
49036	Ōizumi	1147	1991-2020	35.8617	138.3867	867
49052	Otome mizūmi	1417	2008-2022	35.8067	138.6550	1465
50226	Sakuma	2344	1991-2020	35.0567	137.7617	150
50427	Amagisan	4528	1991-2020	34.8717	139.0233	1066
51077	Chausuyama	2443	1991-2020	35.2200	137.6600	1216
52041	Kawai	2050	1991-2020	36.3050	137.1000	471
52081	Shirakawa	2458	1991-2020	36.2733	136.8967	478
52221	Nagataki	3075	1991-2020	35.9233	136.8317	430
52556	Ena	1785	1991-2020	35.4467	137.4033	315
54191	Shimonoseki	1712	1991-2020	38.0917	139.5633	33

54311	Akatani	3252	1991-2020	37.8350	139.4150	135
54396	Sanjō	2056	1991-2020	37.6400	138.9550	9
54462	Miyayose	2929	1991-2020	37.5800	139.1400	125
54472	Murotani	3166	1993-2022	37.5500	139.3700	200
54506	Tochio	2004	1991-2020	37.4750	138.9917	83
54566	Sumon	3105	1991-2020	37.3467	139.0433	222
54651	Takada	2837	1991-2020	37.1067	138.2467	13
55056	Uodzu	2588	1991-2020	36.8217	137.4283	48
55063	Unadzuki	3587	1991-2020	36.8467	137.5567	160
55156	Ōyama	2851	1991-2020	36.6083	137.2833	128
55166	Kamiichi	1358	1991-2020	36.6700	137.4233	296
55191	Nantotakamiya	2597	1991-2020	36.5450	136.8717	91
55217	Tateyamaashikura	2995	2010-2022	36.5767	137.3850	379
55252	Gokayama	2899	2004-2020	36.4300	136.9417	357
55267	Inotani	2331	1996-2020	36.4733	137.2367	215
56036	Suzu	2019	1991-2020	37.4467	137.2867	4
56192	Hōdatsushimizu	1950	2003-2022	36.7883	136.7683	90
56232	Iōzen	1925	1991-2020	36.5200	136.7450	420
56286	Hakusankawachi	2901	1991-2020	36.3967	136.6200	136
56301	Kagasugaya	3086	1991-2020	36.2300	136.3617	83
57121	Ōno	2291	1991-2020	35.9717	136.4967	182
57176	Kuzuryū	2702	1991-2020	35.9083	136.6683	436
57206	Imajō	2608	1991-2020	35.7667	136.2000	128
60051	Imadzu	1947	1991-2020	35.4117	136.0283	88
60131	Hikone	1610	1991-2020	35.2750	136.2433	87
60196	Higashiomi	1441	1991-2020	35.0617	136.1900	128
60236	Tsuchiyama	1640	1991-2020	34.9383	136.2783	248

The ArcGIS software was used to determine the watershed flow length, basin drainage area, and elevation by defining the digital elevation model (DEM) within the boundaries of the watersheds in ArcGIS. Spearman's correlation was performed to produce a correlation matrix figure shown in Figure 13. Annual BFI correlated with mean annual runoff and elevation better than other variables, while $Q7_{10}$ was associated with mean annual runoff, elevation, and mean annual precipitation better than other watershed characteristics. The regression modeling was performed in the case of all basins (53) and specific for basins dominantly classified into sedimentary (25 basins) or igneous lithology (25 basins). Model validation was performed by randomly selected basins (an approximately 20 per cent) for each lithology. No regression modeling was performed for the remaining 4 basins in Table 17 which were classified into metamorphic (Met) lithology. The regression models developed could be applied in poorly gauged watersheds

in Japan to support sustainable water resources management to contribute towards attaining the sustainable development goal 6.

6.2 Results

Prior to model development, the Spearman correlation test was used to determine the correlation between the dependent variables BFI, and $Q7_{10}$ and the independent variables described by various watershed characteristics (Tables 19-20).

Table 19. Watershed characteristics and flow indices for multiple regression modeling.

Watershed characteristics	Abbreviation	Unit
Basin drainage area	A	km^2
Annual runoff	Q	mm
Minimum elevation	Z_{min}	m
Maximum elevation	Z_{max}	m
Mean elevation	Z_{mean}	m
Annual precipitation	P	mm
Annual BFI	BFI_{ann}	No unit
Low flow index	$Q7_{10}$	mm
Flow length	L_{flow}	km

The correlation analysis in the heatmap (Figure 13) showed that mean annual runoff (Q) and mean elevation (Z_{mean}) with correlation coefficients of 0.25 and 0.30 respectively, were independent variables highly correlated with annual BFI (BFI_{ann}), while mean annual runoff (Q) maximum elevation (Z_{max}) with correlation coefficients of 0.51 and 0.28 respectively, were highly associated with $Q7_{10}$ (Figure 13). The Spearman correlation was used when measuring the relationship between two ordinal variables and are significant at 5% significance level (Table 20; Figure 13). Some basin flow length values in the Table 20, were missing because they shoed errors during the flow length analysis with ArcGIS hydrological tools, so they were not considered for correlation

analysis. The values of watershed characteristics used for Spearman's correlation and regression analysis are shown in Table 20.

Table 20. Values of watershed characteristics used for Spearman's correlation.

No.	A (km^2)	Q (mm (yr^{-1})	Z_{min} (m a.s.l.)	Z_{max} (m a.s.l.)	Z_{mean} (m a.s.l.)	P (mm yr^{-1})	BFI_{ann}	$Q7_{10}$ (mm)	L_{flow} (km)
1	172.0	2326	233	1428	677	1666	0.573	0.800	32.935
2	48.5	2709	303	1163	699	2081	0.495	1.080	17.743
3	100.0	3188	128	1133	533	2081	0.452	0.766	28.399
4	195.3	1471	136	1453	491	1344	0.526	0.712	32.155
5	9.7	813	51	317	180	1201	0.173	0.030	8.931
6	89.0	1763	254	1475	726	1834	0.561	0.907	23.324
7	162.0	4722	230	1755	720	3158	0.515	1.467	
8	83.0	727	183	1215	621	1461	0.523	0.211	32.686
9	38.0	3173	340	1336	766	1280	0.553	0.982	14.620
10	126.9	1779	108	1559	520	1712	0.572	1.200	35.267
11	254.0	1458	421	2097	1087	1808	0.521	0.504	
12	169.2	1980	550	1816	993	1561	0.576	0.865	
13	125.0	1565	1266	2464	1618	1627	0.675	1.564	
14	42.0	1103	231	1180	611	1269	0.481	0.371	14.204
15	20.4	1815	594	1581	1028	1300	0.631	0.664	7.989
16	24.0	3492	250	1427	630	2555	0.564	1.519	11.329
17	56.2	1907	186	1298	563	2929	0.341	0.269	14.610
18	59.0	4653	435	1571	876	2446	0.551	1.496	15.236
19	13.0	899	821	1776	1203	1251	0.473	0.174	
20	65.0	2096	866	2315	1399	1624	0.510	0.754	16.377
21	6.1	1930	36	180	100	2056	0.453	0.280	5.120
22	193.0	2910	879	3092	1913	1406	0.708	1.140	
23	46.0	1628	1043	2617	1605	1781	0.675	1.202	16.842
24	40.6	1968	448	1574	956	781	0.579	0.452	9.461
25	83.0	4303	173	1226	640	3166	0.435	0.350	
26	40.5	1283	392	1068	735	1410	0.624	0.968	18.900
27	6.3	2771	85	387	187	2837	0.453	0.183	6.423
28	48.0	4250	139	1407	695	3252	0.641	1.500	14.584
29	16.0	2286	569	1642	1042	3075	0.414	1.040	9.908
30	82.0	1343	397	1694	716	1785	0.464	0.560	13.246
31	88.0	3143	256	2110	1018	3252	0.517	0.750	15.226
32	38.8	1441	898	2271	1479	1436	0.628	0.600	8.305
33	60.0	1353	673	2340	1468	1688	0.265	0.018	18.893
34	15.1	2702	887	2306	1560	2014	0.533	1.150	5.497
35	136.3	1977	460	1390	820	2394	0.386	0.700	
36	76.6	1503	1047	2575	1715	1417	0.620	1.209	11.837
37	72.4	513	784	2587	1559	1417	0.398	0.090	20.321
38	51.7	522	885	2844	1363	1290	0.355	0.029	16.322

39	231.0	3844	361	1963	864	2719	0.633	1.690	33.538
40	63.0	3526	470	1585	862	1857	0.654	1.936	11.981
41	68.2	3334	186	1118	496	2811	0.432	0.970	11.981
42	15.2	1766	330	1217	695	1088	0.544	0.177	7.781
43	22.5	2504	364	1329	729	1039	0.478	0.267	8.554
44	225.5	1781	178	1495	617	1744	0.703	1.667	35.720
45	11.7	1071	72	546	232	1280	0.436	0.020	8.461
46	8.3	3083	232	593	399	1860	0.524	0.045	5.213
47	69.8	4762	171	1706	681	1712	0.610	2.040	12.029
48	11.5	1234	363	1262	686	1671	0.740	1.391	8.589
49	34.5	3287	212	1053	594	2413	0.521	1.060	14.543
50	12.8	1779	89	425	223	2019	0.391	0.260	
51	223.7	1454	339	1606	833	2496	0.505	0.460	32.867
52	70.7	2767	520	1428	816	2496	0.378	0.024	16.274
53	31.1	3004	163	1066	612	3086	0.394	0.530	13.355
54	42.3	2806	314	1273	728	2608	0.584	0.960	11.182
55	11.7	3012	132	530	321	4528	0.504	0.750	5.606
56	54.3	1735	282	1199	607	1640	0.503	0.320	18.762
57	7.8	1342	234	743	507	1525	0.408	0.350	6.130
58	23.4	3755	289	963	616	1947	0.600	0.950	11.882
59	22.4	906	195	1089	455	1441	0.466	0.040	12.770
60	72.2	2925	334	1880	922	3252	0.406	0.020	13.866
61	39.8	2970	298	1697	927	2726	0.545	1.400	11.259
62	38.0	3035	898	1609	1261	2254	0.729	2.200	9.522
63	31.8	2015	95	485	224	1950	0.438	0.310	13.447
64	10.8	2622	260	1122	549	2748	0.459	0.560	7.880
65	24.0	2759	126	1212	509	2177	0.554	0.370	13.633
66	16.2	6750	124	1083	478	2588	0.650	0.400	5.753
67	13.0	6406	289	1765	886	3587	0.650	2.200	4.804

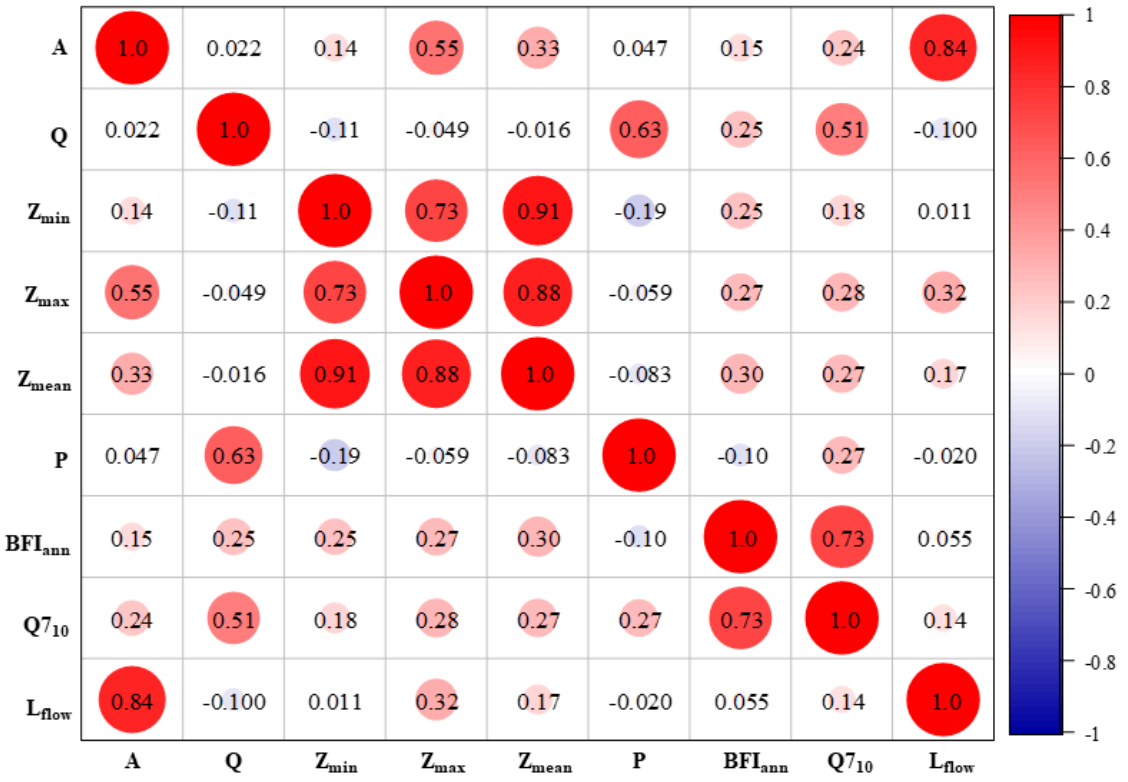

Figure 13. Correlation heatmap showing the correlation coefficients of variables.

Model development steps were followed using two independent variables (i.e., Q and Z_{mean} for Models 1, 3 and 6, and Q and Z_{max} for Models 2, 4 and 6). In the past, similar procedures were used to build an equation for BFI (Ahiablame et al., 2013; Senocak and Tasci, 2022). The models were developed as shown in Table 21 below:

Table 21. Regression models developed.

Dominant lithology	Model no.	Equation	No.
All basins (n=53)	1	$BFI_{ann} = 10^{-1.336}.Q^{0.179}.Z_{mean}^{0.157}$	(1)
	2	$Q7_{10} = 10^{-7.020}.Q^{1.308}.Z_{max}^{0.756}$	(2)
Sedimentary (n=25)	3	$BFI_{ann} = 10^{-1.348}.Q^{0.115}.Z_{mean}^{0.241}$	(1)
	4	$Q7_{10} = 10^{-6.375}.Q^{0.718}.Z_{max}^{1.206}$	(2)
Igneous (n=25)	5	$BFI_{ann} = 10^{-0.861}.Q^{0.149}.Z_{mean}^{0.024}$	(5)
	6	$Q7_{10} = 10^{-7.776}.Q^{1.474}.Z_{max}^{0.773}$	(6)

Table 21 shows the regression models for the BFI_{ann} (Models 1, 3 and 5) which are based on mean annual runoff (Q) and mean elevation (Z_{mean}), while the regression models for the $Q7_{10}$ (Model 2, 4 and 6) are dependent on mean annual runoff (Q) and maximum elevation (Z_{max}) variables.

Table 22. Analysis of variance of annual BFI and $Q7_{10}$ models.

Model	No.	Source	Degree of freedom	Sum of squares	Mean of squares	Signif. F
BFI_{ann}	1	Regression	2	0.170	0.085	**0.000**
		Error	50	0.449	0.009	
		Total	52	0.620		
$Q7_{10}$	2	Regression	2	7.329	3.664	**<0.0001**
		Error	50	7.854	0.157	
		Total	52	15.183		
BFI_{ann}	3	Regression	2	0.127	0.064	**0.007**
		Error	22	0.220	0.010	
		Total	24	0.347		
$Q7_{10}$	4	Regression	2	2.530	1.265	**0.000**
		Error	22	2.284	0.104	
		Total	24	4.814		
BFI_{ann}	5	Regression	2	0.038	0.019	0.194
		Error	22	0.235	0.011	
		Total	24	0.272		
$Q7_{10}$	6	Regression	2	3.713	1.857	**0.015**
		Error	22	7.966	0.362	
		Total	24	11.679		

Bold numbers indicate that they are significant at significance level 0.05

Table 23. Coefficients of determination of annual BFI and $Q7_{10}$ models according to dominant lithology.

Dominant lithology	No.	Model	R^2	Adjusted R^2	Standard error of estimated model
All basins (n=53)	1	BFI_{ann}	0.275	0.246	0.008
	2	$Q7_{10}$	0.483	0.462	0.219
Sedimentary (n=25)	3	BFI_{ann}	0.366	0.309	0.004
	4	$Q7_{10}$	0.526	0.482	0.272
Igneous (n=25)	5	BFIann	0.139	0.060	0.010
	6	$Q7_{10}$	0.318	0.256	0.362

Table 24. Regression coefficients of annual BFI and $Q7_{10}$ models.

No.	Model	Model variables	Unstandardized coefficients		Standardized coefficients		
			Value	Standard error	Value	t	P-value
1	BFI_{ann}	Intercept	-1.336	0.239		-5.592	**<0.0001**
		Q	0.179	0.054	0.425	3.311	**0.002**
		Z_{mean}	0.157	0.052	0.333	3.006	**0.004**
2	$Q7_{10}$	Intercept	-7.020	1.005		-6.983	**<0.0001**
		Q	1.308	0.219	0.608	5.975	**<0.0001**
		Z_{max}	0.756	0.216	0.357	3.506	**0.001**
3	BFI_{ann}	Intercept	-1.348	0.366		-3.687	**0.001**
		Q	0.115	0.099	0.199	1.162	0.258
		Z_{mean}	0.241	0.076	0.546	3.186	**0.004**
4	$Q7_{10}$	Intercept	-6.375	1.313		-4.855	**<0.0001**
		Q	0.718	0.341	0.315	2.102	**0.047**
		Z_{max}	1.206	0.305	0.593	3.960	**0.001**
5	BFI_{ann}	Intercept	-0.861	0.449		-1.918	0.068
		Q	0.149	0.079	0.377	1.879	0.074
		Z_{mean}	0.024	0.110	0.044	0.217	0.830
6	$Q7_{10}$	Intercept	-7.776	3.176		-2.449	**0.023**
		Q	1.474	0.470	0.554	3.133	**0.005**
		Z_{max}	0.773	0.817	0.167	0.947	0.354

Bold numbers indicate that they are significant at significance level 0.05

Table 25. Variance inflation factor (VIF) and Durbin Watson (DW) statistics of models.

Dominant lithology	No.	Model	Independent variables	VIF	DW statistic
All basins (n=53)	1	BFI_{ann}	LogQ $LogZ_{mean}$	1.003 1.003	2.035
	2	$Q7_{10}$	LogQ $LogZ_{max}$	1.001 1.001	2.094
Sedimentary (n=25)	3	BFI_{ann}	LogQ $LogZ_{mean}$	1.018 1.018	2.546
	4	$Q7_{10}$	LogQ $LogZ_{max}$	1.041 1.041	2.368
Igneous (n=25)	5	BFI_{ann}	LogQ $LogZ_{mean}$	1.029 1.029	2.230
	6	$Q7_{10}$	LogQ $LogZ_{max}$	1.008 1.008	2.096

Table 26. Normality test (Shapiro-wilk) of the models.

Dominant lithology	No.	Model	Statistics (W)	Degree of freedom	P-value
All basins (n=53)	1	BFI_{ann}	0.922	50	**0.002**
	2	$Q7_{10}$	0.907	50	**0.001**
Sedimentary (n=25)	3	BFI_{ann}	0.948	22	0.224
	4	$Q7_{10}$	0.952	22	0.275
Igneous (n=25)	5	BFI_{ann}	0.963	22	0.479
	6	$Q7_{10}$	0.746	22	**<0.0001**

Bold numbers indicate that they are significant at significance level 0.05

6.3 Discussion

6.3.1 Regression models of the BFI_{ann} and the $Q7_{10}$ in all basins lumped together

For the regression models 1 and 2 representing all basins lumped together, the significance F values are <0.001 (Table 22) and the adjusted R^2 values are 0.246 and 0.462 (Table 23), respectively. The significance of each independent variable is indicated by the *p*-values, with both mean annual runoff and the mean elevation having a high level of significance (*p*-value = <0.005 in both models) as shown in Table 24. These results show that the all basin lumped models are feasible for the study region, with standard errors of 0.008 and 0.157 for the BFI_{ann} and $Q7_{10}$ dependent variables, respectively (Table 23). In addition, the variance inflation factors (VIF) calculated for the BFI_{ann} and $Q7_{10}$ models were 1.003 and 1.001 respectively indicating that the variables were not correlated under ideal conditions (Table 25). The VIF is used to identify the severity of multicollinearity in the ordinary least square (OLS) regression analysis. The Durbin Watson (DW) statistic values for models 1 and 2 were determined to be 2.035 and 2.094 respectively indicating that there was no autocorrelation (DW is approximately equal to 2) (Table 25). The *P*-values associated with the Shapiro-Wilk test statistic (W) were found to be less than 0.05 for models 1 and 2 indicating that the data significantly deviated from a normal distribution (Table 26).

6.3.2 Regression models of the BFI_{ann} and the $Q7_{10}$ in sedimentary lithology

In the sedimentary classification model, the significance F values were each less than 0.01 and the *p*-values of individual independent variables were lower for $Q7_{10}$ (model 4) than values for BFI_{ann} (Model 3). The value for the adjusted R^2 for the model 4 (up to 0.482), was significantly higher than the value for the model 3 (up to 0.309), although standard error was only reduced for the sedimentary classification (model 3) with 0.004. This may

be associated to the clustered distribution of values for model 3 compared to a more scattered distribution of low flow indices for the model 4. The VIF values determined for both models showed that variables were not correlated under ideal condition and their DW statistic values for each model was within an acceptable range (1.50 - 2.50) implying that there was almost no autocorrelation (Table 25). The results of the test on the normality of the residuals (Shapiro-Wilk) for models 3 and 4 showed that the residuals followed a normal distribution as calculated *p*-values (0.224) for model 3 and (0.275) for model 4 are greater than the significance level 0.05 (Table 26). The Shapiro-Wilk test is based on the following hypotheses: the null hypothesis (H0) is that the residuals follow a normal distribution, and the alternative hypothesis (Ha) is that the residuals do not follow a normal distribution. The results revealed that both BFI_{ann} (model 3) and $Q7_{10}$ (model 4) are viable for the study region dominated by sedimentary lithology.

6.3.3 Regression models of the BFI_{ann} and the $Q7_{10}$ in Igneous lithology

When developing regression models based on Igneous dominant lithology, surprisingly we found that lowest values for the adjusted R^2 could be detected (down to 0.060 for model 5). In comparison with values in sedimentary basin BFI_{ann} model, standard error was only reduced for the igneous classification (models 5) although the significance F and the *p*-values were each >0.01, while for the sedimentary classification model 6 ($Q7_{10}$) the level of significance F was lower, especially for the *p*-value of the mean annual runoff (Q) constant independent variable with 0.003. The results indicated that the regression model 5 did not provide a better fit to the variables although values for VIF, DW and W were within an acceptable range (Tables 25 and 26). The model 6 is viable for the study region dominated by igneous lithology and its calculated values for VIF and DW were with a suitable range. The test on the normality of the residuals (Shapiro-Wilk) for models

6 revealed that the residuals were not normally distributed with *p*-value of 0.001 (Table 26).

6.4 Summary

This paper introduces a simple method to develop regression models that are practical for estimating baseflow and low flow indices through mean annual runoff in combination with data on dominant lithology and either mean elevation or maximum elevation. Average daily flow data were used in 67 watersheds mostly sited in the mountainous region of eastern Japan with high variability in lithology and climate, and often with the influence snowmelt season and partially with typhoon in the Pacific Ocean side. Average annual baseflow index for each individual watershed was quantified by using the Baseflow Index Programme which separates baseflow volume from the total flow volume. BFI is the ratio of baseflow volume to the total flow volume. $Q7_{10}$ is a seven day average minimum flow occurring once in ten years (ten year return period). The regression models for the BFI_{ann} and $Q7_{10}$ dependent variables were built by means of multiple linear regression analysis. When building models dependent on maximum elevation, significantly higher values were found for the adjusted R^2 could be achieved (0.482) for model 4, compared to model dependent on mean elevation (0.309) in dominant sedimentary basin. We discovered the possibility of developing regression models based on a classification of the dominant lithology for each basin as either sedimentary (n=25) or igneous (n=25). Classifying basins by sedimentary dominant lithology leads to an increase in model performance as indicated by the adjusted R^2 values (up to 0.482). The values for F and *P*-values were not significant for the regression model 5 with a reduced $R^2 = 0.06$ for the igneous classification.

If we look at the equation terms of the regression models in Table 21, we can see

that the signs for the explanatory variables of mean annual runoff and elevation are always positive. This is as we expect, with higher annual runoff and higher elevation related with higher baseflow and low flow indices. In this chapter regression models were presented based on two independent variables such as the mean annual runoff (Q) in combination with either mean elevation (Z_{mean}) or maximum elevation (Z_{max}). When comparing models based on mean elevation (BFI_{ann}) with those based on maximum elevation ($Q7_{10}$) (Tables 27 and 28), we can see that in the sedimentary basins, a higher model performance is obtained when using mean annual runoff. However, in the case of models based on Igneous lithology, the lower performance can go either way between mean elevation or maximum elevation as the second explanatory variable. Overall we obtained a slightly higher model performance when using mean annual runoff and maximum elevation as the explanatory variables, with an adjusted R^2 value of 0.482 compared to 0.309 when using mean elevation. Significance of regression analysis results were obtained based on conditions of some assumptions that could reveal the accuracy of the models. A summary of these assumptions are as follows:

- Multiple linear associations between explanatory variables should not exist, thus they should be independent.
- Autocorrelation of estimation errors or residuals should not exist
- The variances of estimation errors must be equal.
- Errors should be distributed normally.

Using more variables in the regression models could increase the accuracy of the estimations, but the associations between variables need to be cautiously assessed by specialists. The DEM used in this study was prepared at a spatial resolution of 90 m as shown in Chapter 3. A finer DEM could produce resolution-based variables that would

give desired accuracy of the model. Further classification of basins based on their proximity to the Sea of Japan side influenced by snowfall and heavy rainfall or Pacific Ocean side influenced with typhoon, could help to improve the accuracy of the models.

Five out of six regression models were accepted as statistically significant and viable for the study area due to significant F values and associated *p*-values (Tables 22-24) and R^2 values of the models (Figure 14) at calibration and validation stages. Tables 27 to 29 show the relative error (RE) expressed as per cent (%). The RE values were calculated in the range between -0.1 and 43.6 was obtained at the calibration stage for the model 1, RE between 3 and 40.5 were obtained at validation stage. Model 2 showed the RE in the range between 2.6 and -77.6 during the calibration stage, RE between -1.6 and -83.2 during validation stage. For the model 3, the RE values between -0.6 and -34 occurred at calibration phase and RE range between -8 and -13.5 at validation phase, while RE values between -3.3 and 79.2 occurred at calibration and RE values ranged between 0.2 and -82 at validation stage for model 4. The RE values calculated ranged between -0.4 and 80.8 at calibration stage for the model 5 and RE between -3.4 and 29.3 at validation. The RE values ranged between -4 and -71 were found at calibration stage for the model 6 and RE values between 0.7 and -82 were found at validation stage.

Table 27. Relative error values for all basins.

Model stage	Basin	Observed BFI_{ann}	Predicted BFI_{ann}	Relative error	Basin	Observed $Q7_{10}$	Predicted $Q7_{10}$	Relative error
Calibration	Minase	0.573	0.512	-10.7	Minase	0.800	0.589	-26
	Hayaguchi	0.495	0.528	6.7	Kamafusa	0.712	0.328	-54
	Subari	0.452	0.521	15.5	Tarumizu	0.030	0.048	59
	Kamafusa	0.526	0.448	-14.7	Tsunatori	0.211	0.114	-46
	Tarumizu	0.173	0.345	99.7	Shoten-Hanayama	1.200	0.444	-63
	Kaihatsu-Okura	0.561	0.492	-12.2	Kusagi	0.504	0.428	-15
	Arasawa	0.515	0.586	13.8	Ikari	0.865	0.573	-34
	Tsunatori	0.523	0.410	-21.6	Chuzenji	1.564	0.530	-66
	Irihata	0.553	0.551	-0.2	Kiryugawa	0.371	0.192	-48
	Kusagi	0.521	0.507	-2.6	Kirizumi	0.664	0.460	-31
	Ikari	0.576	0.528	-8.3	Kariyata	1.519	1.003	-34
	Kirizumi	0.631	0.523	-17.2	Oya	0.269	0.423	57
	Kariyata	0.564	0.544	-3.6	Aburumagawa	1.496	1.570	5
	Aburumagawa	0.551	0.603	9.5	Uchimura	0.174	0.200	15
	Uchimura	0.473	0.472	-0.1	Gejogawa	0.280	0.096	-66
	Gejogawa	0.453	0.367	-19.1	Omachi	1.140	1.418	24
	Omachi	0.708	0.627	-11.5	Narai	1.202	0.584	-51
	Narai	0.675	0.550	-18.6	Nitchu	0.452	0.510	13
	Nitchu	0.579	0.524	-9.4	Hayade	0.350	1.175	236
	Hayade	0.435	0.566	30.1	Higashiyama	0.968	0.217	-78
	Higashiyama	0.624	0.466	-25.3	Shozenji	0.183	0.276	51

Akigawa	0.464	0.468	0.9	Uchinokura	1.500	1.283	-14
Kajigawa	0.517	0.576	11.4	Kajigawa	0.750	1.174	57
Matsukawa	0.265	0.524	98.1	Yokokawa	0.600	0.448	-25
Katagiri	0.533	0.599	12.4	Matsukawa	0.018	0.422	2281
Shintoyone	0.386	0.512	32.7	Katagiri	1.150	1.031	-10
Hirose	0.620	0.548	-11.6	Shintoyone	0.700	0.467	-33
Arakawa	0.398	0.445	12.0	Hirose	1.209	0.520	-57
Daimon	0.355	0.437	23.3	Arakawa	0.090	0.128	42
Sagae	0.633	0.582	-8.1	Daimon	0.029	0.140	384
Takasaka	0.432	0.520	20.2	Sagae	1.690	1.447	-14
Shiramizugawa	0.544	0.489	-10.1	Kijiyama	1.936	1.100	-43
Kamuro	0.478	0.525	9.7	Kamuro	0.267	0.615	130
Aseishigawa	0.703	0.481	-31.6	Aseishigawa	1.667	0.430	-74
Lizume	0.436	0.377	-13.5	Lizume	0.020	0.103	417
Tobe	0.524	0.495	-5.6	Tobe	0.045	0.439	875
Terayama	0.740	0.458	-38.2	Oishi	2.040	1.722	-16
Uchikawa	0.521	0.533	2.3	Uchikawa	1.060	0.736	-31
Oya	0.391	0.410	4.8	Oya	0.260	0.166	-36
Managawa	0.505	0.486	-3.8	Managawa	0.460	0.348	-24
Sasogawa	0.378	0.543	43.6	Ryugahana	0.530	0.660	25
Ryugahana	0.394	0.527	33.8	Hirono	0.960	0.691	-28
Hirono	0.584	0.535	-8.4	Okino	0.750	0.391	-48
Okino	0.504	0.477	-5.3	Ozuchi	0.320	0.352	10
Ozuchi	0.503	0.477	-5.2	Usogawa	0.350	0.175	-50
Usogawa	0.408	0.443	8.5	Ishidagawa	0.950	0.819	-14
Ishidagawa	0.600	0.549	-8.5	Hinogawa	0.040	0.140	250
Mizunashi	0.729	0.592	-18.9	Mizunashi	2.200	0.914	-58

	Konadegawa	0.438	0.419	-4.3	Konadegawa	0.310	0.216	-30
	Johana	0.459	0.506	10.1	Johana	0.560	0.575	3
	Shiroiwakawa	0.554	0.505	-8.8	Shiroiwakawa	0.370	0.651	76
	Kadogawa	0.650	0.586	-9.8	Kadogawa	0.400	1.928	382
	Fusegawa	0.650	0.640	-1.6	Fusegawa	2.200	2.605	18
Validation	Shoten-Hanayama	0.572	0.468	-18.1	Hayaguchi	1.080	0.616	-43
	Chuzenji	0.675	0.546	-19.0	Subari	0.766	0.748	-2
	Kiryugawa	0.481	0.441	-8.4	Kaihatsu-Okura	0.907	0.420	-54
	Oya	0.341	0.480	40.5	Arasawa	1.467	1.740	19
	Oku-Susobana	0.510	0.563	10.3	Irihata	0.982	0.842	-14
	Shozenji	0.453	0.431	-4.7	Oku-Susobana	0.754	0.741	-2
	Uchinokura	0.641	0.572	-10.8	Atagi	1.040	0.641	-38
	Atagi	0.414	0.546	31.8	Akigawa	0.560	0.327	-42
	Yokokawa	0.628	0.531	-15.5	Takasaka	0.970	0.785	-19
	Kijiyama	0.654	0.572	-12.5	Shiramizugawa	0.177	0.364	106
	Oishi	0.610	0.582	-4.6	Terayama	1.391	0.234	-83
	Hinogawa	0.466	0.406	-12.7	Sasogawa	0.024	0.740	2984
	Tainai	0.406	0.559	37.7	Tainai	0.020	0.979	4797
	Kumanogawa	0.545	0.562	3.0	Kumanogawa	1.400	0.925	-34

Table 28. Relative error values for basins classified into sedimentary lithology.

Model stage	Basin	Observed BFI_{ann}	Predicted BFI_{ann}	Relative error	Basin	Observed $Q7_{10}$	Predicted $Q7_{10}$	Relative error
Calibration	Minase	0.573	0.523	-8.7	Minase	0.800	0.703	-12.2
	Hayaguchi	0.495	0.537	8.4	Kamafusa	0.712	0.517	-27.5
	Subari	0.452	0.512	13.4	Tarumizu	0.030	0.054	79.2
	Kamafusa	0.526	0.460	-12.6	Kaihatsu-Okura	0.907	0.599	-34.0
	Tarumizu	0.173	0.337	95.5	Irihata	0.982	0.811	-17.4
	Irihata	0.553	0.559	1.1	Shoten-Hanayama	1.200	0.644	-46.3
	Shoten-Hanayama	0.572	0.476	-16.7	Kusagi	0.504	0.799	58.7
	Kusagi	0.521	0.556	6.8	Ikari	0.865	0.837	-3.3
	Ikari	0.576	0.563	-2.2	Chuzenji	1.564	1.021	-34.7
	Chuzenji	0.675	0.617	-8.6	Kiryugawa	0.371	0.327	-11.9
	Kiryugawa	0.481	0.469	-2.6	Oku-Susobana	0.754	1.168	55.0
	Oku-Susobana	0.510	0.616	20.7	Hayade	0.350	0.909	159.8
	Gejogawa	0.453	0.323	-28.7	Higashiyama	0.968	0.323	-66.6
	Hayade	0.435	0.554	27.2	Shozenji	0.183	0.165	-9.8
	Higashiyama	0.624	0.499	-20.1	Uchinokura	1.500	1.064	-29.1
	Uchinokura	0.641	0.564	-12.0	Takasaka	0.970	0.677	-30.2
	Takasaka	0.432	0.506	17.0	Shiramizugawa	0.177	0.476	169.5
	Shiramizugawa	0.544	0.510	-6.2	Kamuro	0.267	0.679	154.5
	Kamuro	0.478	0.537	12.3	Terayama	1.391	0.384	-72.4
	Terayama	0.740	0.488	-34.1	Oya	0.260	0.135	-48.3
	Oya	0.391	0.389	-0.6	Ryugahana	0.530	0.593	12.0

	Ryugahana	0.394	0.526	33.4	Usogawa	0.350	0.215	-38.4
	Kumanogawa	0.545	0.580	6.5	Hinogawa	0.040	0.257	543.7
	Konadegawa	0.438	0.394	-10.0	Kumanogawa	1.400	1.031	-26.3
	Kadogawa	0.650	0.544	-16.3	Shiroiwakawa	0.370	0.652	76.2
Validation	Kaihatsu-Okura	0.561	0.516	-8.0	Hayaguchi	1.080	0.612	-43.3
	Kirizumi	0.631	0.562	-10.9	Subari	0.766	0.666	-13.0
	Shozenji	0.453	0.392	-13.5	Kirizumi	0.664	0.665	0.2
	Okino	0.504	0.450	-10.5	Gejogawa	0.280	0.050	-82.0
	Usogawa	0.408	0.458	12.2	Okino	0.750	0.256	-65.9
	Hinogawa	0.466	0.427	-8.3	Konadegawa	0.310	0.172	-44.4
	Shiroiwakawa	0.554	0.498	-10.0	Kadogawa	0.400	1.082	170.5

Table 29. Relative error values for basins classified into igneous lithology.

Model stage	Basin	Observed BFI_{ann}	Predicted BFI_{ann}	Relative error	Basin	Observed $Q7_{10}$	Predicted $Q7_{10}$	Relative error
Calibration	Arasawa	0.515	0.566	9.9	Arasawa	1.467	1.408	-4
	Tsunatori	0.523	0.427	-18.3	Tsunatori	0.211	0.067	-68
	Kariyata	0.564	0.540	-4.3	Kariyata	1.519	0.769	-49
	Oya	0.341	0.492	44.1	Aburumagawa	1.496	1.264	-15
	Aburumagawa	0.551	0.568	3.1	Uchimura	0.174	0.123	-29
	Narai	0.675	0.493	-27.0	Narai	1.202	0.399	-67
	Nitchu	0.579	0.501	-13.5	Nitchu	0.452	0.356	-21
	Atagi	0.414	0.513	23.9	Atagi	1.040	0.459	-56
	Akigawa	0.464	0.470	1.3	Akigawa	0.560	0.215	-62
	Kajigawa	0.517	0.538	4.0	Kajigawa	0.750	0.891	19
	Yokokawa	0.628	0.483	-23.1	Yokokawa	0.600	0.299	-50
	Matsukawa	0.265	0.478	80.8	Matsukawa	0.018	0.279	1474
	Katagiri	0.533	0.531	-0.4	Shintoyone	0.700	0.326	-53
	Hirose	0.620	0.488	-21.3	Hirose	1.209	0.350	-71
	Arakawa	0.398	0.415	4.3	Daimon	0.029	0.080	174
	Daimon	0.355	0.415	16.9	Sagae	1.690	1.133	-33
	Sagae	0.633	0.552	-12.8	Kijiyama	1.936	0.846	-56
	Kijiyama	0.654	0.545	-16.7	Lizume	0.020	0.064	220
	Aseishigawa	0.703	0.488	-30.6	Oishi	2.040	1.394	-32
	Lizume	0.436	0.442	1.5	Managawa	0.460	0.231	-50
	Managawa	0.505	0.477	-5.6	Sasogawa	0.024	0.546	2174
	Sasogawa	0.378	0.525	38.7	Hirono	0.960	0.510	-47

	Hirono	0.584	0.524	-10.2	Ozuchi	0.320	0.240	-25
	Ishidagawa	0.600	0.545	-9.1	Ishidagawa	0.950	0.631	-34
	Tainai	0.406	0.531	30.6	Tainai	0.020	0.733	3563
Validation	Uchimura	0.473	0.448	-5.2	Oya	0.269	0.293	9
	Omachi	0.708	0.540	-23.8	Omachi	1.140	1.069	-6
	Shintoyone	0.386	0.499	29.3	Katagiri	1.150	0.764	-34
	Oishi	0.610	0.566	-7.2	Arakawa	0.090	0.072	-20
	Ozuchi	0.503	0.486	-3.4	Aseishigawa	1.667	0.295	-82
	Fusegawa	0.650	0.596	-8.4	Fusegawa	2.200	2.216	1

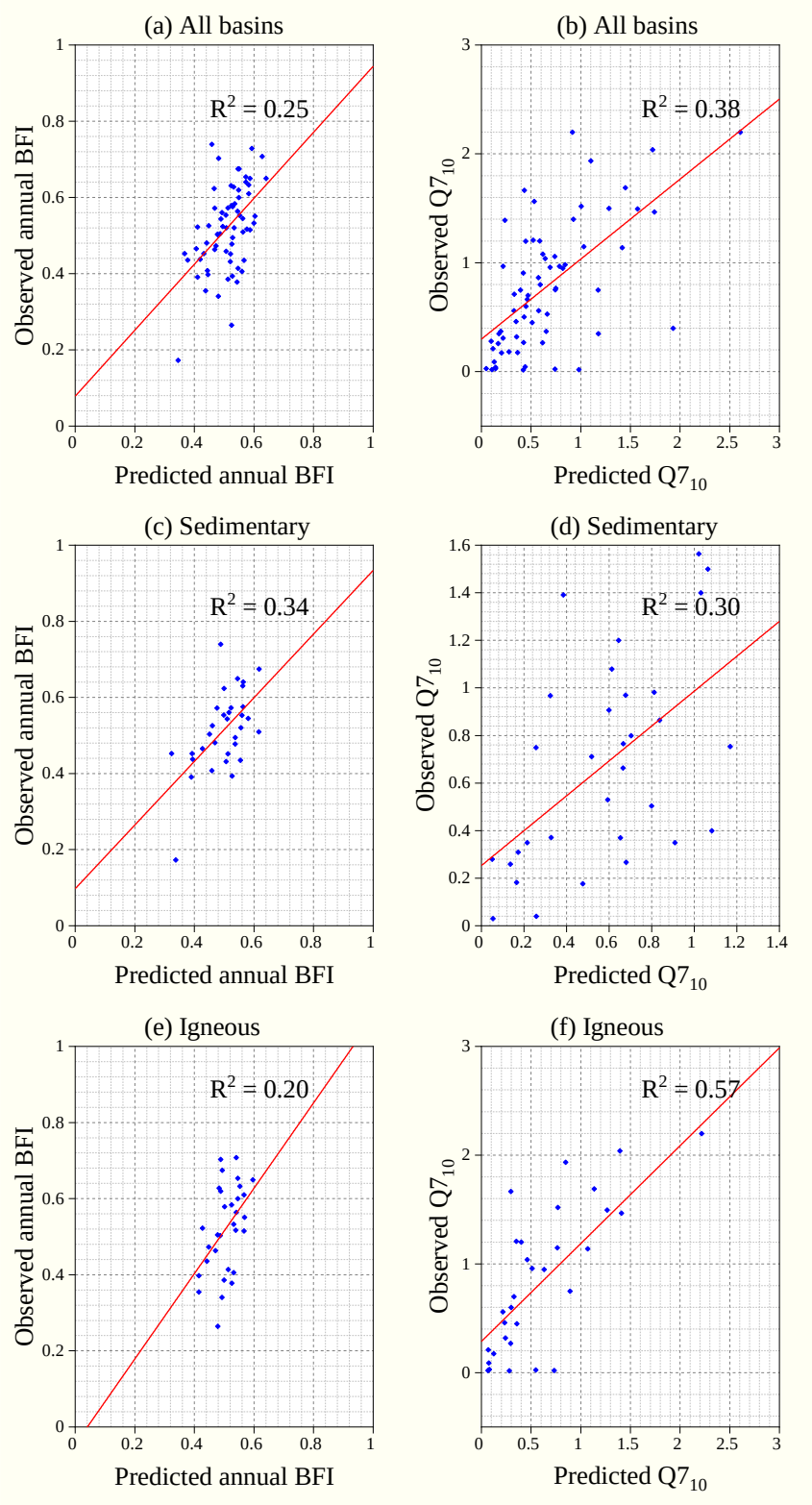

Figure 14. Comparison of observed values and values predicted by BFI_{ann} models (a), (c) and (e), and $Q7_{10}$ models (b), (d) and (f).

Chapter 7 Discussion, Recommendations and Conclusion

7.1 Introduction

Chapter 1 presented the background information, and the aim and objectives of the study. The literature review in Chapter 2 presented the study context and identified study gaps in the literature. Chapter 3 provided the study methods which were used in the thesis and employed three researches. Chapter 4 presented a study article that assessed characteristics and long-term trends of BFI and runoff in the basins located in the eastern Japan. The study is the first one to be conducted in this region. Chapter 5 presented a proposed convenient for the matching strip method in estimating the recession constant by means of the ratio of the streamflow over successive days. The method was put into practice by regression modeling of low flow indices using the estimated recession constant in combination with either mean annual runoff or mean annual precipitation in twenty nine basins located in eastern Japan. Chapter 6 demonstrated the use of watershed characteristics to build annual BFI and $Q7_{10}$ regression models for sixty seven basins with dominant lithology classification.

In this chapter, the complete study findings are discussed in comparison to the study aim and objectives. The study strengths, limitations and contribution are discussed, followed by explanations of the gap filling in the literature. The impressions of the study are discussed and recommendations for future work are expressed. Finally, section 7.4 provides a conclusion of the thesis.

7.2 Discussion

7.2.1 Restatement of aim and objectives

The study aimed to develop regression models to estimate BFI and low flow indices based on watershed characteristics and dominant lithology classification that would allow the estimation and characterization of BFI and low flow indices in ungauged or poorly gauged basins in Japan. The thesis achieved this aim by means of a series of study objectives (SO) as outlined below, which were addressed in the [related chapters]:

④ Characterize the distribution and variability of annual and seasonal BFI in eastern Japan [chapter 4]

⑤ Identify annual and seasonal trends in runoff and BFI across a range of watersheds in eastern Japan [chapter 4]

⑥ Develop regression models that can be used for estimating BFI and low flow indices based on the combination of two of the following independent variables such as elevation, mean annual runoff, mean annual precipitation, and recession constant (λ) in dominant lithological basins [chapters 5-6]

The achievement of each study objective is discussed in the following section.

7.2.2 Achievement of the study objectives

SO1 and SO2

The first and second study objectives were met through a published peer-reviewed paper for publication in chapter 4 using the eastern region of Japan as its study location. The study area is characterized by a distinct climate and hydrological regimes, with 26 watersheds on the Japan Sea and Pacific Ocean sides. The study demonstrated the

baseflow separation technique and quantified annual and seasonal BFI implemented through the use of the BFI Programme.

The study used the daily streamflow with data record periods ranging from twenty-nine to sixty-seven years. This study characterized the BFI in each watershed through the analysis of the relative frequency histograms and box charts which revealed that the distribution of BFI varied with the seasons and that high BFI values with low variability were associated with the impact of hydroclimatology. The analysis of seasonal patterns in BFI and the peak BFI and monthly runoff indicated the influence of snowmelt season on runoff and baseflow.

Annual and seasonal runoff and BFI values for watersheds in the study area were successfully quantified, alongside the detection of the long-term trends and the rate of changes per decade in runoff and BFI values. Evaluation of trends in runoff and BFI values suggested the impact of climate change, especially in basins with significant snowpack.

In the context of the study aim, the study results showed that applying the study methodology to catchments in eastern Japan was successful.

SO3

The third and final study objective was met through an academic peer-reviewed article in chapter 5 (Whitaker et al., 2022) and unpublished work in chapter 6. It demonstrated that the low flow indices ($Q7_{10}$ and $Q97_{10}$), as dependent variables of models, could be estimated based on the baseflow recession constant in combination with either mean annual runoff or mean annual precipitation in 29 dominant lithological basin classifications (Chapter 5).

Regression analysis of $Q7_{10}$ by means of explanatory variables of mean annual runoff and maximum elevation was further performed on a wider study region with 67 basins, as shown in chapter 6. The regression modeling of annual BFI was conducted by using the following independent variables: mean annual runoff and mean elevation. The data period of record ranged from 1993 to 2019.

In the context of the study aim, the study results show the successful application of the study methodology to basins on a wider study region, giving confidence in the effectiveness of the multiple regression modeling.

7.2.3 Strengths

Promotion of using easily open-access data for the study

One strength of the study is the promotion of using open-source data. The thesis used data that were available for free downloads from different online platforms shown in chapter 3. The data may be accessed from anywhere in the world.

Unique and exceptionally different characterization of the BFI

The thesis presents a work that characterizes the BFI in the basins located in eastern Japan. The study is the first of its kind in the study region. Therefore, another strength is the generation of new knowledge on BFI. The study could be linked with the variability of baseflow in basins located on the Japan sea side and Pacific Ocean side. The study was put together according to journal specifications for peer-reviewed publication.

Promotion of usage of already existing tests in hydrology to generate new knowledge

Another strength is the promotion of the already existing tests, such as the Mann-Kendall test, to detect trends in runoff and BFI to generate new results that could be linked to the

current impacts of climate change and land use change on water resources. The newly generated knowledge was published in an academic article by a reputable journal.

Provision of a platform for decision makers to take actions

Another strength of the study is the provision of a platform for policymakers to have information on the study outcomes to manage water resources sustainably.

7.2.4 Limitations

The limitation is defined as a shortcoming or weakness that might have affected the study results. The shortcomings related to this study are summarized as follows:

1. The first limitation concerns the decision to use the DEM prepared at a spatial resolution of 90 m for the regression modeling, as shown in Chapter 3. A finer DEM could produce resolution-based variables that might produce desired model accuracy compared to the accuracy obtained from the models in chapter 6.
2. The second limitation relates to the decision to prevent the inclusion of further classification of basins based on their proximity to the Sea of Japan side influenced by snowfall and heavy rainfall or the Pacific Ocean side influenced by the typhoon. The further classification of basins in chapter 6 could help to improve the accuracy of the models as the BFI and low flow indices could show variability, as demonstrated in chapter 4.
3. The third limitation concerns using only two independent variables to develop the regression models. Adding many independent variables could improve the accuracy and performance of the models in chapters 5-6, as previously reported in related studies (Ahiablame et al., 2013; Senocak and Tasci, 2022). Thus, more variables for regression modeling could be explored.

4. The fourth limitation concerns the decision to use only one turning point (0.9) parameter of the baseflow separation technique, a ‘smoothed minima’ (Tallaksen and van Lanen, 2004), throughout the thesis. The parameter of 0.9 was not adjusted for when determining the baseflow separation points (Tallaksen and van Lanen, 2004). In the future, this limitation could be addressed by adjusting the turning point parameter according to spatial location and climatic conditions of the basins, as suggested in the literature (Stoelzle et al., 2020).

7.2.5 Study contribution

This thesis has contributed to knowledge in many ways. The study contributions are outlined below:

- New investigations regarding the characterization of distribution and variability of the annual and seasonal BFI values have emerged.
- New knowledge has been generated for Japan through the detection of annual and seasonal trends in runoff and BFI across a range of catchments in eastern Japan
- A new proposed convenient procedure for the matching strip method to objectively estimate baseflow recession constant has been discovered.
- New knowledge has been generated for Japan by the development of simple multiple regression models, which could be used to estimate annual BFI and low flow indices in poorly gauged basins in Japan.

7.2.6 Filling of the study knowledge gaps

Chapter 2 provided literature that identified four study gaps. The gaps are repeated below, followed by an explanation of how this thesis dealt with them.

Knowledge gap 1: There is a need to describe the distribution and variability of annual and seasonal BFI across a range of watersheds in eastern Japan.

The results of this study provided critical, innovative insights into the behavior of BFI in watersheds to support sustainable water resources management in Japan. The methodology to address the knowledge gap was presented in Chapters 3 and 4. The study results in chapter 4 show the importance of selecting either annual BFI values or seasonal BFI values for water resources assessments in Japan.

Knowledge gap 2: There is a need to identify annual and seasonal trends in runoff and BFI across a range of watersheds in eastern Japan.

This thesis has addressed knowledge gap two by demonstrating a study methodology that identifies trends in annual and seasonal runoff and BFI in the developed world context, Japan. The methodology to meet the knowledge gap was presented in Chapters 3 and 4. The study outcomes show the success of the method in providing information for policymakers to sustainably manage water resources to achieve sustainable development goal (SDG) 6. This study will be useful to Japan and other countries in assessing the impact of climate change and anthropogenic activity on streamflow in Japan by means of runoff, precipitation, and BFI trend analysis.

Knowledge gap 3: There is a need to build and assess realistic regression models that can appropriately be used to determine low flow indices using the recession constant (λ) and other catchment or climatic characteristics in Japan where there is less related literature.

This thesis filled knowledge gap three by demonstrating the study methodology in Chapter 3, which analyses the regression models for estimating low flow indices based on baseflow recession constant together with either mean annual runoff or mean annual precipitation. The study can be used to promote low flow hydrological assessments, such as calculations of water budgets and environmental flow requirements within the study region in Japan.

Knowledge gap 4: There is a need to develop a regression model that can be appropriately used for estimating BFI by means of catchment or climatic characteristics in Japan.

The thesis addressed knowledge gap 4 through the study output in Chapter 6. Regression models could be applied to poorly gauged watersheds in eastern Japan to support the integrated water resource management and sustainable development goal 6

7.2.7 Impact of the study

This study has important implications for the sustainable management of water resources in support of integrated water resources management and modeling in Japan. The study has also had essential impacts on an improved understanding and modeling of water resources in Japan.

7.3 Recommendations

Knowledge enrichment and generation when carrying out the study provided valuable insights for future work direction. The recommendations for future work as summarized below:

7.3.1 Specific recommendations

① It is recommended that future work should investigate how annual and seasonal BFI may be impacted by continuing changes in climate, as mentioned in Chapter 4.

② Future work on regression modeling of BFI and low flow indices should include the following:

- A finer DEM could yield resolution-based parameters that might produce desired model accuracy compared to the accuracy obtained from the models in chapter 6.
- Seasonal BFI values over the data period of record should be used as the dependent variable in regression model development.
- The further classification of basins based on climate and proximity to the Sea of Japan and the Pacific Ocean side should be considered to improve the performance of the models
- Adding many several explanatory variables should be considered when developing models
- Baseflow separation technique should have a turning point factor adjusted according to spatial location and climatic conditions of the basins as suggested in the literature (Stoelzle et al., 2020).

7.4 Conclusion

In conclusion, the thesis achieved the aim of the study. A study presented investigations regarding runoff and BFI which have not been conducted before in Japan. Regional hydroclimatic characteristics, winter and spring season could have impacts on the variability and trends in BFI and runoff. The study presented a simple method to develop multiple regression models that are reliable statistically for determining low flow indices and annual BFI values with details on dominant lithology and other watershed

characteristics such as mean annual runoff, mean annual precipitation, elevation and recession constants of MRC. The study introduced robust procedure which is suitable extension of the matching strip method to determine baseflow recession constant. The study filled the knowledge gaps found in the literature review. The study findings may be used by water resource experts to perform water resources assessments, and manage water resources sustainably.

The aim was accomplished through several study objectives. Two of the study objectives were achieved by putting them together in an academic writing that was published. The third and last objective was achieved using the publication of the work as shown in chapter 5 and further study analysis was conducted to the expanded number of basins whose results were presented in Chapter 6. In line with this, the thesis is supported by peer reviewed academic papers. The study outcomes have important implications on managing water resources sustainably in Japan to contribute towards attainment of the sustainable development goal 6.

References

Ahiablame, L., Chaubey, I., Engel, B., Cherkauer, K., and Merwade, V.: Estimation of annual baseflow at ungauged sites in Indiana USA, J Hydrol (Amst), 476, 13–27, https://doi.org/10.1016/j.jhydrol.2012.10.002, 2013.

Aksoy, H., Unal, N. E., and Pektas, A. O.: Smoothed minima baseflow separation tool for perennial and intermittent streams, Hydrol Process, 22, 4467–4476, https://doi.org/10.1002/hyp.7077, 2008.

Aksoy, H., Kurt, I., and Eris, E.: Filtered smoothed minima baseflow separation method, J Hydrol (Amst), 372, 94–101, https://doi.org/10.1016/j.jhydrol.2009.03.037, 2009.

Arai, R., Toyoda, Y., and Kazama, S.: Runoff recession features in an analytical probabilistic streamflow model, J Hydrol (Amst), 597, https://doi.org/10.1016/J.JHYDROL.2020.125745, 2021.

Beck, H. E., van Dijk, A. I. J. M., Miralles, D. G., de Jeu, R. A. M., Bruijnzeel, L. A., McVicar, T. R., and Schellekens, J.: Global patterns in base flow index and recession based on streamflow observations from 3394 catchments, Water Resour Res, 49, 7843–7863, https://doi.org/10.1002/2013WR013918, 2013a.

Beck, H. E., van Dijk, A. I. J. M., Miralles, D. G., de Jeu, R. A. M., Bruijnzeel, L. A., McVicar, T. R., and Schellekens, J.: Global patterns in base flow index and recession based on streamflow observations from 3394 catchments, Water Resour Res, 49, 7843–7863, https://doi.org/10.1002/2013WR013918, 2013b.

Berhanu, B., Seleshi, Y., Demisse, S. S., and Melesse, A. M.: Flow regime classification and hydrological characterization: A case study of Ethiopian rivers, Water (Switzerland), 7, 3149–3165, https://doi.org/10.3390/w7063149, 2015.

Bloomfield, J., Gong, M., Marchant, B., Coxon, G., and Addor, N.: How is Baseflow Index (BFI) impacted by water resource management practices?, Hydrology and Earth System Sciences Discussions, 1–34, https://doi.org/10.5194/hess-2021-259, 2021.

Bloomfield, J. P., Allen, D. J., and Griffiths, K. J.: Examining geological controls on baseflow index (BFI) using regression analysis: An illustration from the Thames Basin, UK, J Hydrol (Amst), 373, 164–176, https://doi.org/10.1016/j.jhydrol.2009.04.025, 2009a.

Bloomfield, J. P., Allen, D. J., and Griffiths, K. J.: Examining geological controls on baseflow index (BFI) using regression analysis: An illustration from the Thames Basin, UK, J Hydrol (Amst), 373, 164–176, https://doi.org/10.1016/j.jhydrol.2009.04.025, 2009b.

Bloomfield, J. P., Bricker, S. H., and Newell, A. J.: Some relationships between lithology, basin form and hydrology: a case study from the Thames basin, UK, Hydrol Process, 25, 2518–2530, https://doi.org/10.1002/hyp.8024, 2011.

Bosch, D. D., Arnold, J. G., Allen, P. G., Lim, K. J., and Park, Y. S.: Temporal variations in baseflow for the Little River experimental watershed in South Georgia, USA, J Hydrol Reg Stud, 10, 110–121, https://doi.org/10.1016/j.ejrh.2017.02.002, 2017a.

Bosch, D. D., Arnold, J. G., Allen, P. G., Lim, K. J., and Park, Y. S.: Temporal variations in baseflow for the Little River experimental watershed in South Georgia, USA, J Hydrol Reg Stud, 10, 110–121, https://doi.org/10.1016/j.ejrh.2017.02.002, 2017b.

Brandes, D., Hoffmann, J. G., and Mangarillo, J. T.: Base flow recession rates, low flows, and hydrologic features of small watersheds in Pennsylvania, USA, J Am Water Resour Assoc, 41, 1177–1186, https://doi.org/10.1111/j.1752-1688.2005.tb03792.x, 2005.

Brodie, R., Sundaram, B., and Hostetler, S.: Tools for assessing groundwater-surface water interactions: a case study in the Lower Richmond catchment, NSW, Canberra, 2005.

Brodie, R., Sundaram, B., Tottenham, R., Hostetler, S., and Ransley, T.: An overview of tools for assessing groundwater-surface water connectivity, Canberra, 133: 1-133 pp., 2007.

Cameron, A. C. and Windmeijer, F. A. G.: An R-squared measure of goodness of fit for some common nonlinear regression models, J Econom, 77, 329–342, https://doi.org/10.1016/s0304-4076(96)01818-0, 1997.

Carlier, C., Wirth, S. B., Cochand, F., Hunkeler, D., and Brunner, P.: Geology controls streamflow dynamics, J Hydrol (Amst), 566, 756–769, https://doi.org/10.1016/J.JHYDROL.2018.08.069, 2018.

Caruso, B. S.: Evaluation of low-flow frequency analysis methods, Journal of Hydrology (NZ), 19–47 pp., 2000.

Castiglioni, S., Castellarin, A., and Montanari, A.: Prediction of low-flow indices in ungauged basins through physiographical space-based interpolation, J Hydrol (Amst), 378, 272–280, https://doi.org/10.1016/j.jhydrol.2009.09.032, 2009.

Chiew, F. H. S. and McMahon, T. A.: Detection of trend or change in annual flow of Australian rivers, International Journal of Climatology, 13, 643–653, https://doi.org/10.1002/JOC.3370130605, 1993.

Douglas, E. M., Vogel, R. M., and Kroll, C. N.: Trends in floods and low flows in the United States: Impact of spatial correlation, J Hydrol (Amst), 240, 90–105, https://doi.org/10.1016/S0022-1694(00)00336-X, 2000.

Easterling, D. R., Karl, T. R., Gallo, K. P., Robinson, D. A., Trenberth, K. E., and Dai, A.: Observed climate variability and change of relevance to the biosphere Is the hydrologic cycle changing? Is the weather and climate becoming more extreme or variable?, JOURNAL OF GEOPHYSICAL RESEARCH, 101–121 pp., https://doi.org/10.1029/2000JD900166, 2000.

Eckhardt, K.: How to construct recursive digital filters for baseflow separation, Hydrol Process, 19, 507–515, https://doi.org/10.1002/HYP.5675, 2005.

Eckhardt, K.: A comparison of baseflow indices, which were calculated with seven different baseflow separation methods, J Hydrol (Amst), 352, 168–173, https://doi.org/10.1016/j.jhydrol.2008.01.005, 2008.

Fujibe, F., Yamazaki, N., Katsuyama, M., and Kobayashi, K.: The Increasing Trend of Intense precipitation in Japan Based on Four-hourly Data for a Hundred Years, SOLA, 1, 041–044, https://doi.org/10.2151/sola.2005-012, 2005.

Garg, V., Chaubey, I., and Haggard, B. E.: Impact of Calibration Watershed on Runoff Model Accuracy, Transactions of the American Society of Agricultural Engineers, 46, 1347–1353, https://doi.org/10.13031/2013.15445, 2003.

Gustard, A., Bullock, A., and Dixon, J. M.: Low flow estimation in the United Kingdom, Report No. 108, Crowmarsh Gifford, Wallingford, Oxfordshire, OXIO 8BB, United Kingdom, 1992.

Hagedorn, B. and Meadows, C.: Trend analyses of baseflow and BFI for undisturbed watersheds in Michigan-constraints from multi-objective optimization, Water (Switzerland), 13, https://doi.org/10.3390/w13040564, 2021.

Hall, F. R.: Base-Flow Recessions—A Review, Water Resour Res, 4, 973–983, https://doi.org/10.1029/WR004I005P00973, 1968.

Hara, M., Yoshikane, T., Kawase, H., and Kimura, F.: Estimation of the Impact of Global Warming on Snow Depth in Japan by the Pseudo-Global-Warming Method, Hydrological Research Letters, 2, 61–64, https://doi.org/10.3178/hrl.2.61, 2008.

Helsel, D. R., Hirsch, R. M., Ryberg, K. R., Archfield, S. A., and Gilroy, E. J.: Statistical Methods in Water Resources Techniques and Methods 4 – A3, USGS Techniques and Methods, Reston, VA, 458 pp., https://doi.org/10.3133/tm4a3, 2020.

Hirsch, R. M. and Slack, J. R.: A Nonparametric Trend Test for Seasonal Data With Serial Dependence, Water Resour Res, 20, 727–732, 1984.

Hirsch, R. M., Slack, J. R., and Smith, R. A.: Techniques of Trend Analysis for Monthly Water Quality Data, Water Resour Res, 18, 107–121, 1982.

Hodgkins, G. A. and Dudley, R. W.: Historical summer base flow and stormflow trends for New England rivers, Water Resour. Res, 47, 7528, https://doi.org/10.1029/2010WR009109, 2011.

Institute of Hydrology: Low Flows Studies Report No 3, Wallingford, UK, 1980.

IPCC: Summary for Policymakers. In: Climate Change 2021: The Physical Science Basis. Contribution of Working Group I to the Sixth Assessment Report of the Intergovernmental Panel on Climate Change, edited by: Masson-Delmotte, V., P. Zhai, A. Pirani, S. L. Connors, C. Péan, S. Berger, N. Caud, Y. Chen, L. Goldfarb, M. I. Gomis,

M. Huang, K. Leitzell, E. Lonnoy, J.B.R. Matthews, T. K. Maycock, T. Waterfield, O. Yelekçi, R. Y. and B. Z., Cambridge University Press. In Press, 3949P pp., 2021.

Iwata, Y., Hirota, T., Hayashi, M., Suzuki, S., and Hasegawa, S.: Effects of frozen soil and snow cover on cold-season soil water dynamics in Tokachi, Japan, Hydrol Process, 24, 1755–1765, https://doi.org/10.1002/hyp.7621, 2010.

Jacques, J. M. S. and Sauchyn, D. J.: Increasing winter baseflow and mean annual streamflow from possible permafrost thawing in the Northwest Territories, Canada, Geophys Res Lett, 36, https://doi.org/10.1029/2008GL035822, 2009.

Japan Aerospace Exploration Agency: ALOS World 3D - 30 meter DEM. V3.2, Jan 2021. Distributed by OpenTopography, https://doi.org/10.5069/G94M92HB, 2021.

Jolánkai, Z. and Koncsos, L.: Base flow index estimation on gauged and ungauged catchments in Hungary using digital filter, multiple linear regression and artificial neural networks, Periodica Polytechnica Civil Engineering, 62, https://doi.org/10.3311/PPci.10518, 2018.

Kelly, L., Kalin, R. M., Bertram, D., Kanjaye, M., Nkhata, M., and Sibande, H.: Quantification of temporal variations in base flow index using sporadic river data: Application to the Bua catchment, Malawi, Water (Switzerland), 11, 901, https://doi.org/10.3390/w11050901, 2019.

Kelly, L., Bertram, D., Kalin, R., Ngongondo, C., and Sibande, H.: A National Scale Assessment of Temporal Variations in Groundwater Discharge to Rivers: Malawi, American Journal of Water Science and Engineering, 6, 39–49, https://doi.org/10.11648/j.ajwse.20200601.15, 2020.

Kendall, M. G.: Rank Correlation Methods, 4th ed., Griffin, London, UK, 1975.

Krause, P., Boyle, D. P., and Bäse, F.: Comparison of different efficiency criteria for hydrological model assessment, Advances in Geosciences, 5, 89–97, https://doi.org/10.5194/adgeo-5-89-2005, 2005.

LeBoutillier, D. W. and Waylen, P. R.: A stochastic model of flow duration curves, Water Resour Res, 29, 3535–3541, https://doi.org/10.1029/93WR01409, 1993.

Lei, Y., Jiang, X., Geng, W., Zhang, J., Zhao, H., and Ren, L.: The variation characteristics and influencing factors of base flow of the hexi inland rivers, Atmosphere (Basel), 12, 356, https://doi.org/10.3390/atmos12030356, 2021.

Lins, H. F. and Slack, J. R.: Seasonal and Regional Characteristics of U.S. Streamflow Trends in the United States from 1940 to 1999, Phys Geogr, 26, 489–501, https://doi.org/10.2747/0272-3646.26.6.489, 2005.

Lott, D. A. and Stewart, M. T.: Base flow separation: A comparison of analytical and mass balance methods, J Hydrol (Amst), 535, 525–533, https://doi.org/10.1016/J.JHYDROL.2016.01.063, 2016.

Lyu, S., Zhai, Y., Zhang, Y., Cheng, L., Kumar Paul, P., Song, J., Wang, Y., Huang, M., Fang, H., and Zhang, J.: Baseflow signature behaviour of mountainous catchments around the North China Plain, J Hydrol (Amst), 606, https://doi.org/10.1016/j.jhydrol.2022.127450, 2022.

Mann, H. B.: Nonparametric Tests Against Trend, Econometrica, 13, 245, https://doi.org/10.2307/1907187, 1945a.

Mann, H. B.: Nonparametric Tests Against Trend, Econometrica, 13, 245, https://doi.org/10.2307/1907187, 1945b.

Meals, D. W., Spooner, J., Dressing, S. A., and Harcum, J. B.: Statistical analysis for monotonic trends, nonpoint source monitoring: Tech Notes, U.S. Environmental Protection Agency, 2011.

Meriano, M., Howard, K. W. F., and Eyles, N.: The role of midsummer urban aquifer recharge in stormflow generation using isotopic and chemical hydrograph separation techniques, J Hydrol (Amst), 396, 82–93, https://doi.org/10.1016/j.jhydrol.2010.10.041, 2011.

Mori, N., Takemi, T., Tachikawa, Y., Tatano, H., Shimura, T., Tanaka, T., Fujimi, T., Osakada, Y., Webb, A., and Nakakita, E.: Recent nationwide climate change impact assessments of natural hazards in Japan and East Asia, Weather Clim Extrem, 32, 100309, https://doi.org/10.1016/j.wace.2021.100309, 2021.

Nathan, R. J. and McMahon, T. A.: Evaluation of automated techniques for base flow and recession analyses, Water Resour Res, 26, 1465–1473, https://doi.org/10.1029/WR026I007P01465, 1990.

Nathan, R. J. and McMahon, T. A.: Estimating low flow characteristics in ungauged catchments, Water Resources Management, 6, 85–100, https://doi.org/10.1007/BF00872205, 1992.

Nedelcev, O. and Jenicek, M.: Trends in seasonal snowpack and their relation to climate variables in mountain catchments in Czechia, Hydrological Sciences Journal, 66, 2340–2356, https://doi.org/10.1080/02626667.2021.1990298, 2021.

Oki, D. S.: Trends in streamflow characteristics at long-term gaging stations, Hawaii, U.S. Geological Survey Scientific Investigations Report 2004-5080, 120 pp., 2004.

Penna, D., van Meerveld, H. J., Oliviero, O., Zuecco, G., Assendelft, R. S., Dalla Fontana, G., and Borga, M.: Seasonal changes in runoff generation in a small forested mountain catchment, Hydrol Process, 29, 2027–2042, https://doi.org/10.1002/HYP.10347, 2015.

Piggott, A. R., Moin, S., and Southam, C.: A revised approach to the UKIH method for the calculation of baseflow/Une approche amélioréede la méthode de l'UKIH pour le calcul de l'écoulement de base, Hydrological Sciences Journal, 50, 5, 2005.

Price, K.: Effects of watershed topography, soils, land use, and climate, on baseflow hydrology in humid regions: A review, Prog Phys Geogr, 35, 465–492, https://doi.org/10.1177/0309133311402714, 2011.

Rifai, H. S., Brock, S. M., Ensor, K., and Bedient, P. B.: Determination of Low-Flow Characteristics for Texas Streams, Journal of Water Resources Planning and Management , 126, 2000.

Rougé, C., Ge, Y., and Cai, X.: Detecting gradual and abrupt changes in hydrological records, Adv Water Resour, 53, 33–44, https://doi.org/10.1016/j.advwatres.2012.09.008, 2013.

Sadegh, M., Vrugt, J. A., Gupta, H. v., and Xu, C.: The soil water characteristic as new class of closed-form parametric expressions for the flow duration curve, J Hydrol (Amst), 535, 438–456, https://doi.org/10.1016/j.jhydrol.2016.01.027, 2016.

Saedi, J., Sharifi, M. R., Saremi, A., and Babazadeh, H.: Assessing the impact of climate change and human activity on streamflow in a semiarid basin using precipitation and baseflow analysis, Sci Rep, 12, 9228, https://doi.org/10.1038/s41598-022-13143-y, 2022.

Senocak, S. and Tasci, S.: Shaping a baseflow model through multiple regression analysis: The Çoruh watershed example, Water Supply, 22, 2117–2132, https://doi.org/10.2166/WS.2021.362, 2022.

Sen, P. K.: Estimates of the Regression Coefficient Based on Kendall's Tau, J Am Stat Assoc, 63, 1379–1389, https://doi.org/10.1080/01621459.1968.10480934, 1968.

Serinaldi, F. and Kilsby, C. G.: The importance of prewhitening in change point analysis under persistence, Stochastic Environmental Research and Risk Assessment, 30, 763–777, https://doi.org/10.1007/s00477-015-1041-5, 2016.

Singh, S. K., Pahlow, M., Booker, D. J., Shankar, U., and Chamorro, A.: Towards baseflow index characterisation at national scale in New Zealand, J Hydrol (Amst), 568, 646–657, https://doi.org/10.1016/j.jhydrol.2018.11.025, 2019.

Sloto, R. A., Crouse, M. Y., and Eaton, G. P.: HYSEP: A COMPUTER PROGRAM FOR STREAMFLOW HYDROGRAPH SEPARATION AND ANALYSIS. Water-Resources Investigation Report 96-4040, Lemoyne, Pennsylvania, 1996.

Smakhtin, V. U.: Low flow hydrology: A review, J Hydrol (Amst), 240, 147–186, https://doi.org/10.1016/S0022-1694(00)00340-1, 2001.

Stoelzle, M., Schuetz, T., Weiler, M., Stahl, K., and Tallaksen, L. M.: Beyond binary baseflow separation: a delayed-flow index for multiple streamflow contributions, Hydrol Earth Syst Sci, 24, 849–867, https://doi.org/10.5194/hess-24-849-2020, 2020.

Stuckey, M. H.: Low-flow, base-flow, and mean-flow regression equations for Pennsylvania streams, 84 pp., 2006.

Sugiyama, H.: Analysis and extraction of low flow recession characteristics, Water Resources Bulletin, 32, 491–497, https://doi.org/10.1111/j.1752-1688.1996.tb04047.x, 1996.

Sugiyama, H., Vudhivanich, V., Whitaker, A. C., and Lorsirirat, K.: Stochastic flow duration curves for evaluation of flow regimes in rivers, J Am Water Resour Assoc, 39, 47–58, https://doi.org/10.1111/j.1752-1688.2003.tb01560.x, 2003.

Sun, J., Wang, X., Shahid, S., and Li, H.: An optimized baseflow separation method for assessment of seasonal and spatial variability of baseflow and the driving factors, Journal of Geographical Sciences, 31, 1873–1894, https://doi.org/10.1007/S11442-021-1927-8, 2021.

Tallaksen, L. and van Lanen, H. A.: Hydrological drought. Processes and estimation methods for streamflow and groundwater, edited by: Tallaksen, L. and van Lanen, H. A. J., Elsevier B.V., Amsterdam, 579 pp., 2004.

Tallaksen, L. M.: A review of baseflow recession analysis, J Hydrol (Amst), 165, 349–370, https://doi.org/10.1016/0022-1694(95)92779-d, 1995.

Troendle, C. A. and King, R. M.: The Effect of Timber Harvest on the Fool Creek Watershed, 30 Years Later, Water Resour Res, 21, 1915–1922, https://doi.org/10.1029/WR021I012P01915, 1985.

Vogel, R. M. and Kroll, C. N.: Estimation of baseflow recession constants, Water Resources Management, 10, 303–320, https://doi.org/10.1007/BF00508898, 1996.

Wahl, K. L. and Wahl, T. L.: Determining the Flow of Comal Springs at New Braunfels, Texas, Unknown, 95, 16–17, 1995.

Wakiyama, Y. and Yamanaka, T.: Year-to-year variation in snowmelt runoff from a small forested watershed in the mountainous region of central Japan, Hydrological Research Letters, 8, 90–95, https://doi.org/10.3178/hrl.8.90, 2014.

Whitaker, A. C. and Yoshimura, A.: Climate Change Impacts on the Seasonal Distribution of Runoff in a Snowy Headwater Basin, Niigata, Hydrological Research Letters, 6, 7–12, https://doi.org/10.3178/hrl.6.7, 2012.

Whitaker, A. C., Sugiyama H., and Hayakawa K.: Effect of snow cover conditions on the hydrologic regime: case study in a pluvial-nival watershed, Japan, Journal of American Water Resources Association, 44, 814–828, https://doi.org/10.1111/j.1752-1688.2008.00206.x, 2008.

Whitaker, A. C., Chapasa, S. N., Sagras, C., Theogene, U., Veremu, R., and Sugiyama, H.: Estimation of baseflow recession constant and regression of low flow indices in eastern Japan, Hydrological Sciences Journal, 67, 191–204, https://doi.org/10.1080/02626667.2021.2003368, 2022.

WMO: Manual on Low-flow Estimation and Prediction – Operational Manual Hydrology Report No. 50, edited by: Gustard, A. and Demuth, S., World Meteorological

Organization, German National Committee for the International Programme (IHP) of UNESCO and the Hydrology and Water Resources Programme (HWRP) of WMO, Koblenz, 1–138 pp., 2009.

Yamada, T. J., Seang, C. N., and Hoshino, T.: Influence of the long-term temperature trend on the number of new records for annual maximum daily precipitation in Japan, Atmosphere (Basel), 11, https://doi.org/10.3390/ATMOS11040371, 2020.

Yamanaka, T., Wakiyama, Y., and Suzuki, K.: Is snowmelt runoff timing in the Japanese Alps region shifting toward earlier in the year?, Hydrological Research Letters, 6, 87–91, https://doi.org/10.3178/hrl.6.87, 2012.

Yamazaki, D., Ikeshima, D., Tawatari, R., Yamaguchi, T., O'Loughlin, F., Neal, J. C., Sampson, C. C., Kanae, S., and Bates, P. D.: A high-accuracy map of global terrain elevations, Geophys Res Lett, 44, 5844–5853, https://doi.org/10.1002/2017GL072874, 2017.

Yang, Y., Chen, R., Liu, G., Liu, Z., and Wang, X.: Trends and variability in snowmelt in China under climate change, Hydrol Earth Syst Sci, 26, 305–329, https://doi.org/10.5194/hess-26-305-2022, 2022.

Yoshida, T. and Troch, P. A.: Coevolution of volcanic catchments in Japan, Hydrol Earth Syst Sci, 20, 1133–1150, https://doi.org/10.5194/hess-20-1133-2016, 2016.

Yue, S., Pilon, P., and Cavadias, G.: Power of the Mann–Kendall and Spearman's rho tests for detecting monotonic trends in hydrological series, J Hydrol (Amst), 259, 254–271, https://doi.org/10.1016/S0022-1694(01)00594-7, 2002.

Zhang, J., Zhang, Y., Song, J., and Cheng, L.: Evaluating relative merits of four baseflow separation methods in Eastern Australia, J Hydrol (Amst), 549, 252–263, https://doi.org/10.1016/j.jhydrol.2017.04.004, 2017.

Zhang, J., Song, J., Cheng, L., Zheng, H., Wang, Y., Huai, B., Sun, W., Qi, S., Zhao, P., Wang, Y., and Li, Q.: Baseflow estimation for catchments in the Loess Plateau, China, J Environ Manage, 233, 264–270, https://doi.org/10.1016/j.jenvman.2018.12.040, 2019.

Zhang, X., Vincent, L. A., Hogg, W. D., and Niitsoo, A.: Temperature and precipitation trends in Canada during the 20th century, Atmosphere-Ocean, 38, 395–429, https://doi.org/10.1080/07055900.2000.9649654, 2000.

Appendix A Spreadsheet Procedure to Determine the Master Recession Curve (Modified from Veremu, 2009) for Chapter 5

Step 1:

Using the 3-day moving average of daily runoff, extract recession limbs based initially on a minimum recession period of 14 days. Recession limbs must not include any increase in daily runoff. The minimum recession period may be adjusted through trial and error (e.g. range 12-18 days) to obtain a suitable number of recession limbs, depending on climatic characteristics and the period of record available.

Step 2:

Place time (in days) in column A of the worksheet starting with day 0 (here we use Microsoft Excel). Using the formula $Q_t = Q_0 \exp(-\lambda t)$, generate several common recession limbs in columns B to E as shown in Figure A1, where Q_t is the runoff at time t, Q_0 is the initial runoff and λ is the recession constant. The values of Q_0 are set to cover a range of values, while the slope (recession constant) is the same across all of these common limbs. The extracted recession limbs are aligned in the worksheet so that they all finish on the same row (row 22).

B6 =B$5*EXP($B$3*$A6)

	A	B	C	D	E	F	G	H	I	J	K
1											
2			$Q_t = Q_0 \exp(-\lambda t)$			Extracted recession limbs:					
3	Lambda:	-0.0407				1	2	3	4	5	6
4	Days	Common limb	Common limb	Common limb	Common limb	10/31/1993	9/24/1996	8/30/1998	8/21/2002	7/18/2004	7/13/2005
5	0	1.500	2.000	3.000	6.000						
6	1	1.440	1.920	2.880	5.761						
7	2	1.383	1.844	2.765	5.531						
8	3	1.328	1.770	2.655	5.310			50.491		44.537	
9	4	1.275	1.700	2.549	5.099			33.555		19.286	
10	5	1.224	1.632	2.448	4.895			20.213		17.077	
11	6	1.175	1.567	2.350	4.700	16.554	6.529	14.183	11.093	15.618	12.009
12	7	1.128	1.504	2.256	4.513	10.249	4.532	11.138	7.950	14.692	10.565
13	8	1.083	1.444	2.166	4.333	7.599	4.201	10.178	6.639	10.391	9.913
14	9	1.040	1.387	2.080	4.160	6.434	3.837	9.235	5.865	10.070	9.431
15	10	0.998	1.331	1.997	3.994	5.629	3.503	8.506	5.438	9.209	8.454
16	11	0.959	1.278	1.917	3.835	5.252	3.207	6.784	4.518	8.590	8.251
17	12	0.920	1.227	1.841	3.682	4.874	2.973	5.982	4.107	7.238	7.768
18	13	0.884	1.178	1.767	3.535	4.563	2.868	5.652	3.794	6.856	6.822
19	14	0.848	1.131	1.697	3.394	4.150	2.828	5.161	3.568	6.237	6.001
20	15	0.815	1.086	1.629	3.258	3.818	2.784	4.759	3.515	5.368	5.775
21	16	0.782	1.043	1.564	3.129	3.577	2.667	3.940	3.293	4.698	5.745
22	17	0.751	1.001	1.502	3.004	3.515	2.484	3.401	3.111	4.356	5.636
23											

Figure A1. Extraction of recession periods and generation of common recession limbs.

Step 3:

Calculate average values of Q_{n+1}/Q_n over the last 7-days of each recession limb as shown in Figure A2. Rank these values and use the mean of the largest 5 values as the estimate of the recession constant or slope $(1 - Q_{n+1}/Q_n)$ for the master recession curve.

AN24 =AVERAGE(AN7:AN11)

	A	AG	AH	AI	AJ	AK	AL	AM	AN	AO	AP	AQ
1												
2			Extracted recession limbs, values for Q_{n+1}/Q_n (1-lambda):									
3		11	12	13	14	15						
4	Days	9/5/2011	10/2/2012	9/18/2013	7/25/2015	10/11/2015		Q_{n+1}/Q_n (1-lambda)	Averaged over last 7-days of recession limb			
5	0											
6	1							Rank in decreasing order				
7	2							0.9679	0.0321			
8	3							0.9664	0.0336			
9	4							0.9589	0.0411			
10	5							0.9525	0.0475			
11	6							0.9509	0.0491			
12	7							0.9489	0.0511			
13	8							0.9448	0.0552			
14	9							0.9381	0.0619			
15	10							0.9379	0.0621			
16	11	0.947	0.875	0.929	0.938	0.952		0.9352	0.0648			
17	12	0.978	0.972	0.962	0.899	0.951		0.9312	0.0688			
18	13	0.968	0.971	0.922	0.986	0.973		0.9244	0.0756			
19	14	0.977	0.940	0.940	0.946	0.973		0.9234	0.0766			
20	15	0.952	0.968	0.890	0.955	0.974		0.8993	0.1007			
21	16	0.979	0.939	0.977	0.951	0.969		0.8787	0.1213			
22	17	0.974	0.994	0.946	0.967	0.972						
23										Mean of top 5 values		
24		0.968	0.951	0.938	0.949	0.966			0.0407	= lambda estimate		
25												

Figure A2. Estimation of the recession constant (slope) for the master recession curve based on values of Q_{n+1}/Q_n (1-lambda) over the last 7-days of each recession limb.

Step 4:

Using the worksheet shown in Figure A1, plot the common recession limbs and the extracted recession periods using log scale to give a graph as shown in Figure A3. This allows us to gauge the suitability of the recession constant determined in Step 3. The Q_0 values for the initial runoff in the common limbs can be adjusted to allow visual comparison of the slopes between extracted limbs and the common limbs.

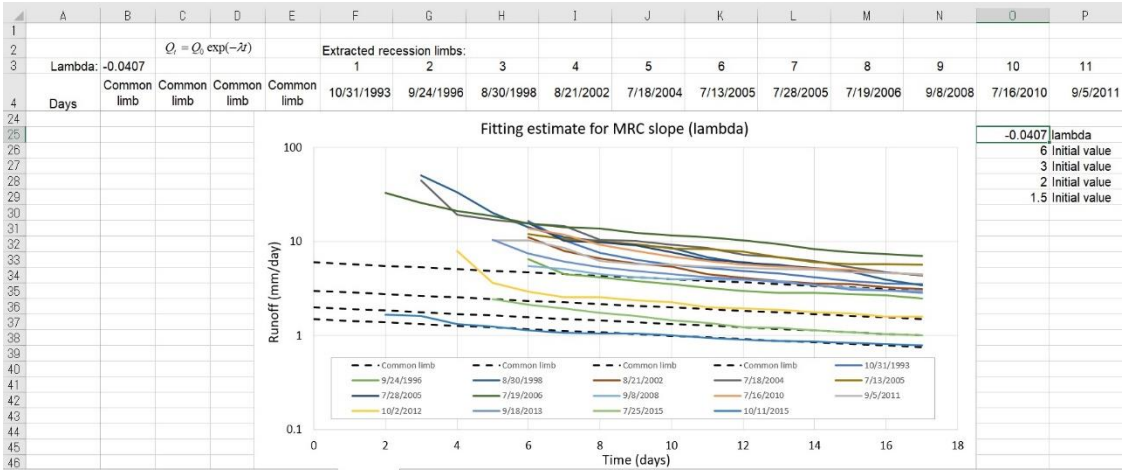

Figure A3. Plotting the extracted recession limbs against common limbs of the same slope (recession constant) to evaluate the suitability of the recession constant for the master recession curve (Figure A4).

Step 5:

Arrange the extracted recession limbs in a separate worksheet so that the final few days of each limb merge with the values in the common limb, and then plot runoff (log scale) against time (Figure A4). In the plot of runoff against time, click on an extracted recession limb, which highlights the corresponding set of values in the worksheet as shown in Figure A4. Place the cursor on the upper right corner and drag upwards (one time-step). This procedure shifts the corresponding limb to the right. The contrary will shift it to the left. This procedure is repeated where necessary until the limbs merge with the common recession limb as shown in Figure A4. This gives the final master recession curve for the Yagisawa basin, as also shown in Figure 3a of the main text (recession constant = 0.0407).

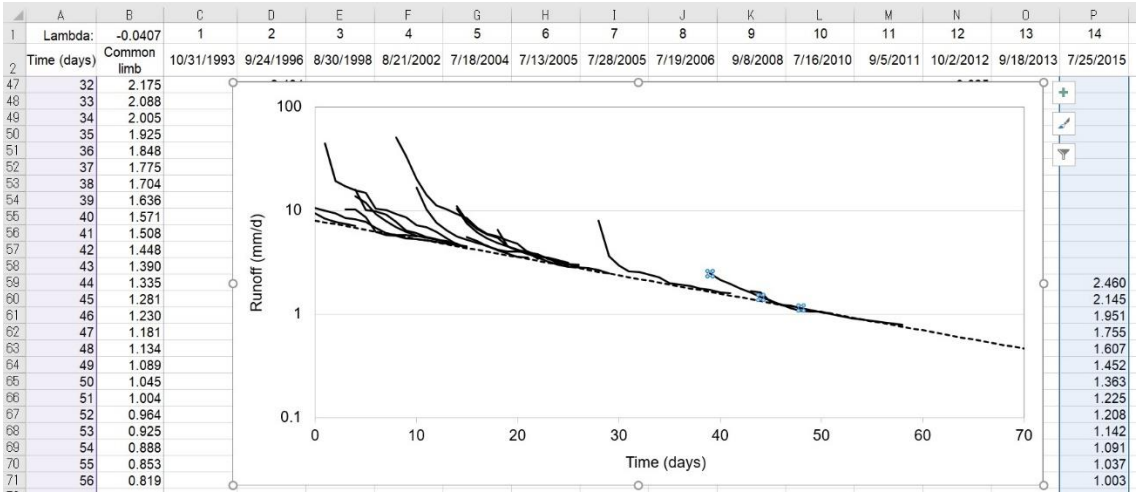

Figure A4. Recession limbs adjusted to the master recession curve.

Appendix B Determination of Annual BFI Values by the BFI Programme

	Data	Q (mm/d)	Baseflow (mm/d)
1	01/10/1993	5.315	
2	02/10/1993	4.790	
3	03/10/1993	5.691	
4	04/10/1993	5.128	
5	05/10/1993	4.752	
6	06/10/1993	4.414	4.414
7	07/10/1993	4.489	4.352
8	08/10/1993	8.396	4.289
9	09/10/1993	6.236	4.227
10	10/10/1993	5.672	4.165
11	11/10/1993	5.203	4.103
12	12/10/1993	4.902	4.040
13	13/10/1993	4.677	3.978
14	14/10/1993	4.451	3.916
15	15/10/1993	4.189	3.853
16	16/10/1993	4.189	3.791
17	17/10/1993	3.963	3.729
18	18/10/1993	3.869	3.667
19	19/10/1993	3.757	3.604
20	20/10/1993	3.663	3.542
21	21/10/1993	3.569	3.480
22	22/10/1993	3.456	3.417
23	23/10/1993	3.418	3.355
24	24/10/1993	3.306	3.293
25	25/10/1993	3.231	3.231
26	26/10/1993	3.212	3.118
27	27/10/1993	3.005	3.005
28	28/10/1993	3.118	3.056
29	29/10/1993	3.268	3.106
30	30/10/1993	12.378	3.157
31	31/10/1993	6.874	3.207
32	01/11/1993	5.053	3.258
33	02/11/1993	4.470	3.309
34	03/11/1993	4.207	3.359
35	04/11/1993	3.944	3.410
36	05/11/1993	3.850	3.460
37	06/11/1993	3.738	3.511
38	07/11/1993	4.132	3.561
39	08/11/1993	4.095	3.612
40	09/11/1993	3.663	3.663
41	10/11/1993	3.569	3.569
42	11/11/1993	3.587	3.537
43	12/11/1993	3.475	3.475
44	13/11/1993	4.921	3.504
45	14/11/1993	4.395	3.534
46	15/11/1993	4.001	3.563
47	16/11/1993	3.888	3.593
48	17/11/1993	3.700	3.622
49	18/11/1993	3.963	3.652
50	19/11/1993	3.681	3.681
51	20/11/1993	4.282	3.689
52	21/11/1993	6.536	3.696
53	22/11/1993	5.409	3.704
54	23/11/1993	5.053	3.711
55			

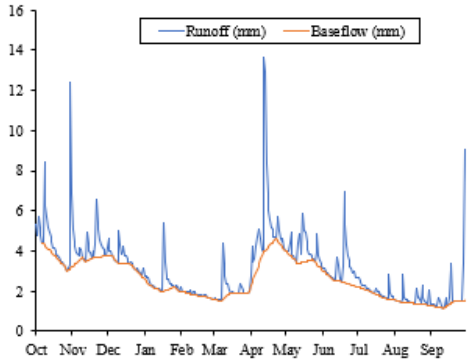

Load Sample Data | Reset | Calculation of BFIs | 1994

Results: Whole series	
BFI	0.673
Mean of annual BFIs	0.675
Season Information	
Season start day	1
Season start month	10
Season end day	30
Season end month	9
Year shift during season	Yes
Series information	
Start of entire series	10/1/1993
Start of base flow line	10/6/1993
End of base flow line	12/21/2019
End of entire series	12/31/2019

Results: Annual values

Year	BFI	Lost days
1994	0.830	5
1995	0.713	0
1996	0.761	0
1997	0.636	0
1998	0.609	0
1999	0.604	0
2000	0.760	0
2001	0.684	0
2002	0.697	0
2003	0.659	0
2004	0.700	0
2005	0.689	0
2006	0.596	0
2007	0.694	0
2008	0.764	0
2009	0.725	0
2010	0.612	0
2011	0.597	0
2012	0.729	0
2013	0.696	0
2014	0.714	0
2015	0.689	0
2016	0.641	0
2017	0.711	0
2018	0.582	0
2019	0.688	0
2020	0.445	284

Figure B1. An example above shows the determination of annual BFI values using the BFI Programme for the Narai basin in the Shinano-gawa river system (26 water years).

Appendix C Determination of $Q7_{10}$ Flow Index

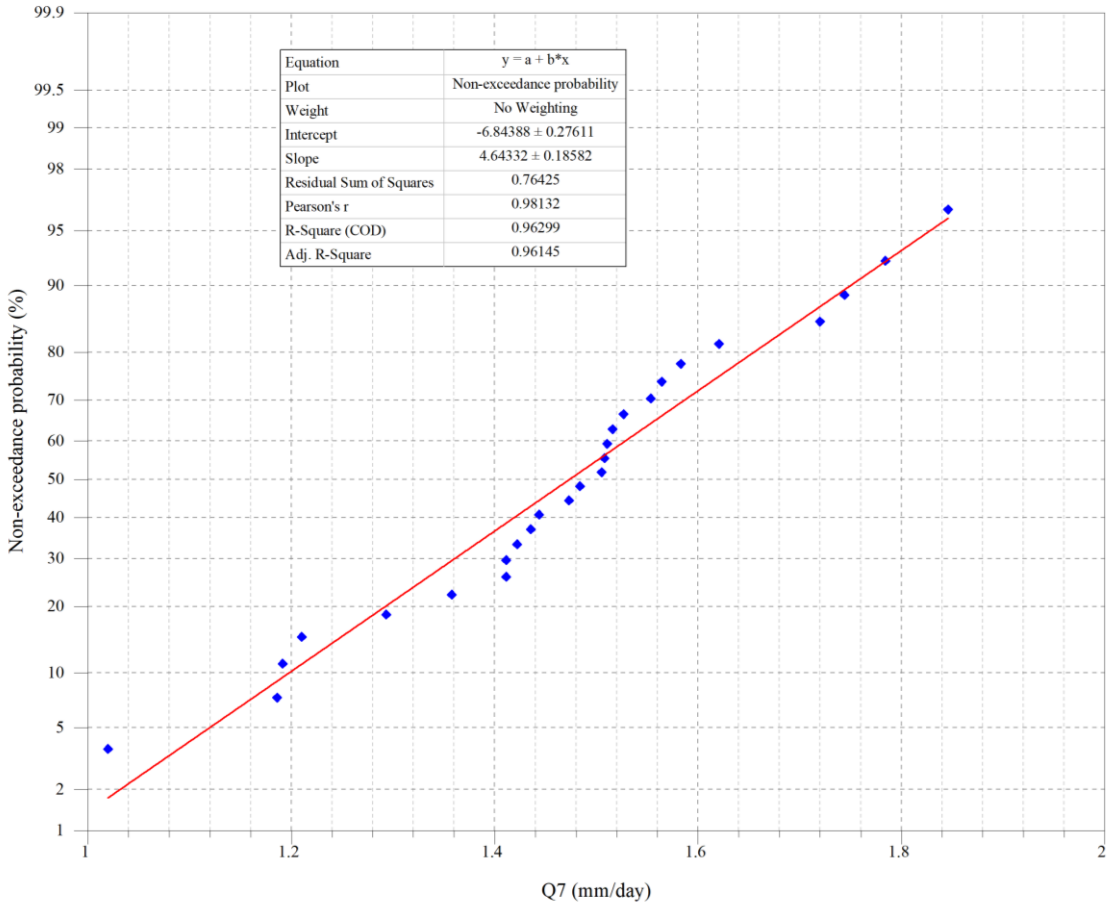

Figure C1. An example above shows that $Q7_{10}$ = 1.2 mm/day for the Narai basin in the Shinano-gawa river system (1993-2019).